GROUND VIBRATIONS NEAR EXPLOSIONS

Thesis by

Benjamin F. Howell, Jr.

In partial fulfillment of the requirements

for the degree of

Doctor of Philosophy

California Institute of Technology

Pasadena, California

1949

Acknowledgments.

The author wishes to thank the United Geophysical Company, particularly Dr. Raymond A. Peterson and Mr. Merrill Swan, for making this research possible. The apparatus used to make the observations was supplied by the United Geophysical Company; much of it was specially purchased or made for these studies, and the explosions observed were detonated as a part of their work in testing new equipment. The generously given cooperation of the many men conducting these tests made possible the records on which this dissertation is based.

The author wishes to express special thanks to Dr. Beno Gutenberg of the California Institute of Technology, whose advice and guidance was of inestimable assistance throughout the investigation, and without whose help the present project probably never would have been completed.

Many others, including Dr. Hugo Benioff, Dr. C. H. Dix and Dr. C. F. Richter, reviewed this report and made helpful suggestions in the writing of it, for which the author wishes to express his appreciation.

The two illustrations in section IX of ground motion recorded at other places than at Los Alamitos are reproduced thru the courtesy of L. Don Leet. Permission to include these is appreciated by the author.

Abstract.

Records are shown of the three components of ground vibration taken at distances out to 3284 meters following small explosions of dynamite about ten meters underground. The apparatus used to record this motion is described, and its limitations discussed. The refracted compressional waves recorded are used to calculate roughly the thickness of the near surface layers. Three principal dispersed waves are recognized and described. It is shown that two of these do not behave like any well known type of wave motion. It is pointed out that this is not surprising since the near surface material is probably neither homogeneous nor elastic and these conditions are required by the classical theories. The third dispersed wave is shown to closely resemble a modified Rayleigh wave. Three published theories of such modified motion are reviewed and compared with the observations. The recorded data are also compared with other similar records copies of which have been published.

Table of Contents.

Table of contents continued.

List of Illustrations.

List of illustrations continued.

List of illustrations continued.

List of charts. All charts are included in the envelope at the back of the report.

GROUND VIBRATIONS NEAR EXPLOSIONS.

I. PREVIOUS EXPERIMENTAL WORK.

Introduction.

One would expect that since seismic waves from explosions are the basis of a whole industry (seismic surveying), their nature would have been thoroughly investigated and described. A seismic crew commonly sets off in a normal day's operation some tens of charges of dynamite, photographically recording the ground motion following each explosion at sometimes as many as 24 separate locations. The records made are later studied in detail by specially trained engineers and scientists. Yet in spite of the tremendous amount of data thus accumulated, our knowledge of the detailed character of the energy radiated from such an explosion is very limited. In particular, the aspects of the problem which have no obvious, immediate, commercial application have largely been neglected.

One reason for this is that the records regularly taken in geophysical exploration for possible oil reservoirs are not well suited for such studies. Only one component of the motion is recorded; and the apparatus used to measure that is commonly not carefully calibrated, so that the amplitude of the original ground motion can not be accurately determined. Often the

gain of the amplifiers is caused to vary during the time of reception of the energy from a single explosion. Also, only a very limited frequency spectrum is normally recorded. The reason for this restricted type of recording is that the exploration geophysicist is not primarily interested in the shapes of the seismic pulses, but in the paths they travel to his instruments. Great care is taken to determine the velocities of compressional waves in the ground where such surveys are conducted, by making well velocity surveys, and refraction records to determine "weathering corrections"; and much work has been done on studying the phenomena of reflection and refraction (Gutenberg, 1944; Dix, Fu, and McLemore, 1945)*. But in general, little effort has been made to investigate the physical properties of the ground itself, such as its absorption and dispersion characteristics.

It is common practice in studying seismic exploration records to assume that all of the significant energy recorded represents compressional waves, though occasionally the presence of some transverse wave energy is postulated to explain otherwise incomprehensible observations. Other types of wave motion are treated as part of the background noise, and wherever possible are excluded from the recorded spectrum by the use of

---

* All references are made to the bibliography at the end of the paper.

appropriate filters in the amplifiers.

However, proper interpretation of the records obtained requires some knowledge of the detailed character of the ground motion; and therefore any information on the nature of the seismic energy which is generated by an explosion is certain to have some value in the science of exploration geophysics. The series of experiments described herein was undertaken with the intent of increasing the knowledge of the basic seismic forms to be expected in the record of an explosion.

Work of J. A. Sharpe.

Some previous work has been done on this problem, and a certain amount of information is available from researches primarily pointed in other directions. A very fine approach was made by J. A. Sharpe (1942). He made a series of observations of the energy from small explosions at depths from 2.4 meters to 94 meters, with seismometers located in holes 1.5 meters to one side, and at various depths above and below the shots. Unfortunately his observations were limited to measurements of the vertical component of ground motion. Since his geophones were always close to directly above or below his shots, and responded only to vertical movements, his observations give a good picture of the nature only of the compressional pulse generated by an

explosion.

Sharpe's paper is of particular interest because he analyses the pulse shape to be expected from theoretical considerations, and compares it with those observed. Since the initiating forces in the ideal case are entirely radial, there should be no shear waves directly generated, a conclusion born out, in general, by observation for explosions buried at sufficient depth beneath the surface. Shear waves are, however, to be expected from a superficial explosion, as predicted by Lamb (1904) for the case of a force applied vertically to the surface.

Limitations on this theory.

In practice we do not encounter a homogeneous, isotropic, elastic medium thru which the seismic energy can be transmitted from the explosion to the recording mechanism. Most rock in place consists of a number of different formations. Where these formations are sedimentary, as is often the case at the surface of the earth, the formations are arranged in sheets, each of which is relatively uniform throughout, and which may be flat, or folded either gently or sharply, or faulted, or both folded and faulted. Where the deformation is not too complex the paths of the seismic waves thru the rocks are relatively simple (provided the classical theory applies), energy from the

original explosion reaching the recording station by a number of paths, being split into reflected and refracted compressional and shear components each time it encounters the boundary between two media of distinctly different physical properties. Thus a large part of the energy received from an explosion consists of pulses which have followed such paths. This is the basis of seismic exploration, and the details of such transmission are well known.

However, this model of the earth's structure, is only a very rough first approximation to the true conditions. Although the deeper layers of rock may be considered to be homogeneous, the surface layer itself certainly is not, and can be satisfactorily approximated only by assuming that it varies in nature at least in the vertical direction. In this case the ray paths can still be calculated. As a second approximation we can say that our earth departs from homogeneity only in simple ways.

The same is true of the condition of isotropy. Most rocks may be considered isotropic, although for some rocks this is known not to be the case. Foliated and bedded rocks can be shown to have different elastic constants perpendicular and parallel to the foliation or bedding (Birch and Leet, 1942, p.73-77). In practice, however, these differences are generally

small. Even if the rocks are not isotropic the theory can be extended to include any case where the departure from isotropy is of a regular nature (see for instance Macelwane, 1936, Chapter III), though the equations become much more complex.

The third necessary condition for the simple classical theory is that the rocks be elastic, that is that the strain be proportional to the stress, and that the body return to its original state on removal of the stress. Study of the transmission of body waves thru the earth indicates that this condition is held to a first approximation except right at the earth's surface. The layer of decomposed and decomposing, or for other reasons unlithified material which overlies the "solid" rock almost everywhere is not elastic. Although equations have been developed to describe the response of such material to long continued stresses of one polarity (Gutenberg, 1939, Ch. XV), the wave mechanics in such media are largely undescribed, though some special cases have been treated (Frenkel, 1944). Yet it is at the upper boundary of this layer that most of our observations in geophysical exploration are made.

In spite of the inaccuracies of our assumptions as to the nature of the medium, our simple theory of wave transmission is adequate to explain most of the

observed motions of the ground. However, when observations do not seem to fit the theory, we have a ready possible explanation in the differences between our assumptions as to these conditions and fact. Conversely, if we could make our theory more general to include more varied ground conditions, we might be better able to explain our observations.

Besides the body waves in the earth, surface waves are generated at its surface; and possibly, though this has never been proven for an explosion, in the interfaces between the formations. Thus the record of an explosion consists of a series of motions, which commonly overlap, being the results of transmission of the different types of elastic waves (plus any other types of waves which may be present, if such exist) along a multiplicity of different paths.

The techniques of sorting out and identifying the nature of each of these different pulses are well known, and need not be reviewed here. They are the same as those used in seismic exploration and in studying teleseisms. At small distances from the explosion the different pulses overlap, and are hard to identify. At larger distances they are more distinct, but of smaller amplitude. Thus the pulses possessing little energy are difficult to examine except from large explosions.

Studies of very large explosions.

For this reason most of the work done in the past has been on large explosions. These are often recorded at nearby permanent seismic observatories. Such a case was the Oppau explosion, or explosions, on Sept. 21, 1921 (Hecker, 1922, also Wrinch and Jeffreys, 1922), which was recorded at seismic stations from Heidelberg, 29 km. away, to Munich, 307 km. away. Most of the recorded energy from this explosion, and the others mentioned below, does not travel directly to the recording seismographs, but follows complex refracted paths penetrating to considerable depth into the crust of the earth, or even thru it.

Wood and Richter published two studies (1931 and 1933) on the records from quarry blasts recorded at southern California seismic stations; Byerly and others have similarly treated explosions in the San Francisco region (Byerly and Dyk, 1932; Byerly and Wilson, 1934: Byerly, 1946). Gutenberg and Richter published brief descriptions of records of the experimental atomic bomb explosions at Los Alamos and Bikini atoll (Gutenberg, 1946; Gutenberg and Richter, 1947); and Jeffreys (1947) has described the records of an explosion in England. Willmore (1947) has reported briefly on the Heligoland explosion. All of these papers deal primarily with data recorded many kilometers from their source. Pulses

of compressional and transverse waves coming along refracted ray-paths are discussed, and in some cases possible surface wave components mentioned. However, the principal aim of these studies is to determine something of the structure of the crustal layers of the earth. Because of the large distances from the explosions the ray-paths for the body waves penetrate so deeply into the earth, that the effect of individual formations is lost, the identified wave paths being associated with the major divisions of the crust. The shapes of the pulses are altered by the selective attenuation of certain frequencies, by dispersion, and by resonance effects of the ground near the recording station (Lee, 1932). Such literature as has been published on material recorded in this manner places little emphasis on surface waves, which are not prominent on records of this type. Thus only limited information on the character of seismic waves from explosions is to be expected from studies of explosions recorded at permanent seismic stations.

Work of L. D. Leet.

Besides Sharpe's paper mentioned earlier, another direct approach to the problem was made by L. D. Leet (1939, 1946; also Leet and Ewing, 1932). Leet recognizes two other types of waves in records from explosions besides the well known compressional,

transverse, Love and Rayleigh waves. The first of these, the "C" or "Coupled" wave is characterized by simultaneous in-phase motion on all three components. The second, the "H" or "Hydrodynamic" wave, is similar to the Rayleigh wave, except that whereas the particle motion in a Rayleigh wave is retrograde with respect to the direction of propagation, in the Hydrodynamic wave the particle motion is direct, being like that of a gravity wave in a liquid. H has been observed up till now only in the atomic bomb record made during the Los Alamos test and in the record of one explosion in New England. C was observed also in these records, and in other records from blasts in New England. These results will be considered in greater detail in section IX at the end of this paper.

From the above brief review of previous work it can be seen that of the various kinds of seismic waves initiated by explosions only the compressional waves have been studied in great detail. In the work which is described below, therefore, the emphasis is upon the less well known types. The compressional waves, though well recorded, will not be discussed in detail.

II. THE APPARATUS.

The apparàtus used in this research was very generously loaned by the United Geophysical Company. A considerable number of different types of seismometers and amplifiers were used in the early stages of the research; but eventually the assemblage described below became available, and as it proved to be well adapted to the requirements of studying seismic waves from explosions, it was the one used to obtain all of the significant information presented in this report. Figure 1 is a block diagram of this apparatus.

The Seismometers.

The seismometers were manufactured by Engineering Laboratories, Inc., of Tulsa; and are their type GS 13. They were designed primarily for use in refraction type seismic surveying. They are electromagnetic induction type instruments, with the acoustical energy transformed into electrical energy by the relative motion of a permanent magnet with respect to a coil suspended by springs in the gap of the magnetic assembly. Their electrical output, when properly damped, was uniform for constant velocity of the ground from about eight cycles per second to the highest frequencies recorded by the rest of the apparatus. Below four cycles per second their sensitivity rapidly decreased.

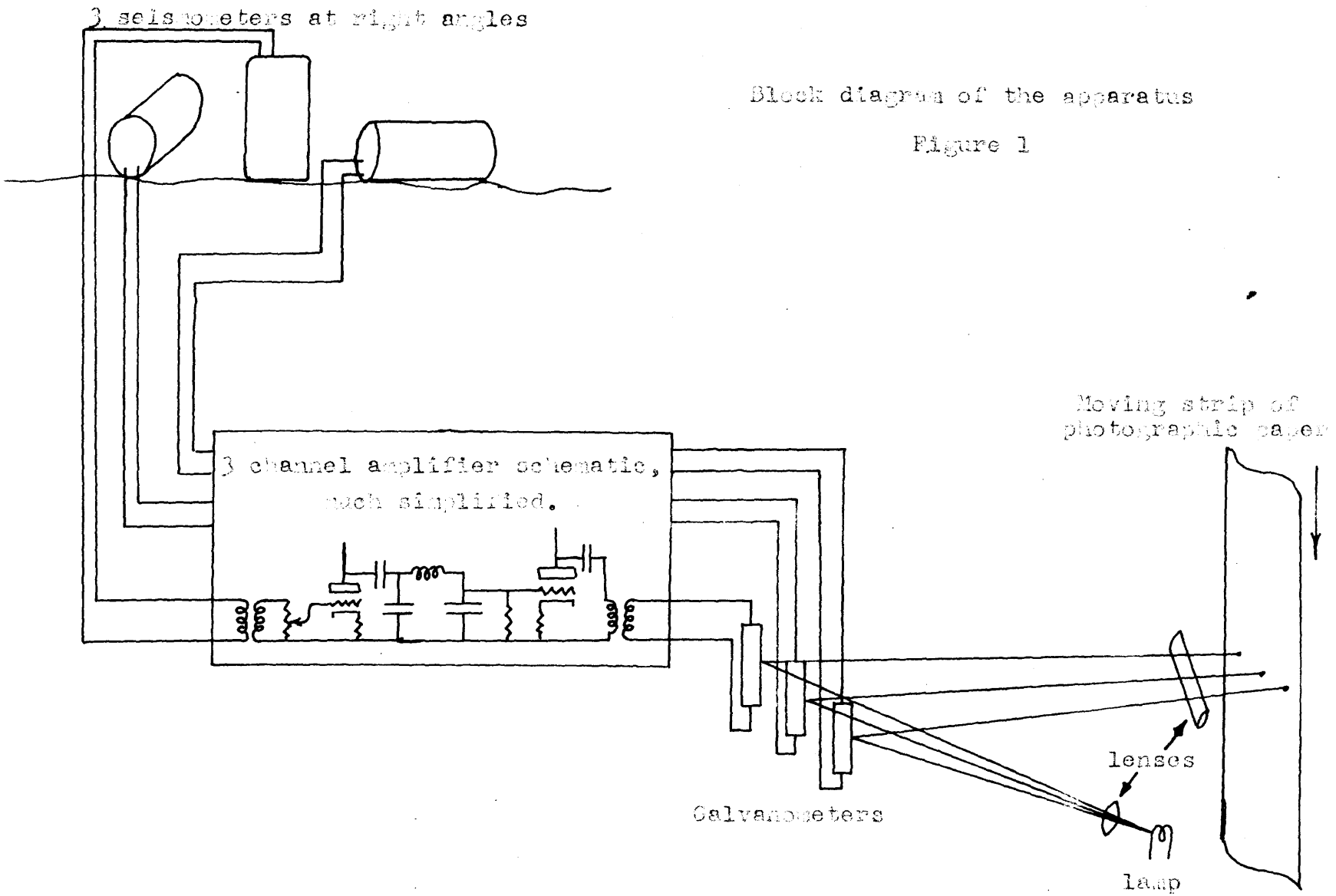

Block diagram of the apparatus

Figure 1

Three seismometers of this type were used. One measured the vertical component of the ground motion, one the horizontal component radially from the shot point, and the third the horizontal component in a direction perpendicular to the other two.

The seismometers were originally intended to be used only in the vertical position, and some modification was required before they could be used to measure the horizontal components of the ground motion. Unfortunately, because of the nature of the instruments, it was impossible to make them completely insensitive to the vertical component of motion without completely rebuilding them, so that both of the horizontal units responded slightly to vertical movement.

The Amplifiers.

The amplifiers used were also designed for refraction type seismic surveying. Their outputs were essentially uniform for constant electrical input from below four cycles per second to over one hundred cycles per second. They also contained filters which could be used to decrease the sensitivity of the apparatus to the higher frequencies. These filters had sharp cut-offs at nominally 10, 20, 40 and 80 cycles per second. The amount of amplification could be varied by the use of calibrated voltage dividers.

The recording oscillograph.

The electrical output of each amplifier was fed to a D'Arsonval type moving coil galvanometer. Transformers were used to match the amplifiers to both the galvanometers and seismometers. A small mirror was mounted on each galvanometer coil. The galvanometers were part of a recording oscillograph wherein the rotary motions of the galvanometer coils and attached mirrors displaced beams of light which fell on a moving strip of photographic paper. When developed, the photographs showed three wavy lines, one for each light beam. The amount each of these lines was displaced from a straight line at any point was proportional to the corresponding component of the velocity of the ground at the time it was recorded. As the sensitivity of the galvanometers decreased rapidly above 120 cycles per second, they provided an upper limit to the frequency response of the recording system.

The same recording oscillograph was not available at all times for this investigation; but the same type of instrument was used throughout, so that the records differ only in the width of the photographic paper used and the speed with which it was drawn past the light spots.

A means was provided in the oscillograph whereby marks were placed on the photographic record every

one hundredth of a second. The frequency of these lines was controlled by a 50 cycle per second tuning fork. The timing lines were checked against standard time signals sent out by radio station WWV in Washington, and were known to be of the frequency indicated with an error of less than 1/100 second in a minute. The possible error of timing any motion recorded is appreciably less than the accuracy with which the time of that phase of the pulse can be read from the record.

In order to determine the interval from the time of the explosion until the arrival of any phase of the recorded energy, a signal was transmitted by radio at the instant of the explosion, and was recorded on the photographic record on a fourth trace beside those representing the three components of ground motion.

Calibration of the seismographs.

Figures 2, 3 and 4 show the overall response characteristics of the three channels. Figure 2 is for the vertical component; figure 3, for the longitudinal component (horizontal component radially from the shot point); and figure 4, for the transverse component (horizontal component perpendicular to the other two components). The calibrations are given in decibels above 1 millimeter peak to peak displacement of the light spot on the paper per 1/1000 millimeter

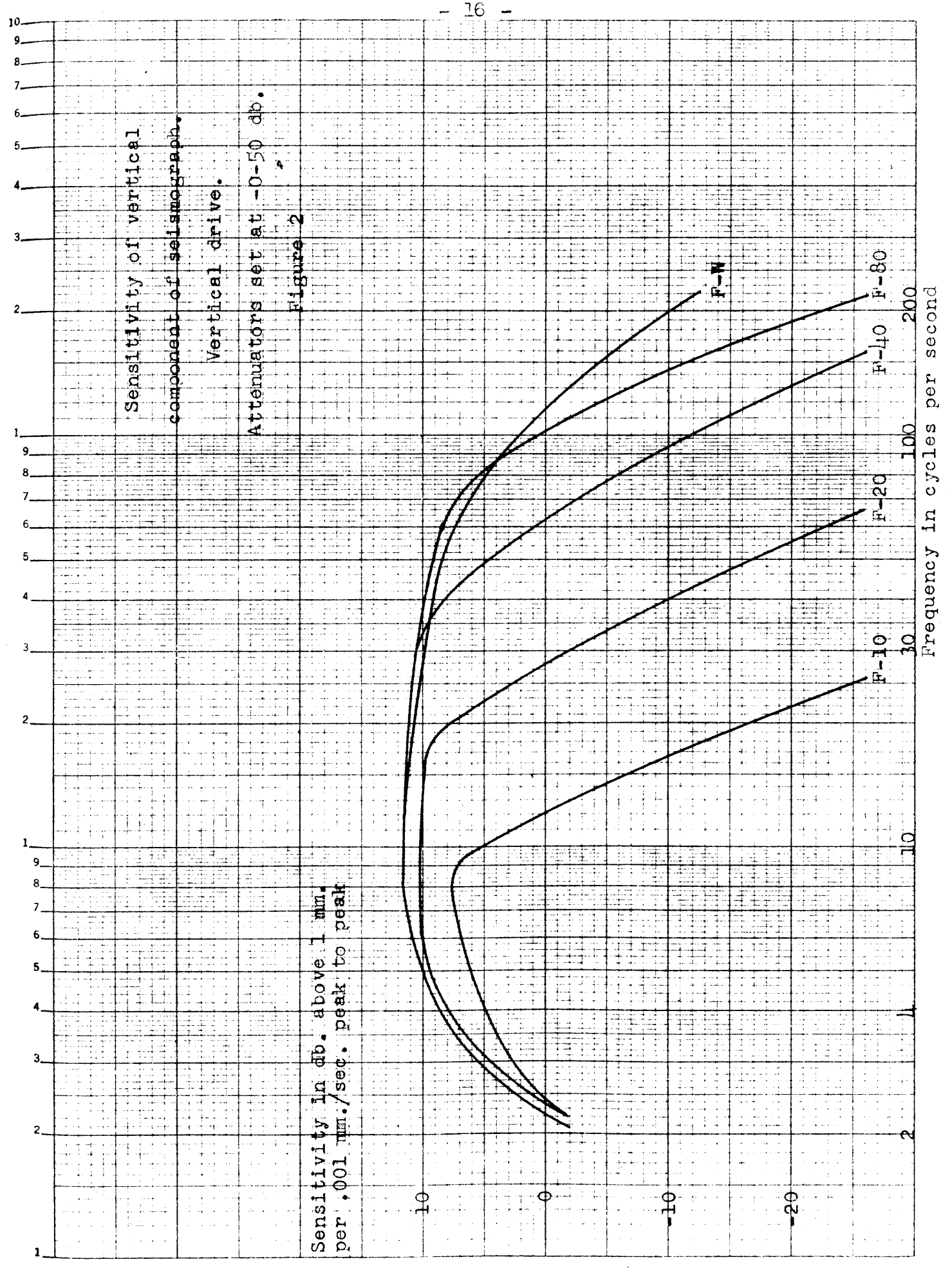
Sensitivity of vertical component of seismograph.
Vertical drive.
Attenuators set at -0-50 db.
Figure 2
Sensitivity in db. above 1 mm. per .001 mm./sec. peak to peak
F-W
F-80
F-40
F-20
F-10
10
0
-10
-20
1
2
10
30
100
200
Frequency in cycles per second

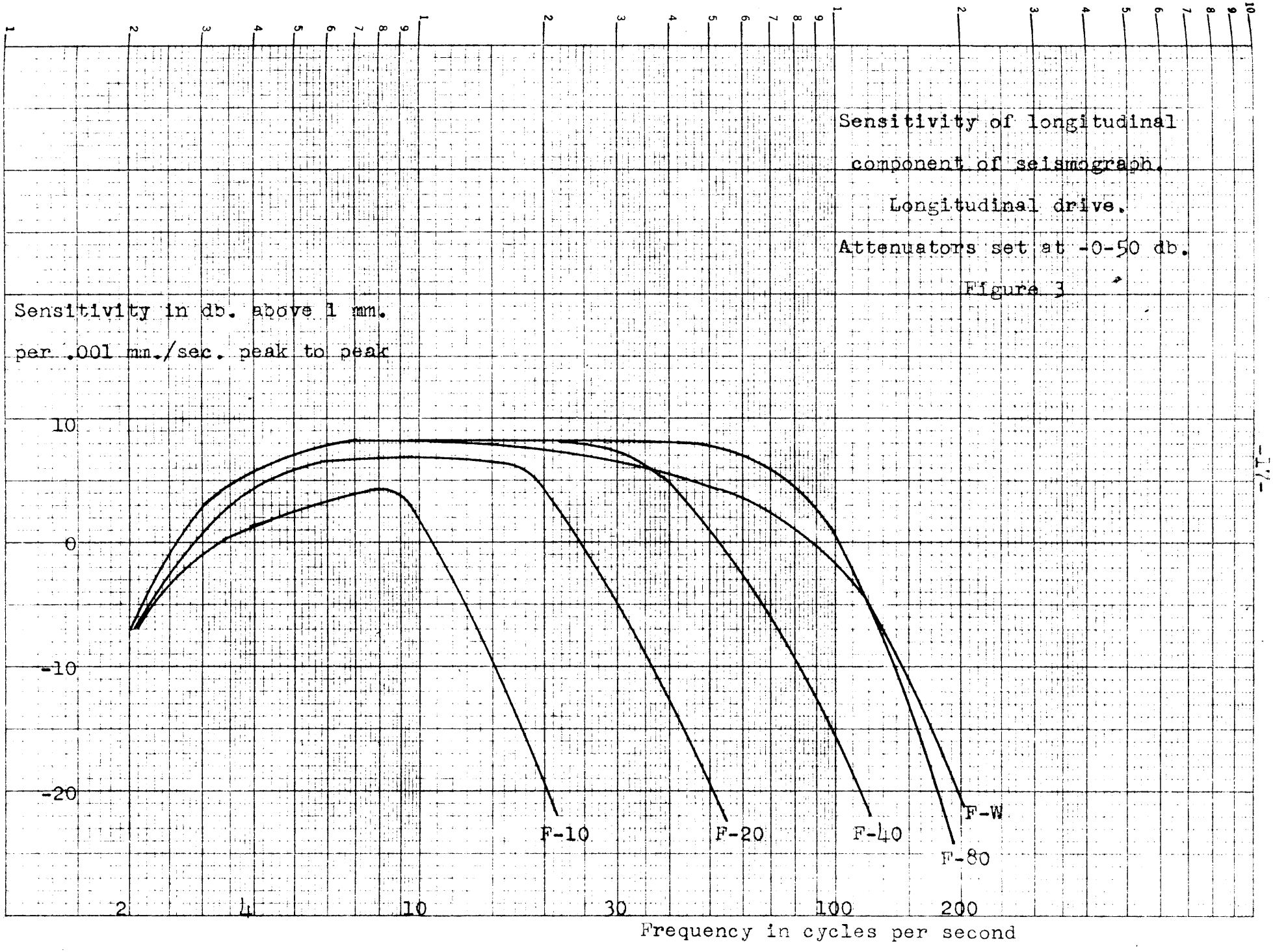
Sensitivity of longitudinal component of seismograph.
Longitudinal drive.
Attenuators set at -0-50 db.
Figure 3
Sensitivity in db. above 1 mm. per .001 mm./sec. peak to peak
10
0
-10
-20
F-10
F-20
F-40
F-80
F-W
2
4
10
30
100
200
Frequency in cycles per second

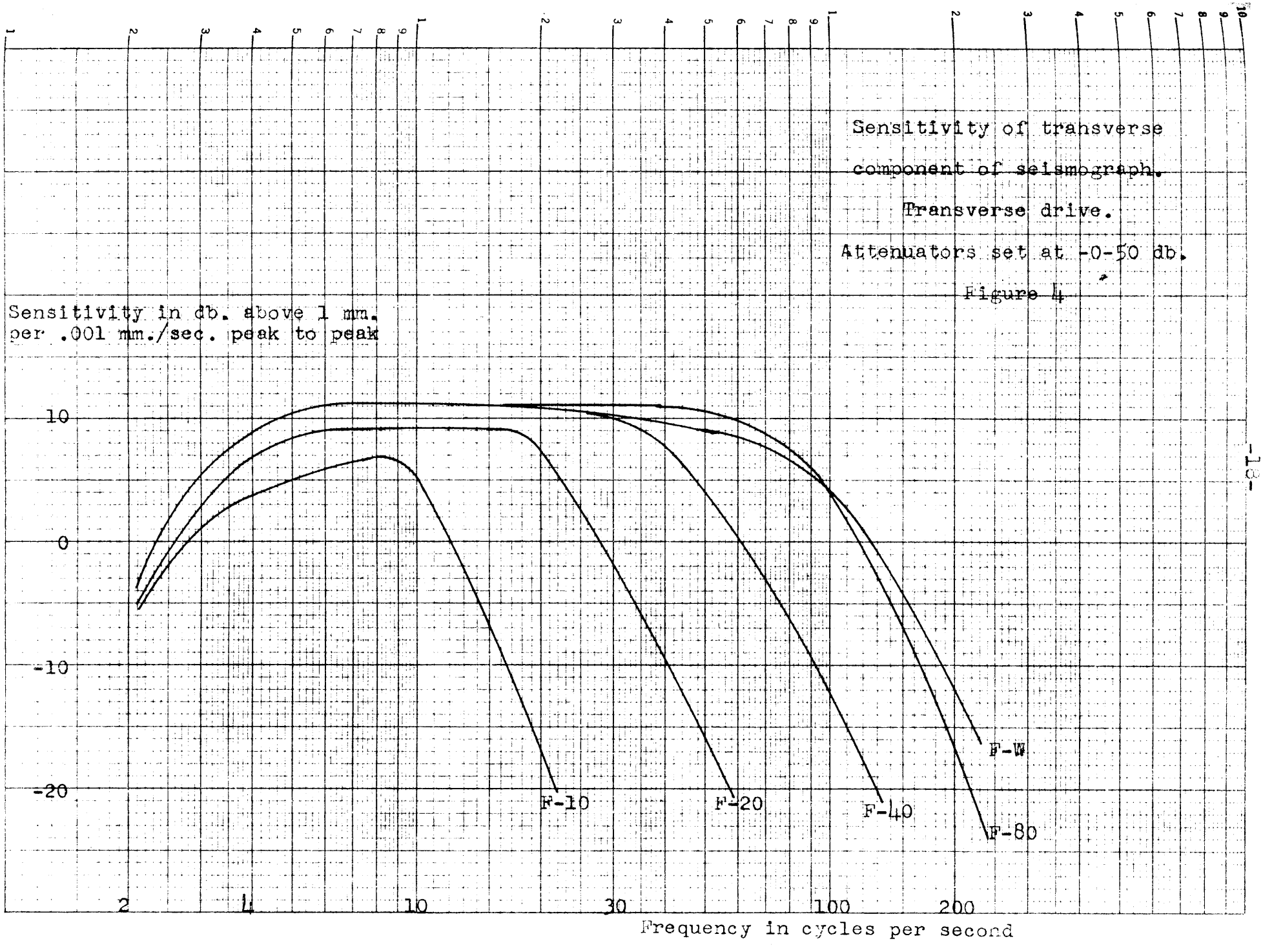
Sensitivity of trahsverse
component of seismograph.
Transverse drive.
Attenuators set at -0-50 db.
Figure 4
Sensitivity in db. above 1 mm.
per .001 mm./sec. peak to peak
10
0
-10
-20
F-10
F-20
F-40
F-80
F-W
2
4
10
30
100
200
Frequency in cycles per second

per second peak to peak ground velocity. (The ratio of two amplitudes, A and B, expressed in decibels is $20 \log_{10} A/B$. Six decibels, abbreviated "db.", corresponds approximately to a ratio of 2; ten db., to a ratio of 3; 20 db., to a ratio of 10.) The five curves in each chart correspond to the five different settings of the filters in the amplifiers. When the filters are set for 10 cycles per second cut-off (F-10), the amplifier is overdamped, causing considerable loss of gain as compared to the gain at the other filter positions. The "unfiltered" connection (F-W) is accomplished by shorting out the inductance of a π section filter, resulting in an awkward match between two stages of the amplifier, which causes the amplifier response to droop throughout the range of frequencies to which it responds. Its upper limit of frequency response is eventually determined by the natural frequency of the galvanometer, since above that frequency (approximately 120 cycles per second) the galvanometer rapidly loses sensitivity. The low frequency response is limited by the failure of the seismometers to respond to ground motions of less than their natural frequencies (3 1/2 cycles per second).

Figures 5, 6, and 7 show the relative sensitivities of the three channels to motions perpendicular to their principal direction of response with the filters on

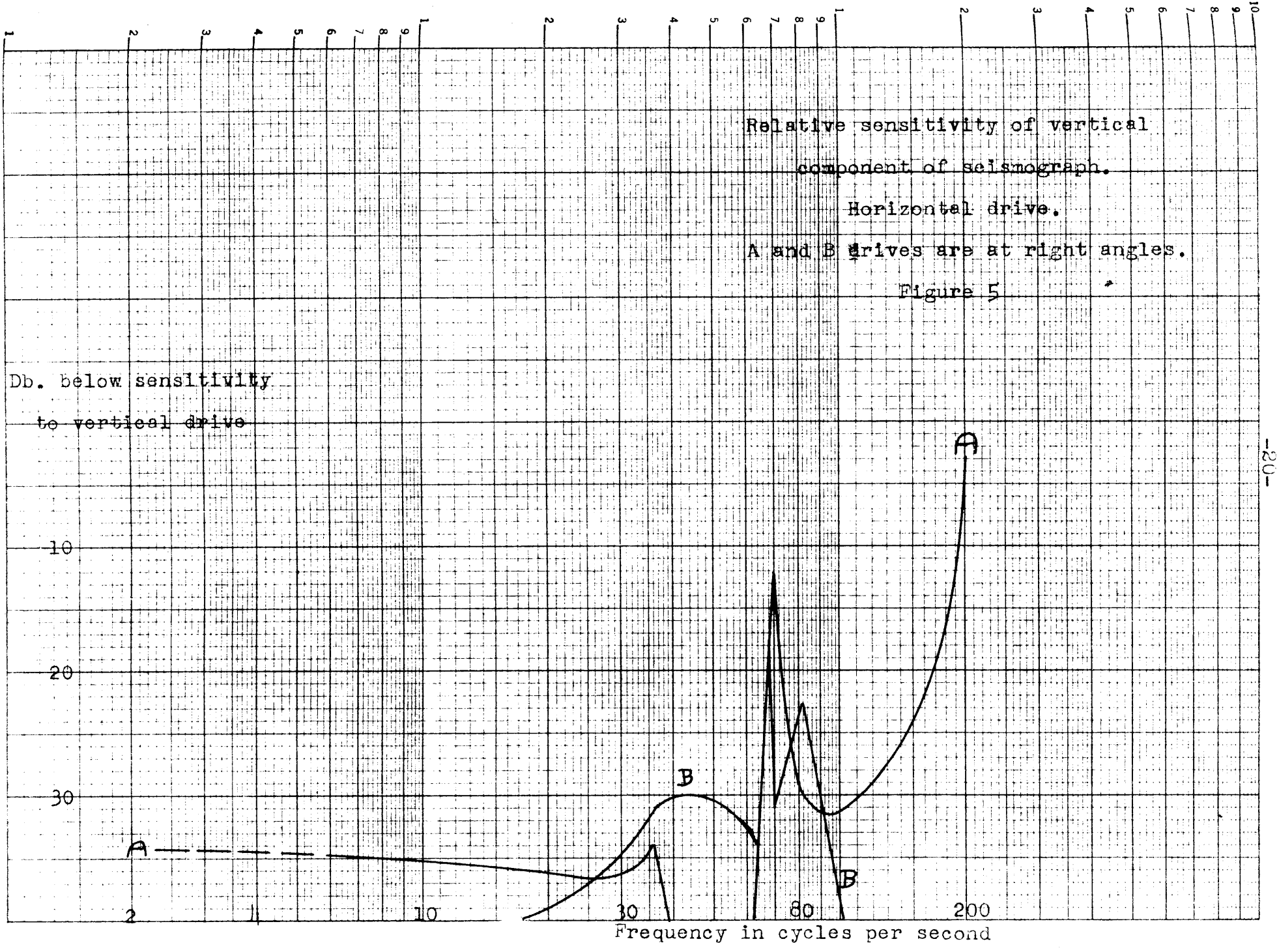
Relative sensitivity of vertical component of seismograph.
Horizontal drive.
A and B drives are at right angles.
Figure 5
Db. below sensitivity to vertical drive
10
20
30
A
B
A
B
2
4
10
30
60
200
Frequency in cycles per second

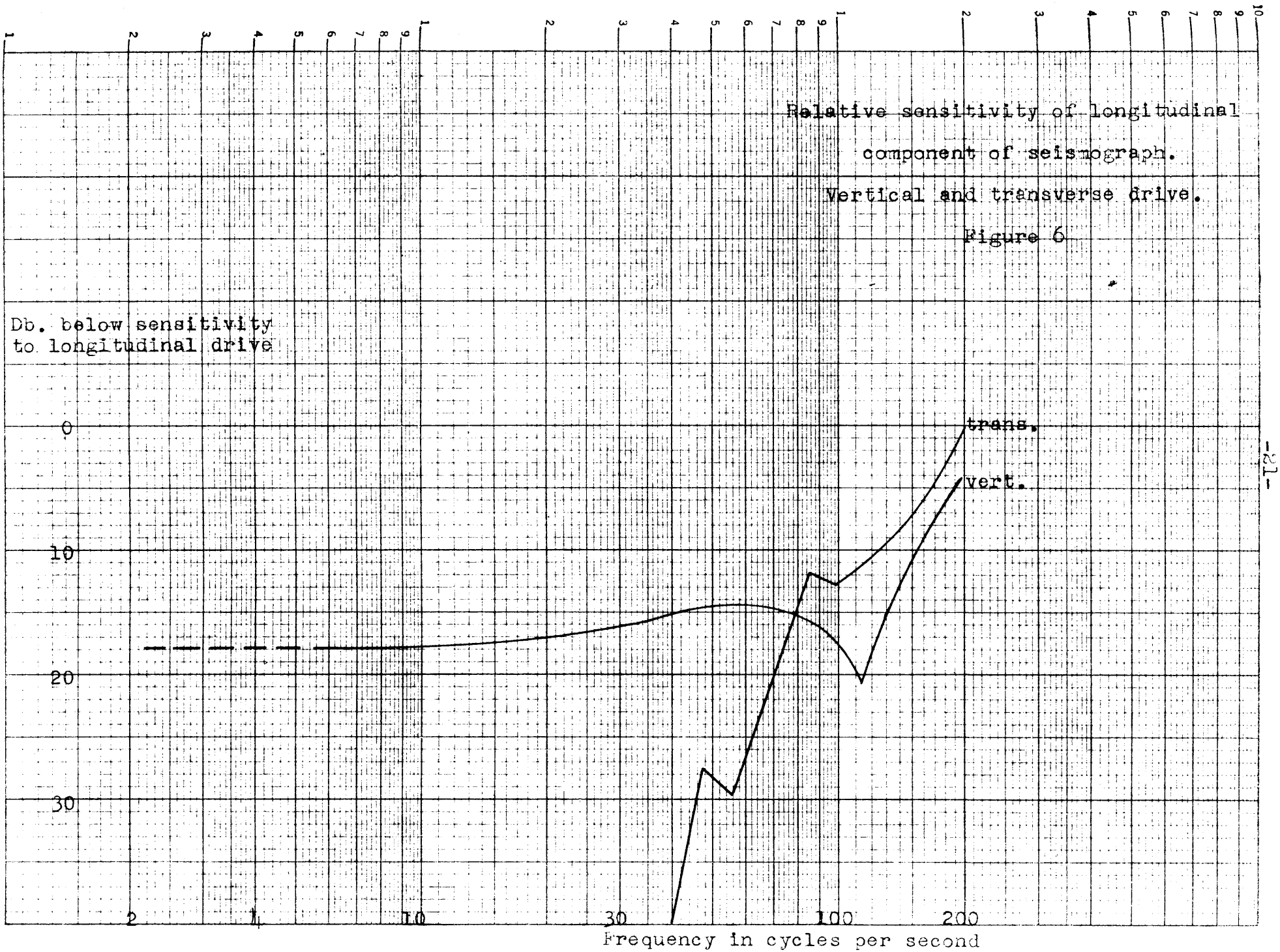
Relative sensitivity of longitudinal component of seismograph.
Vertical and transverse drive.
Figure 6
Db. below sensitivity to longitudinal drive
0
10
20
30
trans.
vert.
2
1
10
30
100
200
Frequency in cycles per second

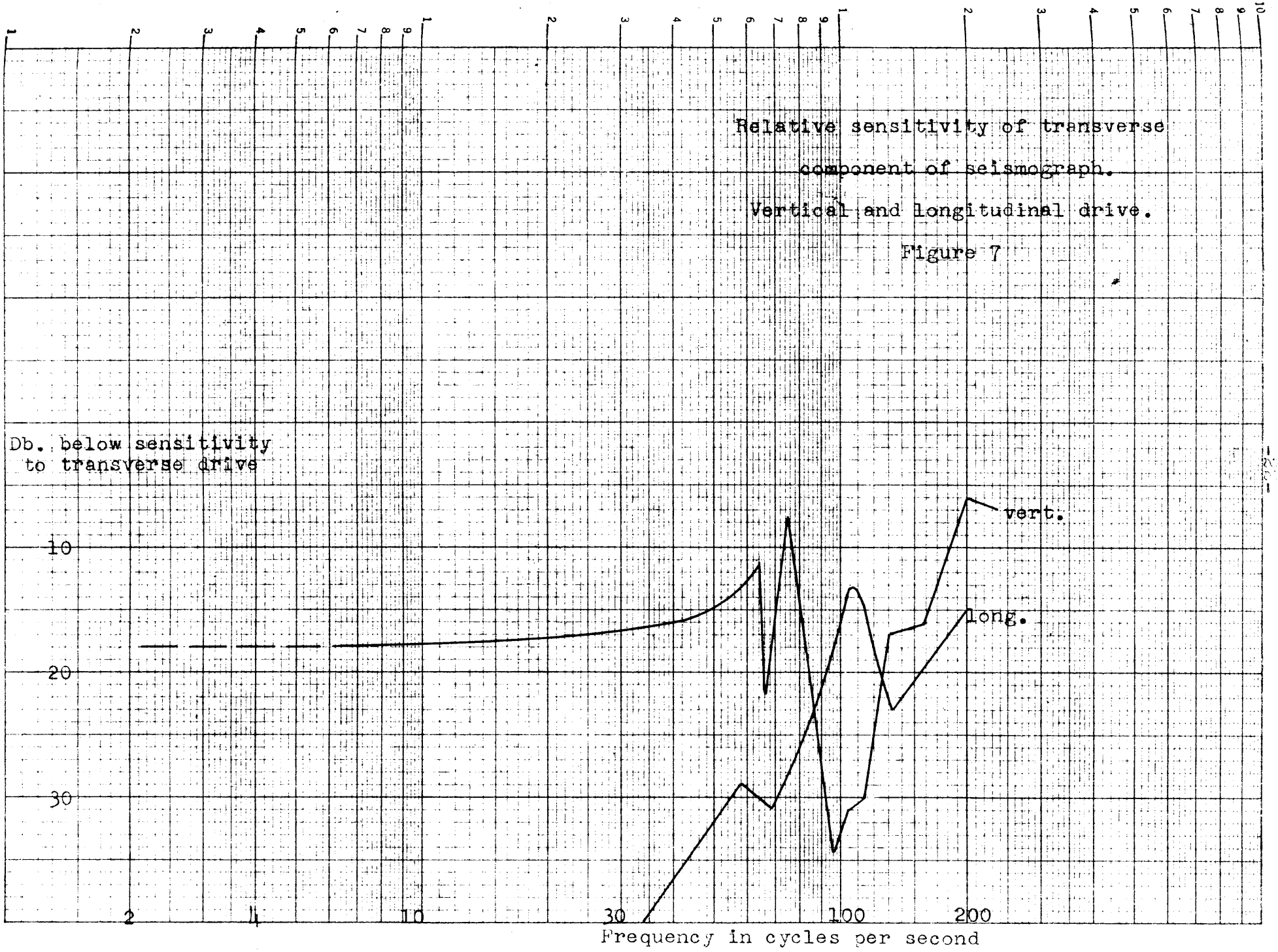
Relative sensitivity of transverse component of seismograph.
Vertical and longitudinal drive.
Figure 7
Db. below sensitivity to transverse drive
10
20
30
vert.
long.
2
4
10
30
100
200
Frequency in cycles per second

position F-W. At low frequencies the apparatus is relatively insensitive to this motion, but above about 70 cycles per second there are "parasitic" frequencies in the response. This is presumably due to undamped modes of the spring suspension of the coil of the seismometer. Where these parasitic frequencies were within the pass-band of the filters, their presence could sometimes be detected, since they caused an almost continuous background of vibration of low amplitude at 70 to 80 cycles per second.

The method of obtaining the overall frequency response curves was to place the seismometer on an electrodynamically driven shaking table, using a sinusoidal driving force, and photographically recording the output of the amplifier with the oscillograph, exactly as was done in recording explosions in the field. At the same time the output of a "standard" vibration pickup, sitting on the shaking table beside the seismometer, was measured. The standard pickup (an M B Manufacturing Company type 124) had previously been calibrated on a mechanical shaking table whose amplitude of motion could be measured with a scale, and hence from its output the motion of the shaking table used here could be calculated. Records were taken at a series of frequencies, and from the measurement of these records

the sensitivities calculated. Figures 2-7 were drawn using this data.

Limitations in accuracy.

The curves obtained in this way were repeatable within two decibels (a ratio of 1.26) from about 6 cycles per second to the top of the pass band of the seismograph. However, outside of the pass band the accuracy decreases with distance from the cut-off frequency. Since the method of calibration was essentially the same as that used to record explosions, except for the difference in the source of the driving motion, corresponding inaccuracies enter in both cases, and will be discussed together.

The principle known sources of error are: 1. errors in leveling the seismometers; 2. errors in measuring the amplitude of the recorded trace; 3. inaccuracies in measuring the frequencies of the motions; 4. possible errors in measuring the output of the standard pickup; and 5. variations in the voltages of the batteries supplying the amplifiers.

To a first approximation, the output of each seismometer was proportional to the cosine of the angle between its axis and the direction of the driving force. Therefore, the sensitivity was changed by tilting the instrument. Near the direction of maximum response the sensitivity changed slowly; but near the

direction of minimum response the reverse was true. Thus a slight misalignment had little effect on the response in the proper direction, but greatly increased the sensitivity to motion at right angles to this.

The horizontal instruments were so constructed that, when they lay flat the coils were not free to move. Therefore, to keep the coils freely suspended, they had to be mounted with a tilt of approximately 2 1/3° from the horizontal. This is why the horizontal components were so much more sensitive to vertical motion than the vertical component was to horizontal motion.

During the calibrations a spirit level was used in setting up all the instruments; but in making observations in the field, the vertical instrument was leveled by eye, and the spirit level was used only for the horizontal instruments. The alignment of the horizontal instruments along directions toward the shot and transverse to that direction was also done by eye. The result was that no component was completely independent of motion in the other two directions.

The amplitudes of the records were measured by drawing lines tangent to the crests and troughs of the recorded traces, and measuring the distances between these lines to the nearest hundredth of an inch. On the calibration records this amplitude was about one inch except outside of the pass band of the amplifiers,

where it sometimes decreased to as little as 1/20 of an inch. In the records from explosions the amplitude between successive peaks and troughs was in most cases between 1/5 and 2½ inches. Therefore, except at frequencies rarely encountered in this investigation the accuracy of the actual measurements of the records was good.

However, as these traces were not sinusoidal in shape, a large amount of uncertainty was introduced, since the trace amplitude depended greatly on how the amplitudes of components of ground velocity of different frequencies added. It must be remembered that because of the frequency discrimination of the system, most frequencies were suppressed on the records, and only those lying within a narrow band recorded with sufficient amplitude to be measured.

The frequency of the motion was determined by measuring the period between successive peaks or troughs on the records using the 1/100 second timing lines. For the shaking table calibrations this method was very accurate, as the motion was sinusoidal. In the observations of ground motion, on the other hand, the periods thus obtained were dependent on the phase relations between the various frequency components present in the motion, and large errors were possible. Since much of the measured motion had "periods" determined in this fashion of more than 1/4 second,

they corresponded to parts of the response curves where the gain was varying with frequency, and appreciable error would be introduced by computing the amplitude of motion for the wrong frequency.

Thus the measurements of amplitude made in this investigation, though good for comparison with each other where the frequency is within the pass band of the amplifiers, or where it is alike, are not of great absolute accuracy.

The output of the standard pickup was measured with a Ballantine Vacuum Tube Voltmeter which could easily be read to the nearest half decibel. However, the absolute accuracy of this instrument is unknown, so that the absolute magnitude of the ground motion is also unknown. On the other hand, the relative magnitudes at the different frequencies could be accurately measured except below 10 cycles per second. At these frequencies the needle of the voltmeter was inadequately damped, and vibrated at the frequency being studied. Therefore, at low frequencies it was necessary to depend on the doubtful linearity of the driving mechanism to obtain a calibration curve.

Three batteries were used to supply each channel. Two 45 volt dry batteries supplied the plate and screen voltages. The voltage of these batteries was not observed to change during the whole series of experiments.

Storage batteries were used to supply the filament voltage, and they were recharged before each day's observations. Therefore, there is no reason to suspect that variation in battery voltages caused variations in the sensitivity of the apparatus during the experiments.

Indicial admittance of the seismographs.

Another way to study the response of the apparatus is to examine its indicial admittance, or response to a "step wave" input. A typical response of this sort for one channel is illustrated in figure 8. The indicial admittance for filter position F-W, which is not shown, is almost identical with that for position F-80. The indicial admittance can be obtained in several ways. The ideal way is to give the seismometer a small mechanical displacement, photographically recording the output of the amplifier in the usual way. If the mechanical displacement is of the form of a step wave, this gives the true indicial admittance. However, it is difficult to produce mechanically a true step wave motion. Electrically it is easy, since this can be done by simply introducing a sudden change of voltage across the input of the circuit whose response is being studied. To obtain the indicial admittances shown, the electrical "equivalent" circuit of the seismometer was constructed, and a small voltage

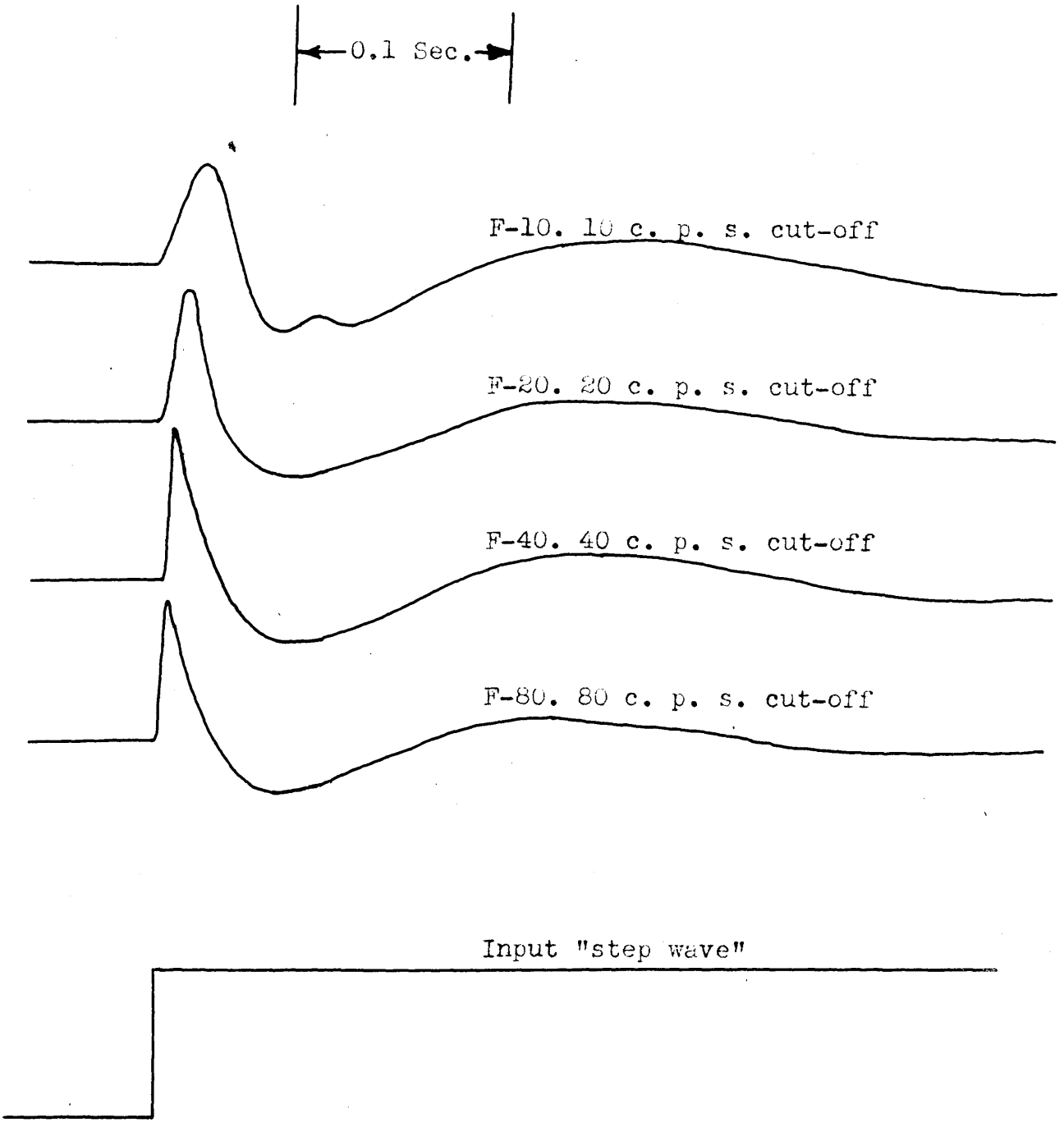

Indicial admittance of one of the recording seismographs used in this survey. The response includes the effect of the seismometer, amplifier, and galvanometer.

Figure 8.

introduced in series with the "equivalent coil" of the instrument, as shown in figure 9. (This produces the same response as suddenly giving the real seismometer a constant velocity).

The indicial admittance is a measure of the response of the recording apparatus to any type of pulse of motion. Since any pulse can be looked upon as a sum of step waves of different sizes and phases, the response of the system can be found by adding replicas of the indicial admittance of appropriate size and in proper phase relationship. Since the energy received from an explosion consists of a series of pulses, a knowledge of the shape of the indicial admittance is desirable to get some idea of the shape of the ground motion before it has been reshaped by transmission thru the amplifier.

Amplitude control.

Since the maximum amplitude of ground motion resulting from an explosion decreases rapidly as one goes farther from the shot, some mechanism had to be provided to adjust the gain of the recording system so that the trace of the light spot stayed on the photographic paper. At distances up to 600 feet from the explosions, a resistive pad was placed across the seismometers, whereby only 1/100 of their output was fed to the amplifiers. At larger distances the two attenuators in the amplifiers were adequate to cover

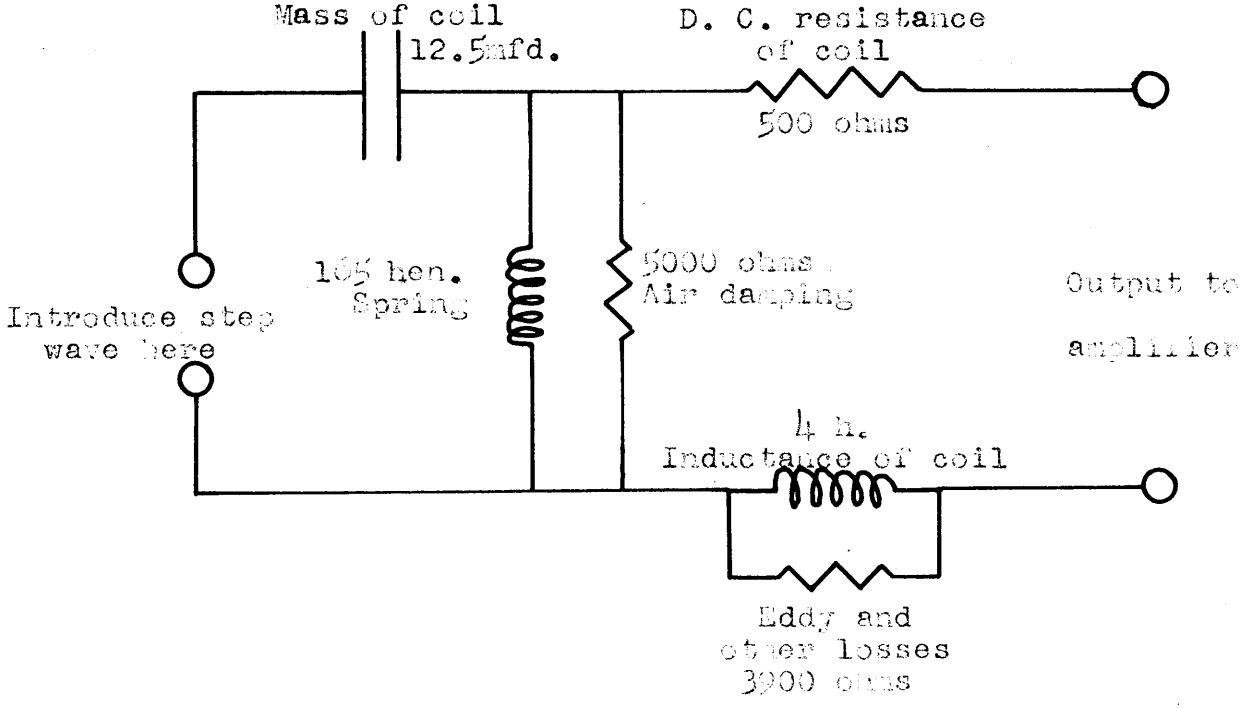

Equivalent circuit of seismometer.

Figure 9

the range of signals encountered. These attenuators are situated in the grid circuits of the first two stages of the amplifier, and consist of tapped resistors whereby the grids are fed only a fraction of the total input signal to that stage. These dividers were calibrated by measuring the relative amount of input signal required to give a constant spot deflection on the photographic paper for each tap on the divider as compared to a "standard" setting for which the frequency response calibration curves were made.

III. LOCATION OF THE SURVEY AND FIELD PROCEDURE.

The location where the records were taken lies near the center of the Los Alamitos, California, quadrangle of the United States Geological Survey, 42 kilometers southeast of Los Angeles. The exact location is shown on the map, figure 10. Measurements were taken at 14 different locations along an east-west line at from 97 to 3284 meters from the place where the explosions were set off. The distances from the shots to the recording locations were measured using a 100 foot steel tape. In all, 33 explosions were recorded here.

The seismometers were set on the surface, or half buried in the ground at the side of the road, or in a dry irrigation ditch about a meter deep. The rest of the recording apparatus was mounted in a truck provided with dark room and developing facilities, so that each record could be developed as soon as it was taken, and changes in the amplification or filtering made before recording the next explosion. The charges set off consisted of either $2\frac{1}{2}$ or 5 pounds of Hercules 60% Petrogel. The charges were being detonated in the course of routine testing of new seismic apparatus by the United Geophysical Company. The records were taken between October 1947 and February 1948, whenever such routine testing was being made so that explosions were available.

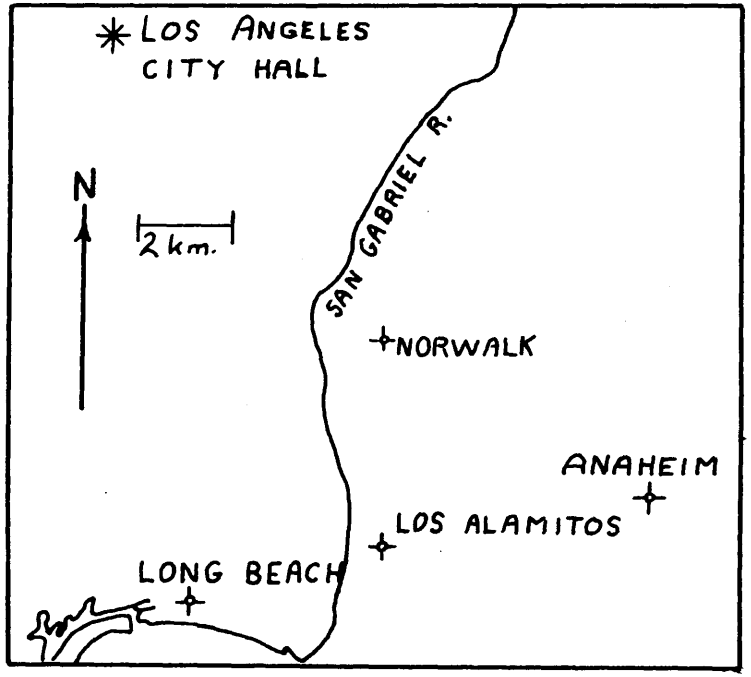

Map showing location where the measurements were made

Figure 10

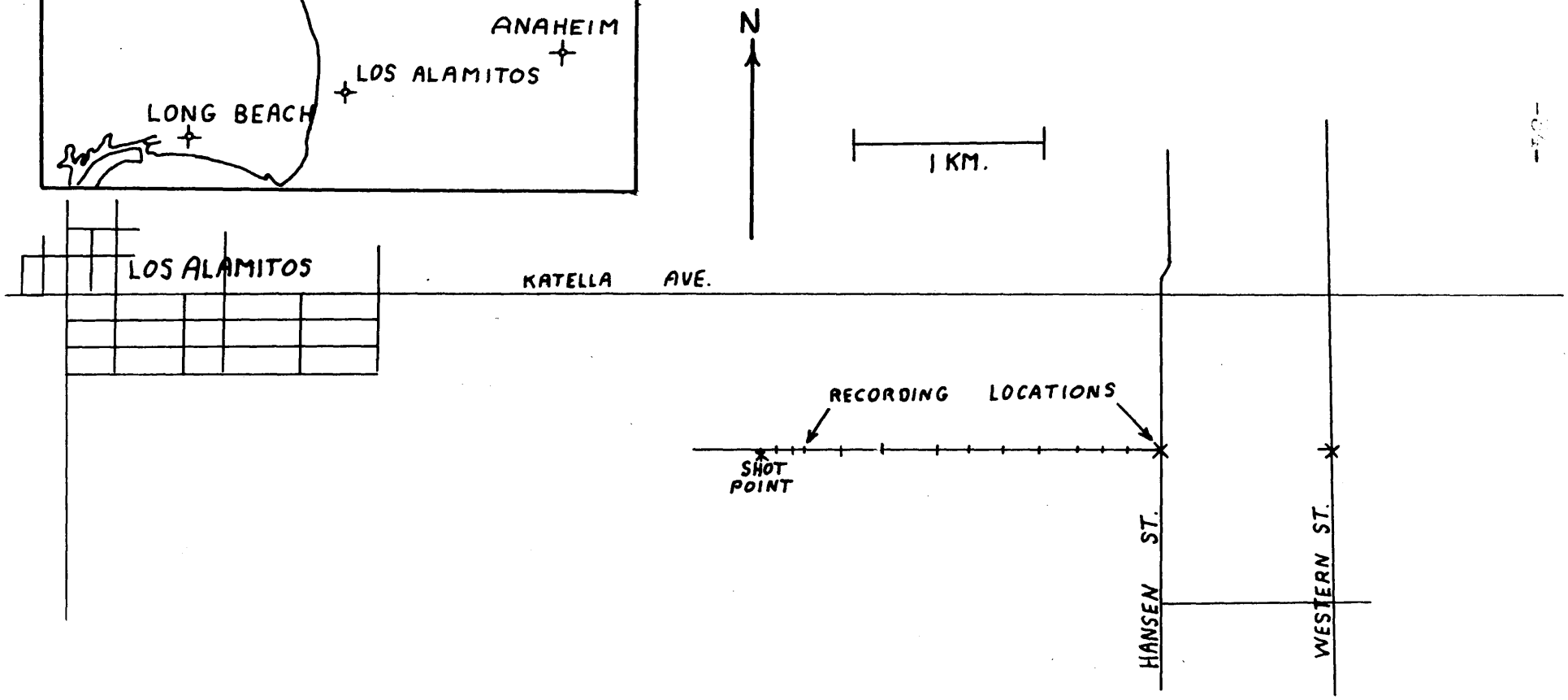

The explosions were detonated in different holes on different occasions, but all were within a radius of approximately 6 meters. The charges were fired at depths ranging from 6.7 to 12.5 meters.

Little detailed information is available on the geology of the district where this investigation was made. There are no surface outcrops of solid rock. The surface material is everywhere a fine grained clayey soil. The driller's log for the shot holes shows nothing but "sand-loam" except for "clay ledges" at 10.7 and 13.1 meters. Hoots (1932, plate 6, p.28 and figure 1, p.24) shows the surface rocks to be recent alluvium, probably overlying Pleistocene marine terrace and alluvial fan deposits of unknown thickness, possibly 500 meters or more. These deposits are believed to overlie a thick section of Tertiary marine deposits.

The water table is shallow, but varies, probably seasonally. When observed during loading of the dynamite into the holes it was at 3 meters.

IV. THE BODY WAVES.

The records.

Charts I-III are tracings of a selected group of the records taken. They are arranged in order of increasing distance from the shot. In each case the three traces represent from top of the group to the bottom, vertical motion, longitudinal motion, and transverse motion. An upwards deflection of the trace on the record corresponds to a downward velocity of the ground, a velocity away from the shot, or a velocity to the left as one stands at the recording position facing the shot. The sensitivities of the three channels are not identical, so the relative amplifications of the horizontal channels with respect to the vertical in decibels at 10 c. p. s. are given beside each horizontal trace. Positive values correspond to greater amplification in the horizontal channel, negative to lesser amplification.

To the left of each record is given the amplification of the vertical channel in db. also at 10 c. p. s. The units are millimeters peak-to-peak spot deflection on the paper compared to millimeters per second peak ground velocity. Also given are the nominal cut-off frequency of the high frequency filter, the distance from the shot to the recording station in meters, the size of the charge of explosive in pounds, and the

depth in meters beneath the surface at which it was detonated. Timing marks are given representing half second intervals following the shot. A correction for the time of the explosion before or after the first timing line is written beside it. ("+" corrections mean that the marked t_o is late,; "-" corrections mean it is early.)

Principal compressional waves.

Where the author has succeeded in correlating the separate pulses, a representative symbol is given above the beginning of that pulse. "P" as defined here is the first wave to arrive at the recording station regardless of by what path it travelled. It is a compressional wave, and it is always refracted. It arrives at the surface at angles of 28° or less with the vertical, in general decreasing as the distance from the shot increases, as shown in Table I (p.38). This steep angle of incidence suggests that the near surface material has a much lower compressional wave velocity than the deeper material, as would be expected.

From the travel time curve, Chart IV, it appears that the deepest layer to which any identified, refracted wave has penetrated has a compressional wave velocity of 1950 meters per second. Arrival times at short distances suggest that above this layer there is another layer whose compressional wave velocity is 1565 meters

Table I.

Angle of incidence of P at surface.

Distance from shot	Angle of incidence
97 meters	28°
478	22° Roughly
762	5° Roughly
1095	10°
1285	15°
1493	10°
1711	12°
2441	15°
3284	11°

per second. (See also figure 11.) Above this layer there must be a layer of even lower velocity material, since the average uphole velocity is much less than 1565 meters per second.

Layer thicknesses.

If we assume that we are concerned only with horizontal layers of constant thickness, we can use the data from figure 11 to investigate the thickness of the uppermost layer. Figures 12 and 13 are the ray paths of P for this case, figure 12 applying if the shot was

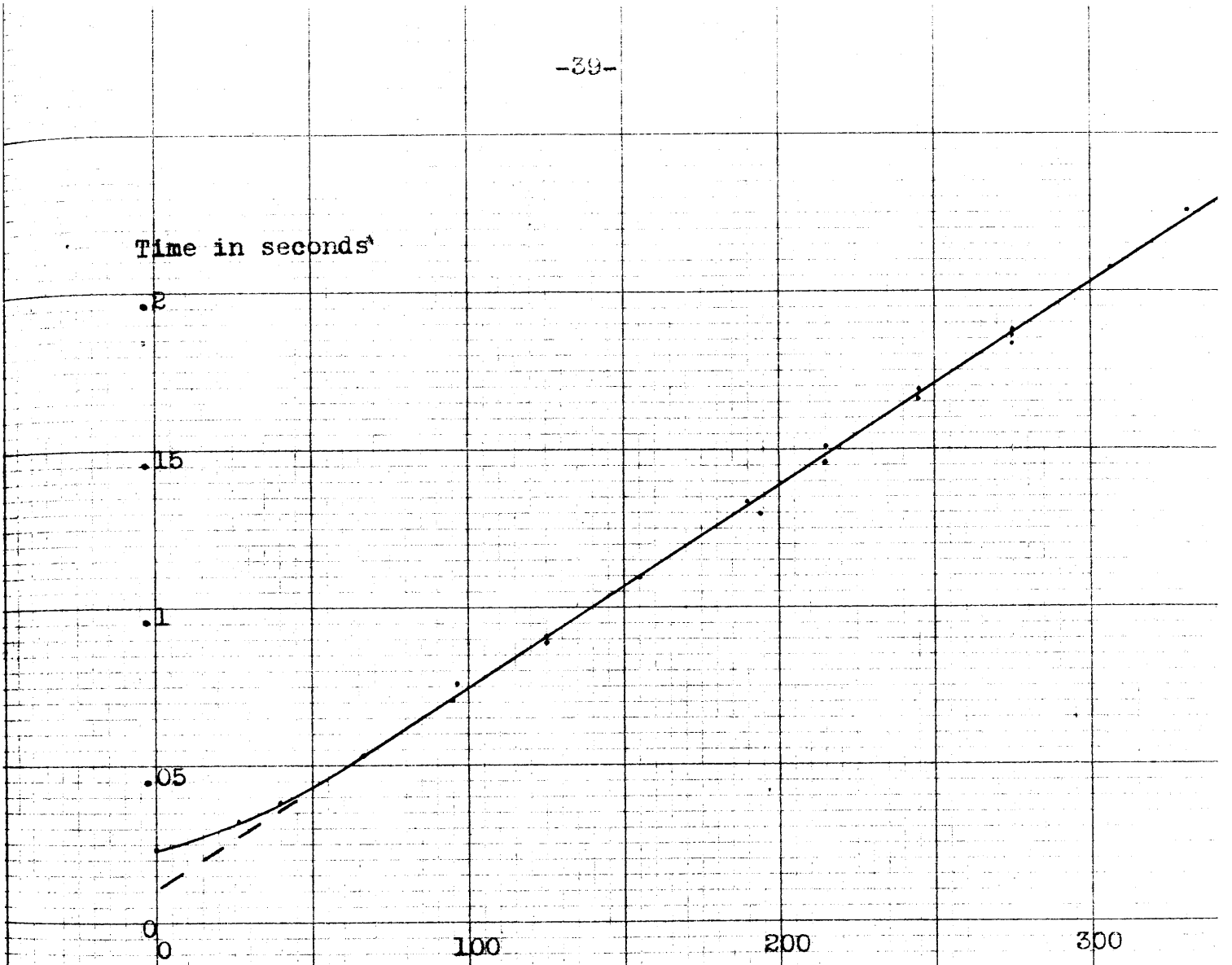

Arrival times of "P" out to 350 meters.

Figure 11.

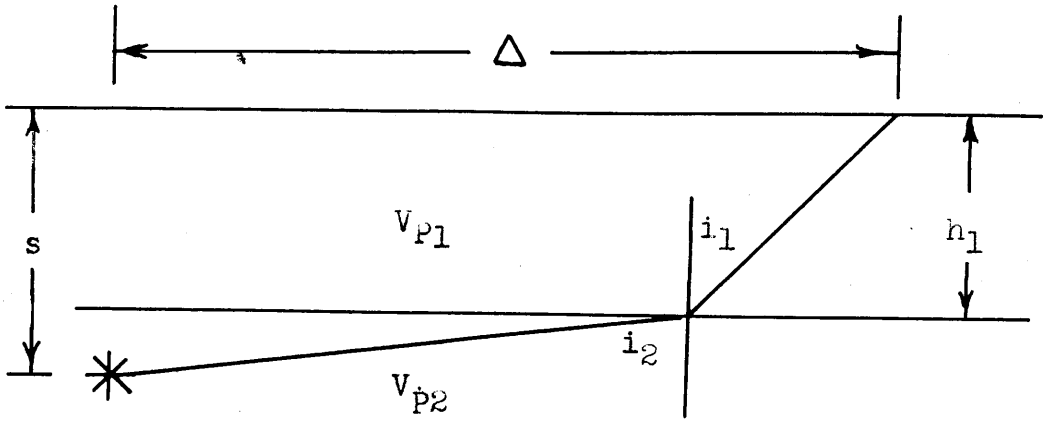

Ray path for explosion in second layer.

Figure 12.

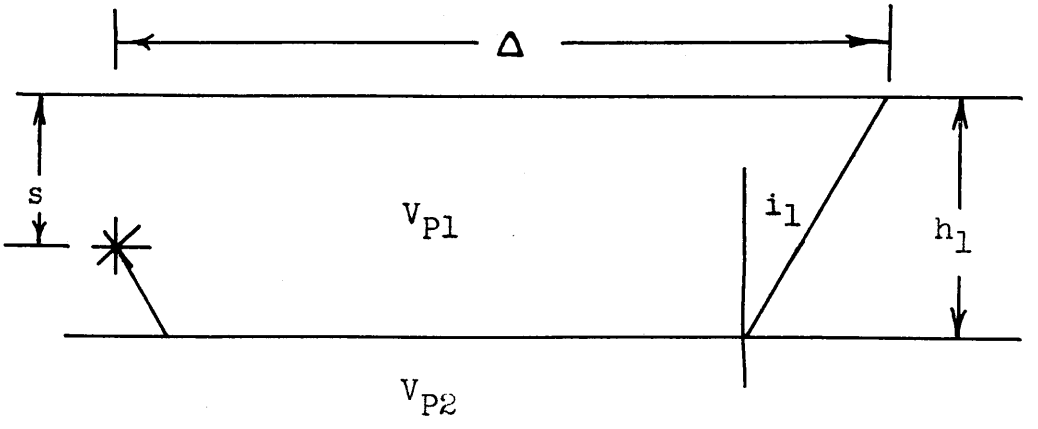

Ray path for explosion in first layer.

Figure 13.

detonated in the second layer; figure 13, if the shot was in the first.

If Δ is the distance along the surface of the ground from the explosion to the recording point, s is the depth at which the explosion occurs, h_1 is the depth of the uppermost layer, i_n is the angle of incidence of the recorded ray in the nth layer, T is the time required for the explosion to travel to the recording point, V_{Pn} is the compressional wave velocity in the nth layer, and the explosion takes place in the second layer, then:

$$T_\Delta = \frac{\Delta - h_1 \tan i_1}{V_{P2} \sin i_2} + \frac{h_1}{V_{P1} \cos i_1} \qquad (4\text{-}1)$$

For $\Delta \gg s$, $\sin i_2 \approx 1$, and (4-1) becomes:

$$T_\Delta = \frac{\Delta - h_1 \tan i_1}{V_{P2}} + \frac{h_1}{V_{P1} \cos i_1} \qquad (4\text{-}2)$$

In this case Snell's law states:

$$\sin i_1 = \frac{V_{P1}}{V_{P2}} \qquad (4\text{-}3)$$

The tangent to the travel-time curve for large Δ's will intercept the time axis at a value $T = T_0$. Since equation (4-2) is the equation of this straight line, we can say:

$$T_0 = -\frac{h_1 \tan i_1}{V_{P2}} + \frac{h_1}{V_{P1} \cos i_1} = \frac{h_1}{\cos i_1}\left(\frac{1}{V_{P1}} - \frac{\sin i_1}{V_{P2}}\right) \qquad (4\text{-}4)$$

Substituting (4-3) into (4-4) we get:

$$T_0 = \frac{h_1}{\cos i_1}\left(\frac{1}{V_{P1}} - \frac{V_{P1}}{V_{P2}^2}\right) = \frac{h_1}{\cos i_1}\left(\frac{V_{P2}^2 - V_{P1}^2}{V_{P1} V_{P2}^2}\right) \qquad (4\text{-}5)$$

But (4-3) is equivalent to:

$$\cos i_1 = \left[1 - (\sin i_1)^2\right]^{1/2} = \frac{(V_{P2}^2 - V_{P1}^2)^{1/2}}{V_{P2}} \tag{4-6}$$

And therefore:

$$T_o = h_1 \frac{(V_{P2}^2 - V_{P1}^2)^{1/2}}{V_{P1} V_{P2}} \tag{4-7}$$

If we solve this for V_{P1} we get:

$$V_{P1} = \frac{h_1 V_{P2}}{(T_o^2 V_{P2}^2 + h_1^2)^{1/2}} \tag{4-8}$$

If, on the other hand, the explosion takes place in the first layer, (4-1) becomes:

$$T_\Delta = \frac{h_1 - s}{V_{P1} \cos i_1} + \frac{\Delta - (h_1 - s)\tan i_1 - h_1 \tan i_1}{V_{P2}} + \frac{h_1}{V_{P1} \cos i_1} \tag{4-9}$$

and in the same manner as before:

$$T_o = \frac{2h_1 - s}{V_{P1} \cos i_1} - \frac{(2h_1 - s)\tan i_1}{V_{P2}} \tag{4-10}$$

Which is the same as (4-4) except that $(2h_1 - s)$ replaces h_1. Therefore, (4-8) becomes:

$$V_{P1} = \frac{(2h_1 - s) V_{P2}}{\left[T_o^2 V_{P2}^2 + (2h_1 - s)^2\right]^{1/2}} \tag{4-11}$$

From figure 11 we see that T_o equals .010 sec. and V_{P2} = 1565 meters per second. Using these values equations (4-8) and (4-11) are the relations which V_{P1} and h_1 must satisfy to give the travel-time curve of figure 11. This relation is plotted in figure 14.

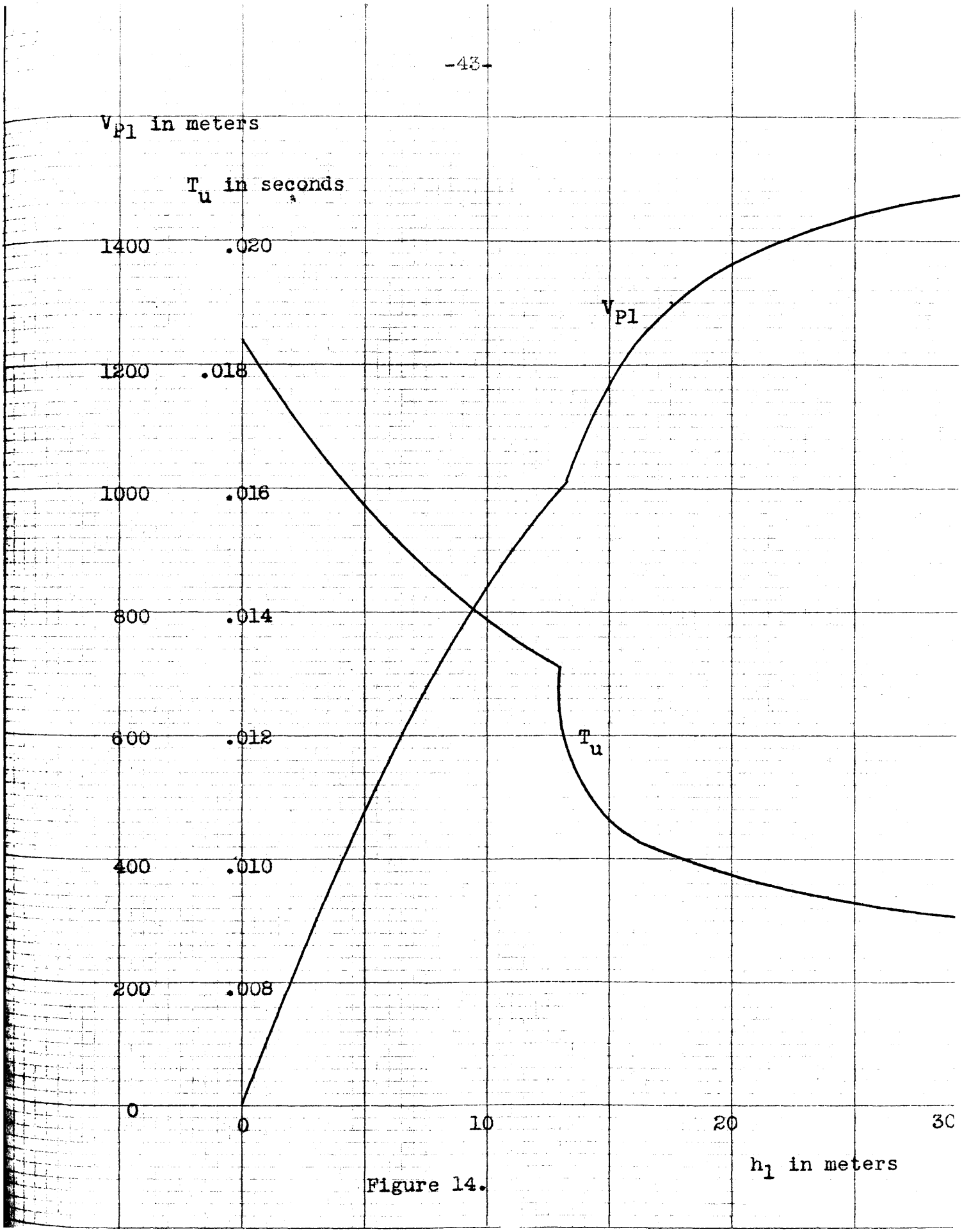

Figure 14.

Values of V_{P1} and uphole time, T_u, for different thicknesses, h_1, of the uppermost layer which will give the travel-time curve of figure 11 at large distances from the shot.

Figure 11 was made using an explosion at 13.1 meters depth. Using V_{P_2} of 1565 m/s., and the values of V_{P1} and h_1 from figure 14, we can calculate the uphole time, T_u, which the sound of the explosion would take to reach the surface from 13.1 meters depth using the formulas:

$$T_u = \frac{h_1}{V_{P1}} + \frac{s - h_1}{V_{P2}} \qquad \text{if } h_1 \leq s \qquad (4\text{-}12)$$

$$T_u = \frac{s}{V_{P1}} \qquad \text{if } h_1 \geq s \qquad (4\text{-}13)$$

The values of T_u found in this manner are also shown in figure 14. T_u should lie between .00838 sec. for very large h_1 and .01838 sec. for $h_1 = 0$. However, the observed T_u was actually .023 seconds. There is no reconciling this data under the assumption of uniform, horizontal formations. We must, therefore, conclude either that the uppermost layer was thicker at the shot point than at the recording point, that the velocity of compressional waves in our formations changes laterally, or that our assumption of only two layers is too simple a picture.

Since the travel-time curve strongly suggests the existence of a second layer with a uniform compressional wave velocity of 1565 m/s., perhaps our difficulty arises out of some error in our assumptions as to the simple nature of the first layer.

This is not unlikely. It is common knowledge that

at most places very near to the surface there exists a layer of material in which the seismic wave velocities are relatively very low. This layer is thought to be in some fashion related to the layer of material lying above the water table, where the rocks are decomposed or decomposing, and the pores filled with air instead of water. It is known as the "weathered" layer. The weathered layer is often variable in thickness and in its elastic constants from place to place. Such a variation may explain the inconsistency of the observed and calculated uphole times. It could also explain the late arrivals of P at distances between 2106 and 2441 meters.

It is also likely that in the weathered layer the velocity of compressional waves increases with depth from the surface to the bottom of the layer. This velocity distribution may in itself be enough to account for the large uphole time.

There is, however, another likely explanation. A great many explosions had previously been detonated in the same hole before the one which was used to make the records from which figure 11 was made; and as a result of this, the ground had been very much disturbed. It is possible that the uphole time was greater than it would otherwise have been as a result of this. Hence, none of the uphole times taken at the shot location are dependable for calculating layer thicknesses. Explosions

at 21.3 meters depth detonated about 1/3 kilometer from the shot location under consideration had uphole times of .023 to .024 seconds. If we assume that all of the material below 13.1 meters has a compressional wave velocity of 1565 m/s., and that there are only two layers above 21.3 meters, then the pair of values of h_1 and V_{P1} in figure 14 which will give an uphole time of .023 sec. for a shot depth of 21.3 meters is $h_1 = 1.2$ meters and $V_{P1} = 120$ m/s.

Another approach is to consider what velocity in the first layer would give the observed angle of incidence at the surface. The angle of incidence at $\Delta = 97$ meters is, from table 1, 28°. From (4-3) we find that for $V_{P2} = 1565$ m/s. and $i_1 = 28^\circ$, $V_{P1} = 735$ m/s. Similarly at $\Delta = 478$ meters, $i_1 = 22^\circ$, giving $V_{P1} = 586$ m/s. However, the first compressional wave arriving at 478 meters may have penetrated deeper than the second layer. If $V_{P1} = 735$ m/s., we find from figure 14 that $h_1 = 8.4$ meters, while if $V_{P1} = 586$ m/s., $h_1 = 6.3$ meters. In loading the dynamite into the shot hole, it was found that the water table lies at 3 meters depth. Thus considering all the evidence, it appears probable that our explosion was detonated in a second layer whose compressional wave velocity is 1565 m/s. lying beneath a first layer, whose thickness most likely is between 1.2 and 8.4 meters, and whose compressional wave velocity

most likely is between 120 m/s. and 735 m/s.

At distances greater than 600 meters from the shot the first compressional waves to arrive have penetrated to a layer whose compressional wave velocity is 1950 m/s. The time of arrival of this wave is given by the formula:

$$T_\Delta = \frac{h_1 + h_2 - s}{V_{p2}\cos i_{23}} - \frac{\Delta - (h_1 + h_2 - s)\tan i_{23} - h_2 \tan i_{23} - h_1 \tan i_{13}}{V_{p3}}$$

$$+ \frac{h_2}{V_{p2}\cos i_{23}} + \frac{h_1}{V_{p1}\cos i_{13}} \qquad (4\text{-}14)$$

The symbols are the same as those used previously except that we now use i_{nm} for the angle of incidence in the nth layer of the ray whose deepest penetration is the top of the mth layer. h_n is the thickness of the nth layer. Figure 15 shows the ray path of a ray whose deepest penetration is the third layer.

(4-14) can be solved giving:

$$h_2 = \frac{T_\Delta + \frac{s - h_1}{V_{p2}\cos i_{23}} - \frac{\Delta + (s - h_1)\tan i_{23} - h_1 \tan i_{13}}{V_{p3}} - \frac{h_1}{V_{p1}\cos i_{13}}}{\frac{2}{V_{p2}\cos i_{23}} - \frac{2\tan i_{23}}{V_{p3}}} \qquad (4\text{-}15)$$

We now use Snell's law in the form:

$$\frac{\sin i_{nm}}{V_n} = \frac{1}{V_m} \qquad (4\text{-}16)$$

From chart IV we see that for Δ = 2441 m., T = 1.342 sec., V_{P3} = 1950 m/s. We know that V_{P2} = 1565 m/s., and for this explosion s = 12.2 meters. From (4-16):

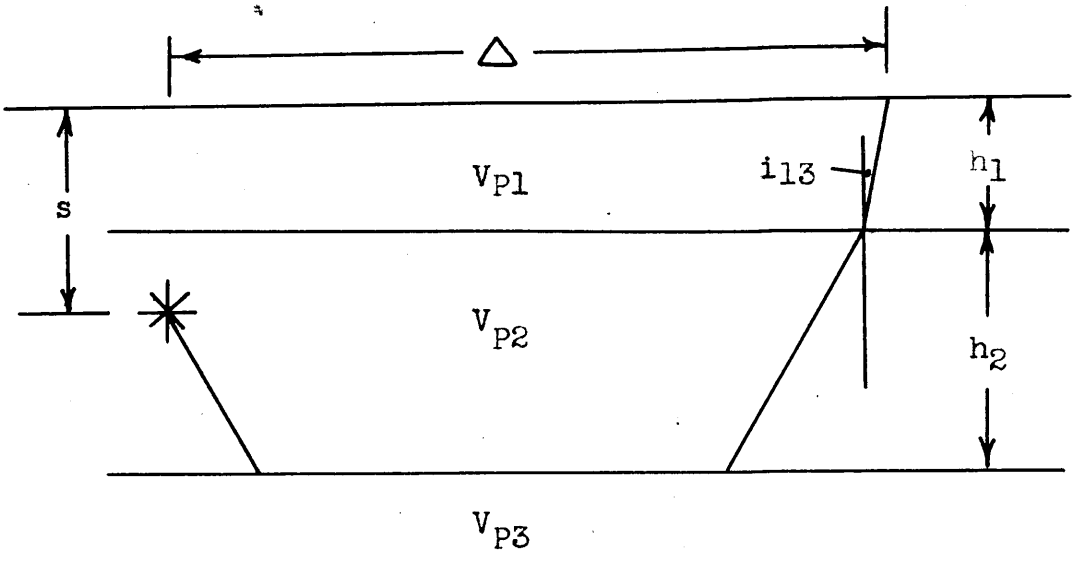

Ray path when ray penetrates to third layer.

Figure 15.

if V_{P1} = 120 m/s., h_1 = 1.2 meters, then h_2 = 29 meters.

if V_{P1} = 735 m/s., h_1 = 8.4 meters, then h_2 = 106 meters.

At 2441 meters the observed angle of incidence was 15°. Using equation (4-16) we find that this corresponds to a value of V_{P1} of 505 m/s., which is within the range of values we have found for the first layer.

Our best estimate, therefore, as to the structure of the Los Alamitos area is that there is a weathered layer between 1.2 and 8.4 meters thick whose compressional wave velocity lies between 120 m/s. and 735 m/s., a second layer between 29 and 106 meters thick whose compressional wave velocity is 1565 m/s., and a third layer of unknown thickness whose compressional wave velocity is 1950 m/s.

Other body waves.

Following P on the records are a number of more obscure pulses, several of which can, however, be correlated on a large percentage of the records. There are also a number of other pulses which represent arrivals of some sort of seismic disturbance, but which can not be correlated from one record to another. The four pulses which were correlated are marked on the travel-time curves, chart IV, together with a few of the more prominent non-correlatable pulses. These four

are also marked on charts I-III. Unfortunately, the beginnings of the pulses are not distinct, so the data are too inaccurate to use for detailed calculations of subsurface relations, or even to determine accurately the velocities of these seismic waves.

The first of the four pulses is labeled "P_3". It appears to be in general similar to P in the nature of its motion. It is probably a refracted compressional pulse which has penetrated deeper than P.

Next to arrive is "X_1". This pulse, and "X_2" and "X_3" which follow, can be recognized on all the components, but usually not clearly on all three on any one record. X_1 is often a prolonged oscillation, so it may be a combination of several pulses. X_1 commonly has a vertical component, but X_2 and X_3 are normally recognizable only on the horizontal components. They are probably body waves penetrating beneath the third layer. One or more of them may be shear waves.

V. DISPERSED WAVES ON THE LONGITUDINAL COMPONENT.

Description of the pulse.

The next group of waves to arrive, which start with the emergent pulse marked "C" on the records, consists of motion predominantly in the longitudinal direction (figures 16 and 17). There is some motion also on the vertical component at short distances. Simultaneously with the arrival of C on the longitudinal and vertical is a train of waves arriving on the transverse. That these are two separate wave trains is made clear by the lack of correlation of the periods of the two motions.

It should be noted that the motion illustrated by figures 16 and 17 and the other diagrams like them which follow is given in terms of velocity, not displacement, so the diagrams do not give a true picture of the particle path. For a sine wave the relations between the horizontal and vertical components of the frequency and displacement are identical at any one frequency, but there is a relative phase shift between different frequency components in the two cases, and a frequency factor in the expression for the amplitude. Since the pulses recorded are the sum of many frequency components, the shape of the particle path will be different from what is shown in the figures, although these diagrams do give an indication of the nature and direction of the particle motion during the passage of the pulse.

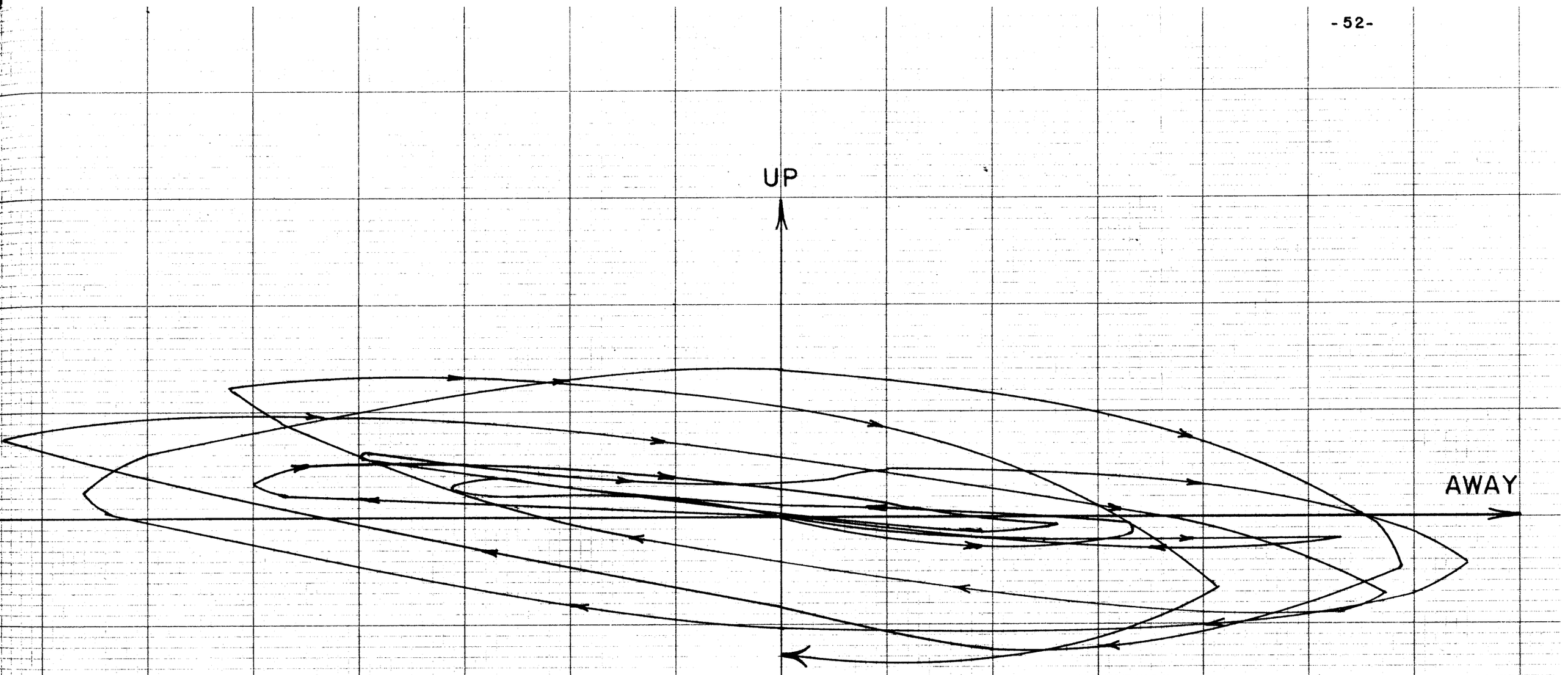

GROUND VELOCITY IN A VERTICAL PLANE DURING THE ARRIVAL OF C AT 1285 METERS FROM AN EXPLOSION

.0095 MM./SEC.
PEAK GROUND VELOCITY

FIGURE 16

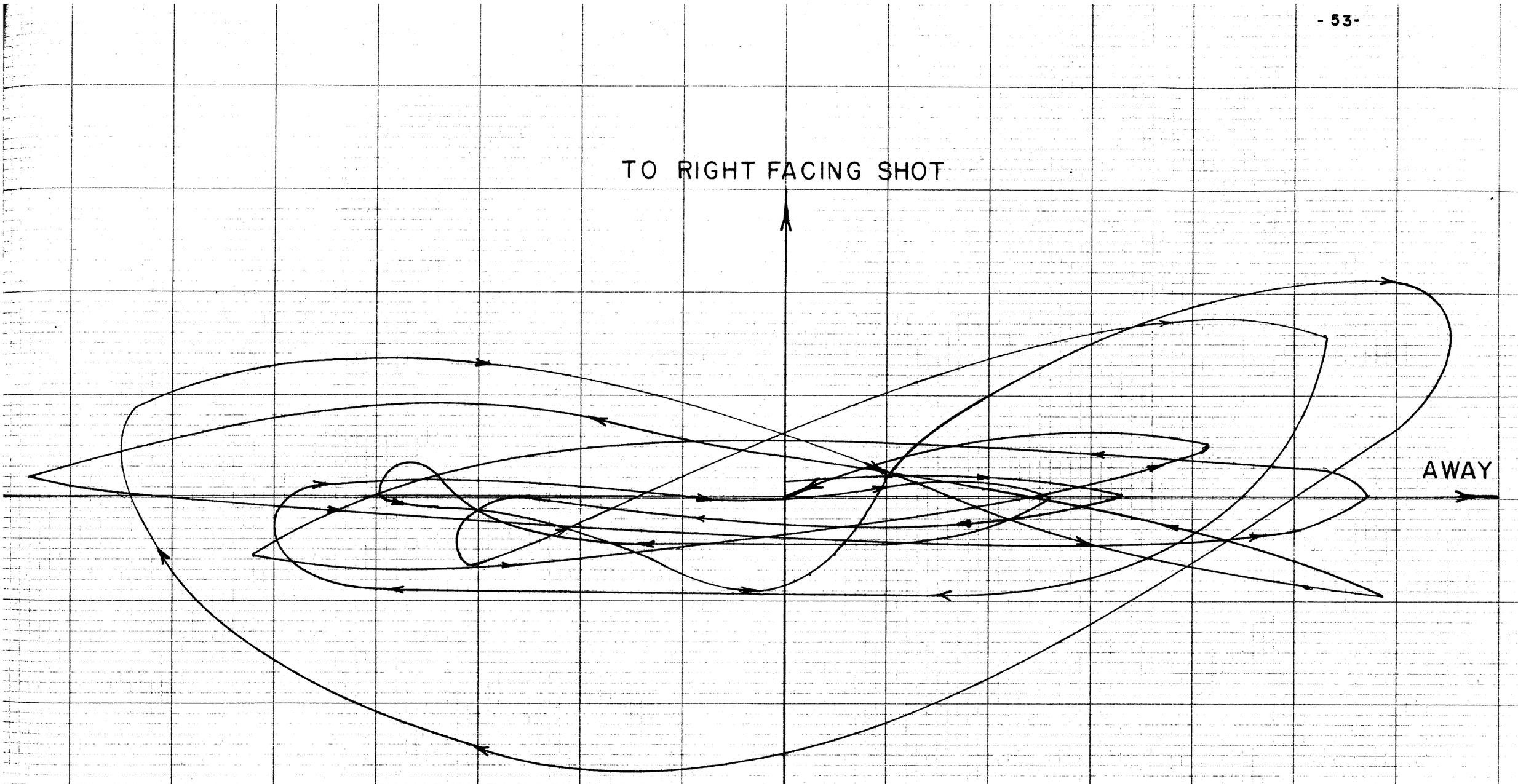

GROUND VELOCITY IN A HORIZONTAL PLANE DURING THE ARRIVAL OF C AT 1285 METERS FROM AN EXPLOSION

.0095 MM. /SEC.
PEAK GROUND VELOCITY

FIGURE 17

The beginning of C is not clear, being recognizable only by a gradual growth in amplitude of the ground motion, especially at low frequencies. In general the average amplitude increases throughout the time of arrival of this pulse, building up to a series of maxima, with lower amplitudes in between. These maxima can sometimes be correlated on records taken at successive distances, but can never be correlated continuously over long distances. A number of such correlations are shown in Chart IV. Their pattern is that of group velocity showing that unquestionably C is dispersed.

To demonstrate the dispersion the times of arrival of all of the outstanding maximum away-from-the-shot velocities of C have been plotted. The last C motion commonly includes a series of strikingly large maxima marked C_{M1}, C_{M2} and C_{M3} on charts I-III and CM on Chart IV. It is clear that these maxima do not correlate throughout the record. In general they belong to a family of group velocity correlations in which the maximum amplitude migrates to later and later correlations as one gets farther from the source of the waves.

Following the last recognized C motion, a line can be roughly drawn which represents the minimum recorded phase velocity of C, just as the emergent pulse labeled C on the records is the observed maximum velocity phase. The period of this lowest velocity C wave, as measured from the records, lies between .22

and .31 seconds (figure 18). Since 4 cycles per second is the approximate cut-off frequency of the recording system, this may explain the abrupt decrease in amplitude at this point. The seismometer fails to respond to motion of lower frequencies. Figure 18 shows that the dispersion is one wherein the velocity decreases as the frequency decreases.

An interesting feature of C is that, like P, it seems to be refracted. Its travel-time curve appears to have two "legs" and possibly three. This is apparent both for the maximum and minimum velocities.

After attaining its largest amplitude on the longitudinal trace, C appears to terminate suddenly, or to decrease rapidly in amplitude. However, as a different type of motion has already begun on the longitudinal and transverse before C is ended, the suddenness of its cessation is not certain. This later arriving pulse will be discussed in section VI. The suddenness of the termination of motion of C suggests a minimum group velocity, such as observed by Jeffreys (1925) for both the Love and Rayleigh waves from earthquakes, and predicted from theory by Stoneley (1925) and others (for instance Press and Ewing, 1948). However, as pointed out above, this apparent minimum is very likely due to the lesser sensitivity of the seismograph below 4 cycles per second.

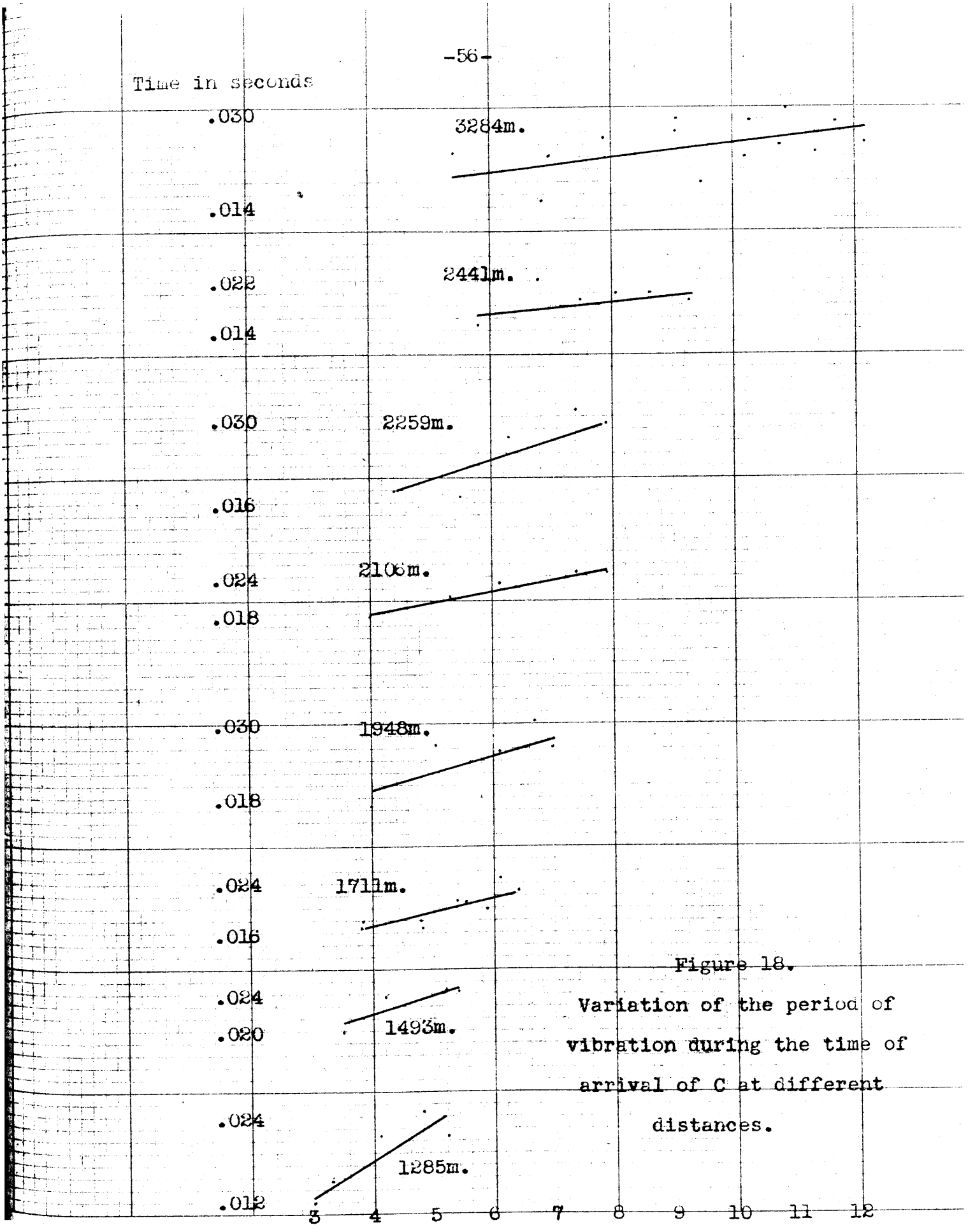

Figure 18.

Variation of the period of vibration during the time of arrival of C at different distances.

Nature of C.

The motion of the ground during the arrival of C is not that of any of the well known wave types of seismology. Seismic body waves do not exhibit appreciable dispersion, and seismic surface waves can not, by definition, be refracted. Therefore, we must conclude either that C is a different type of wave motion from those found and described in earthquake seismograms, or that the ground at Los Alamitos is in some way so different from that assumed by classical theory that under these conditions one of the well known body or surface waves will be modified to the type of motion observed. The wide variance of the rocks at Los Alamitos from those assumed by classical theory was discussed in the first section of this paper.

If the wave motion is a new type, for which the theory has not yet been worked out, then we must wait for the mathematical physicists to explain our observed phenomena. On the other hand, if the peculiarities of our data are a result only of the special conditions of the ground near the surface, then we can with profit seek to determine which of the already known types of wave motion most nearly resembles what we have observed.

C compared to described surface waves.

Since our waves are dispersed, the suggestion is strong that they are surface waves. But since the

motion is largely restricted to the longitudinal component, it resembles neither a Love wave in which the particle motion is in the transverse direction, nor a Rayleigh wave in which the particle motion is elliptical. Therefore, it is unlikely that the observed waves are related to either of these common types of surface waves.

In approaching the problem of what types of ground motion can be propagated the waves are usually assumed to be plane. If this limitation is dropped the problem becomes much more complex. Fu (1947) has considered the waves resulting from the incidence of spherically symmetrical compressional waves on an interface, and concluded that besides body and Rayleigh waves there result several other types including a compressional surface wave travelling with the velocity of the body shear wave, and falling off in amplitude as the square of the distance from the source of the energy.

The decrease in amplitude of such a wave would follow the formula:

$$A_n = A_o \frac{1}{\Delta_n^2} e^{-\alpha \Delta_n} \qquad (5\text{-}1)$$

where A_n is the amplitude of the vibrational velocity at distance Δ_n from the source of the waves, and α is the absorption coefficient. This can be written:

$$\frac{A_1 \Delta_1^2}{A_2 \Delta_2^2} = e^{\alpha(\Delta_2 - \Delta_1)} \qquad (5\text{-}2)$$

or:

$$\alpha = \frac{1}{\Delta_2 - \Delta_1} \log_e \frac{A_1 \Delta_1^2}{A_2 \Delta_2^2} \qquad (5\text{-}3)$$

Figure 19 is a plot of $A_n \Delta_n^2$ vs. Δ_n.
It is clear that the rate of decrease of the amplitude against distance is not as great as that required by Fu's theory, since the observed amplitudes would indicate that α was negative, an impossibility.

If C were an ordinary surface wave (5-1) would become:

$$A_n = A_o \frac{1}{\Delta_n^{1/2}} e^{-\alpha \Delta_n} \qquad (5\text{-}4)$$

and in the same manner as before the absorption would be:

$$\alpha = \frac{1}{\Delta_2 - \Delta_1} \log_e \frac{A_1}{A_2} \left(\frac{\Delta_1}{\Delta_2} \right)^{1/2} \qquad (5\text{-}5)$$

From figure 20 we see that in this case α is approximately equal to .0012.

Other types of surface waves were described by Uller (see Gutenberg, 1932, p.115-124), but no attempt has been made to correlate what was observed here with Uller's complicated wave mechanics.

C compared to body waves.

Since the ground motion is largely longitudinal, it could be caused by shear waves arriving close to vertically from below, or by compressional waves travelling in the upper layer nearly parallel to the

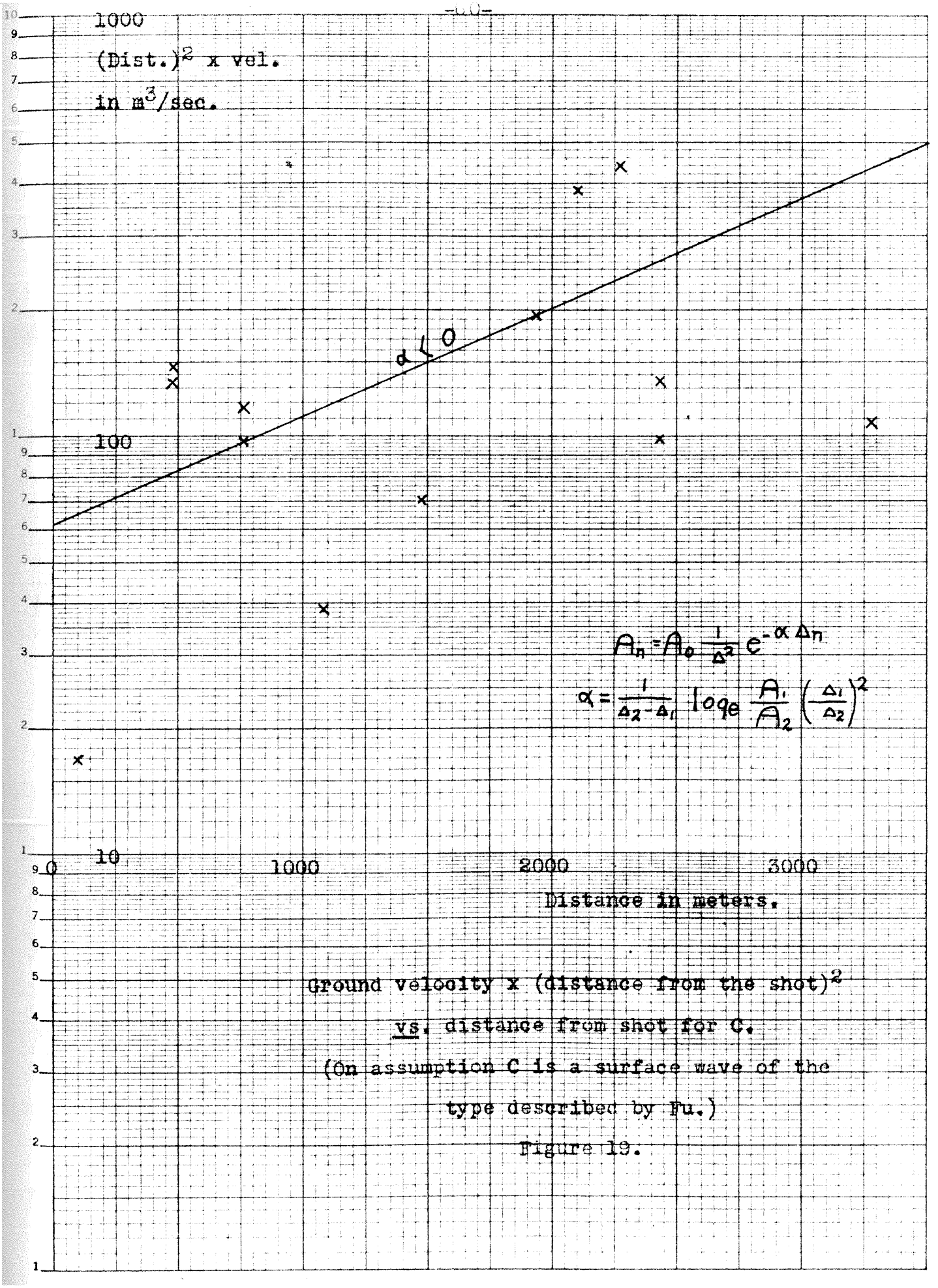

Ground velocity x (distance from the shot)²
vs. distance from shot for C.
(On assumption C is a surface wave of the
type described by Fu.)

Figure 19.

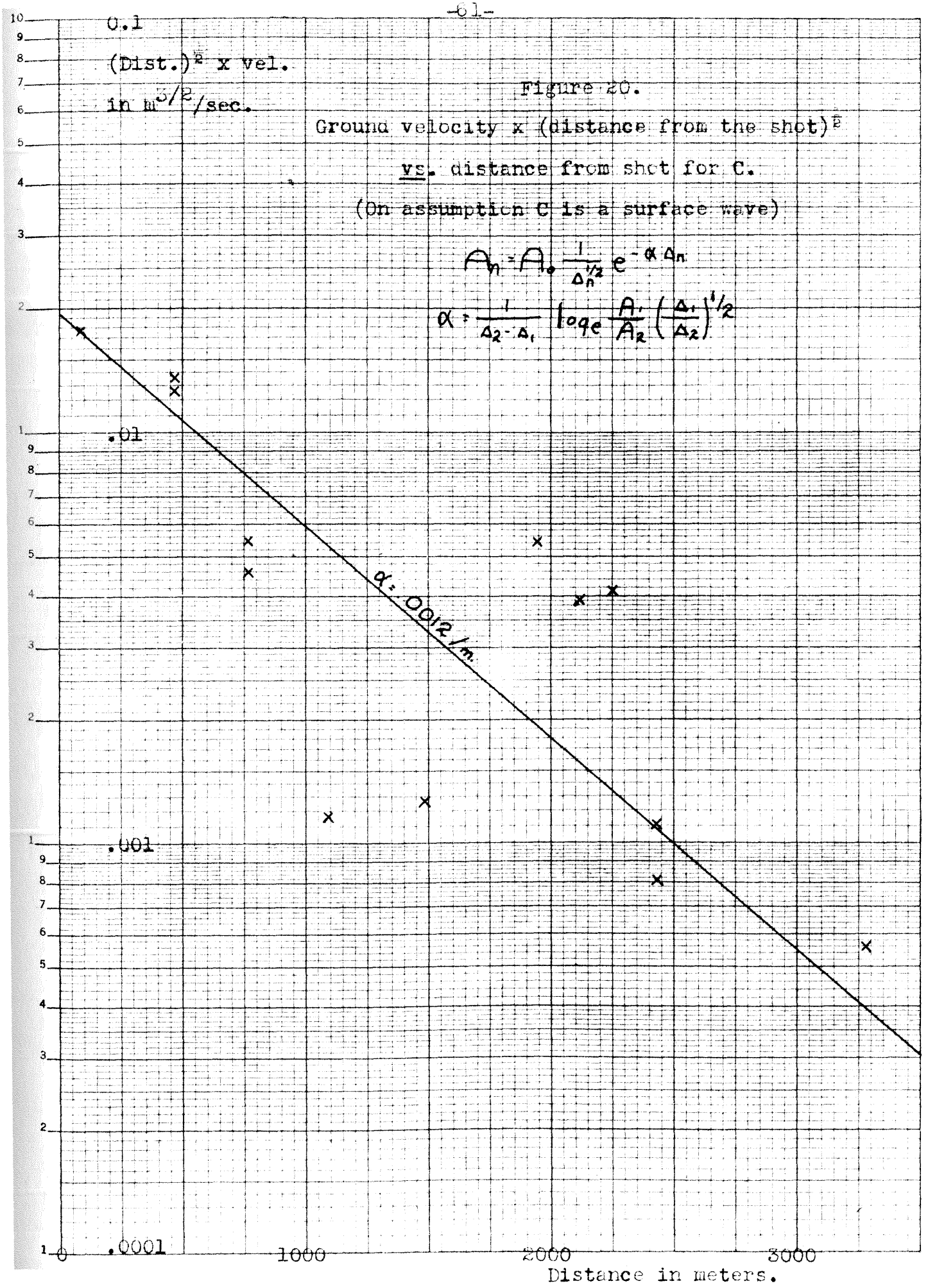

Figure 20.

Ground velocity x (distance from the shot)$^{\frac{5}{2}}$ vs. distance from shot for C.

(On assumption C is a surface wave)

$$A_n = A_0 \frac{1}{\Delta_n^{1/2}} e^{-\alpha \Delta_n}$$

$$\alpha = \frac{1}{\Delta_2 - \Delta_1} \log_e \frac{A_1}{A_2} \left(\frac{\Delta_1}{\Delta_2}\right)^{1/2}$$

surface, that is a train of waves coming directly from the shot location without passing thru the deeper layers. It might also be the sum of two waves of these kinds, which is the type of motion that corresponds to the degenerate solutions of Rayleigh's equation when the velocity of the surface waves exceeds that of the body waves. The equations for this case are developed in section VII. If Poisson's ratio is exactly zero, $V_R = V_p$, there is a compressional wave only, and no vertical component of motion at all. If the surface velocity, V_R, differs slightly from V_p the direction of particle motion makes an angle with the surface as indicated by equation (7-34).

The observed motion, though largely confined to the longitudinal, has an appreciable vertical component at short distances. If C is one pulse and not the sum of two, the angle of this motion with respect to the horizontal is such as to favor the view that C consists of longitudinally polarized shear waves, as shown in figures 21 and 22. The change of angle of incidence with distance might be a result of the deeper penetration of the waves recorded farthest from their source. It is not necessary that the explosion take place in the first layer as indicated in figure 22, as the surface motion at large distances will be similar even if the explosion occurs at greater depth.

Another noteworthy feature of C is that it often

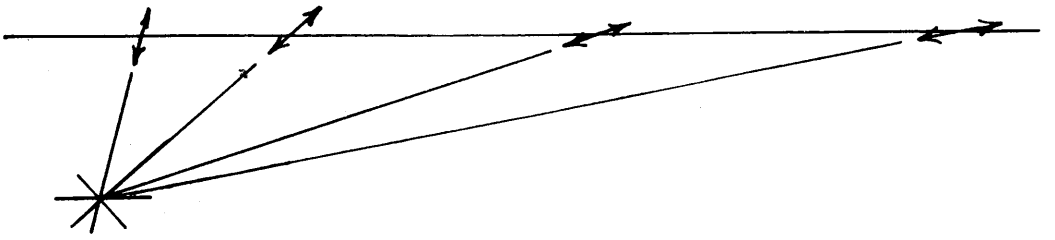

Direction of particle motion of direct compressional ray arriving at the surface. Near the shot the motion is up-away and down-toward the shot location. At large distances the vertical component vanishes.

Figure 21.

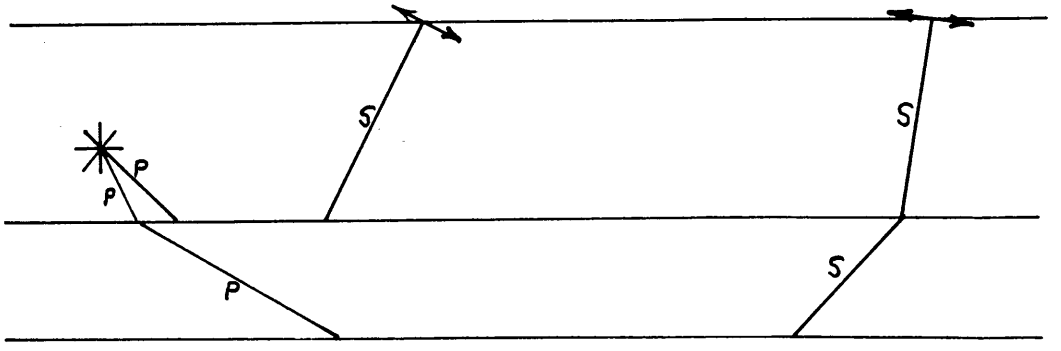

Direction of particle motion of refracted shear ray arriving at the surface. Near the shot the motion is down-away and up-toward the shot location. The deeper it penetrates the steeper its arrival at the surface.

Figure 22.

has the largest amplitude on the record, and since it also arrives during a longer interval of time than any other pulse it must carry the largest share of the energy of the explosion. This is surprising, as no shear wave would be expected to be generated by an underground explosion, as pointed out by Sharpe (1942). However, at each interface both a reflected and a refracted shear wave will be produced, the relative amplitudes depending on the angles of incidence (Gutenberg, 1944). At some angles the transverse refracted ray has the greatest amplitude. This is of particular significance near the surface where the wave velocities increase rapidly with depth, as then comparatively little energy will be transmitted into the lower medium, as shown in figure 23. Only waves arriving at the interface at angles no larger than the critical angle, i_c, will enter the lower medium. i_c is small if the velocity in the second medium greatly exceeds that in the first. At angles between the critical angle for compressional waves and that for shear waves, there will be a refracted transverse ray only; at larger angles, no refracted waves. Furthermore if the surface lies not far above the interface, when i_c lies between these two critical angles, the reflected P will soon again reach the interface after reflection from the surface, and at such an angle that more of its energy will be fed into the second layer as refracted

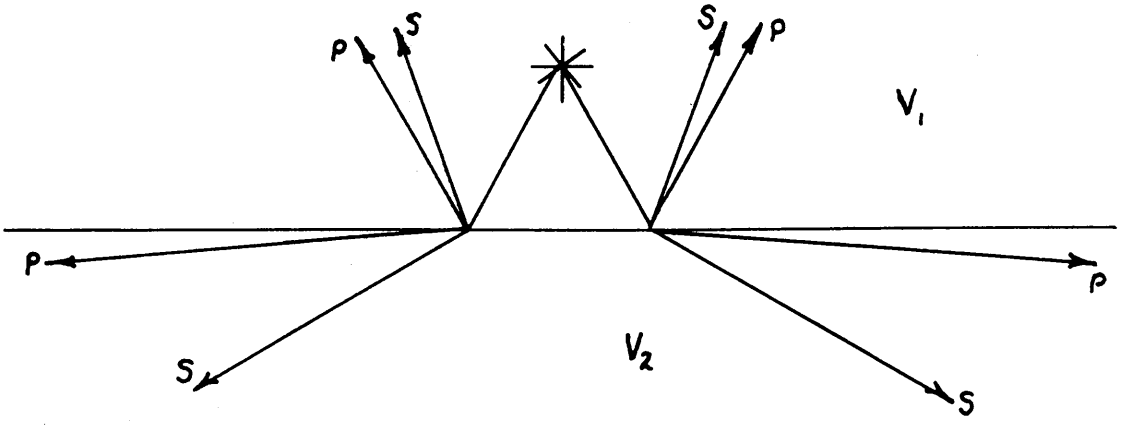

Division and spreading of an incident compressional ray at an interface where V_2 is greater than V_1.

Figure 23.

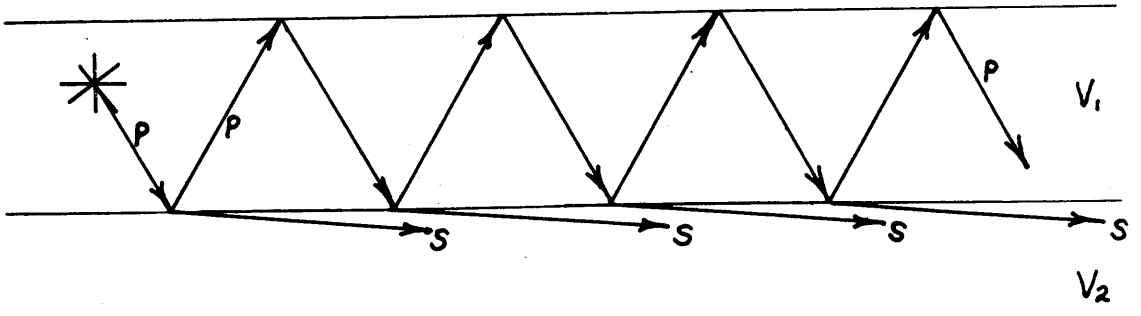

Loss of energy from a compressional ray confined to a superficial layer by refraction as shear rays in the underlying material.

Figure 24.

shear waves. This is shown in figure 24. These later generated shear waves will not arrive at a distant point simultaneously with the first refracted waves, but will result in a series of pulses of shear waves, or a long continuous sequence of shear waves. This is very like the motion of C. The phenomenon is related to the "multiple reflections" of exploration geophysics. (See for instance, Gutenberg and Fu, 1948.)

This suggests an explanation of why it is desirable to detonate the explosions of exploration geophysics beneath the low velocity layer, besides the reduction of surface wave amplitude. If the shot is not deep enough there may be a beam of strong direct compressional and refracted transverse waves arriving at the same time as the compressional reflections that are being sought. The surface waves, which have up till now been thought to cause most of the interference with seismic exploration, have periods largely much longer than one tenth of a second, as will be discussed later; but this is not necessarily true for the direct compressional and refracted transverse waves. Also the fanning out of the cone of waves entering the lower medium is avoided.

It is notable that C is longitudinally polarized. This is what would be expected if it owed its existence solely to the incidence of compressional waves on

horizontal or nearly horizontal interfaces, as theory predicts no transversely polarized waves in such a situation. The same applies to the absence of surface shear waves, as they must arise either from the initial disturbance of the surface by the explosion or from the incidence of compressional waves on the surface, and in both cases the motion would be radial from the explosion. Any waves originating at an interface as a result of a radial motion arriving at the interface should have particle motions lying in the plane which is perpendicular to the interface and contains the incident ray. The particle motion of transversely polarized shear waves is in a direction perpendicular to this plane.

We have seen that the particle motion is close to that of either a direct compressional wave or a refracted shear wave. The difficulty lies in the dispersed nature of the waves. In the case of surface waves, dispersion will result if the elastic constants of the ground near the surface change rapidly with depth. It is possible that if the elastic constants change sufficiently rapidly within a distance of one wave length in a direction parallel to the wave fronts of body waves, these waves will also be dispersed. As will be discussed in detail later, surface waves of the Rayleigh type were recorded at Los Alamitos,

and were dispersed, showing that the elastic constants do change rapidly with depth. There remains, however, the problem of proving theoretically that body waves can be dispersed in this manner.

Another way in which body waves might be dispersed is by absorption. Alexander Wood (1941, p.129-136) shows that absorption of sound waves in gases results in dispersion. In the notation of (5-1) the absorption for a body wave would follow the formula:

$$A_n = A_o \frac{1}{\Delta_n} e^{-\alpha \Delta_n} \qquad (5\text{-}6)$$

Or:

$$\alpha = \frac{1}{\Delta_2 - \Delta_1} \log_e \frac{A_1 \Delta_1}{A_2 \Delta_2} \qquad (5\text{-}7)$$

From figure 25 it follows that $\alpha = .00073$ per meter.

As pointed out above, the wave length of C is of the order of 90 meters. Therefore, for body waves α would be about .066 per wavelength, while for surface waves α would be about .11 per wavelength. In either case this is a very large absorption, though it is not necessarily enough to account for the dispersion.

Since α is so unusually large, the fact that it is smaller on the assumption that C is a body wave than on the assumption that it is a surface wave is in itself an argument in favor of C being a modified form of body wave. However, as will be shown later, the above values of α are not as great as the absorption

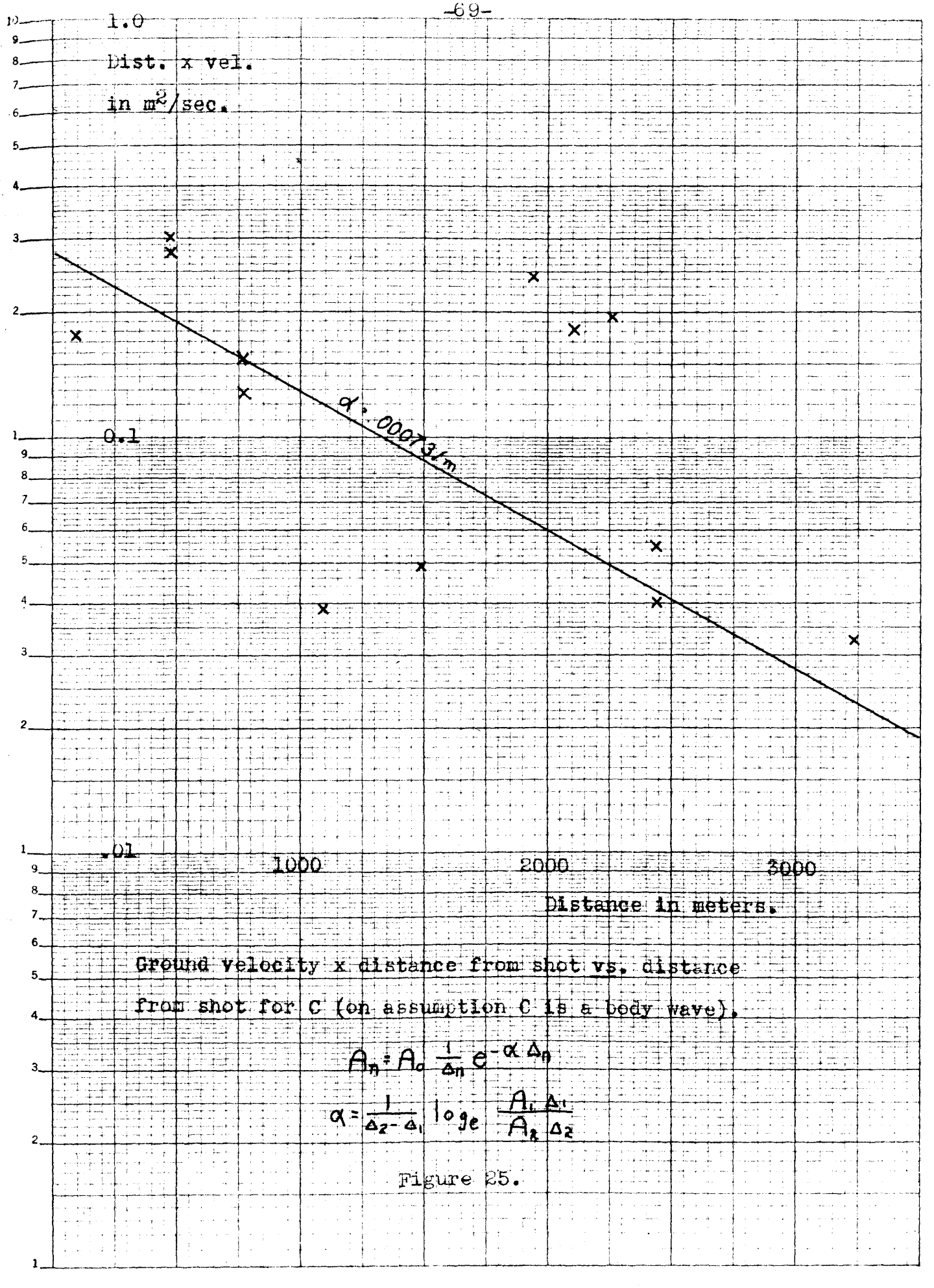

Ground velocity x distance from shot vs. distance from shot for C (on assumption C is a body wave).

$$A_n = A_o \frac{1}{\Delta_n} e^{-\alpha \Delta_n}$$

$$\alpha = \frac{1}{\Delta_2 - \Delta_1} \log_e \frac{A_1 \Delta_1}{A_2 \Delta_2}$$

Figure 25.

coefficient calculated for the observed Rayleigh waves in section VII.

Inferences as to layer thickness if C is a shear wave.

Although the forces generated by an explosion in the ground are presumably entirely radial, it is not completely certain that no shear waves would be generated in a medium whose nature is as little known as the outermost part of the earth's crust. It may be that C is simply a modified shear wave. If this is the case, it should be possible to check the thickness of the upper layers found in section IV using the velocities and arrival times of C as determined from the travel-time curves. Since C has both a maximum and a minimum velocity, we will use both sets of data. The two sets should give us about the same answer if they are the phase velocities of body waves transmitted at different speeds along the same paths.

We define V_{C_n} and V'_{C_n} as the maximum and minimum phase velocity of C in the nth layer. Otherwise our notation is the same as that of section IV. From the travel-time curves we get:

V_{C_1}	= 225 m/s.	V'_{C1}	= 163 m/s.
V_{C_2}	= 675 m/s.	V'_{C2}	= 275 m/s.
V_{C_3}	= 1225 m/s.	V'_{C3}	= 385 m/s.

For waves penetrating to the second layer only, where

the explosion is in the first layer, equation (4-10) holds. It can be rewritten:

$$T_o = \frac{2h_1 - s}{V_{c1}\cos i_1} - \frac{(2h_1 - s)\tan i_1}{V_{c2}} \qquad (5\text{-}8)$$

This can be solved for h_1 giving:

$$h_1 = \frac{1}{2}\left[s + \frac{T_o \cos i_1}{\frac{1}{V_{c1}} - \frac{\sin i_1}{V_{c2}}}\right] \qquad (5\text{-}9)$$

Where i_1 is defined by Snell's law as:

$$\frac{\sin i_1}{V_{c1}} = \frac{1}{V_{c2}} \qquad (5\text{-}10)$$

Using this relation (5-9) can also be written:

$$h_1 = \frac{s}{2} - \frac{T_o V_{c1} V_{c2}}{2(V_{c2}^2 - V_{c1}^2)^{1/2}} \qquad (5\text{-}11)$$

Similar formulas hold on substituting V'_{Cn} for V_{Cn}.

(5-11) unfortunately depends on the shot depth, s, which is not the same for all shots, varying from 8.2 meters to 12.1 meters. However, if we assume $s = 10.1$ meters for the purposes of calculation, not more than 1.05 meters error will be introduced in h_1. From the travel-time curves, chart IV, we see that for the minimum phase velocity of C, $T_o = .62$ sec. Using these figures equation (5-11) gives $h_1 = 79$ meters. For the maximum phase velocity of C, $T_o = .55$ sec., and $h_1 = 66$ meters. The average

of these two depths is 72.5 meters.

In section IV we estimated that the total thickness of the first two layers lay between 30.2 and 114.4 meters. Thus the value of h_1 calculated from the C wave velocities is not unreasonable if we assume that in this case the first layer corresponds to the first two layers of the previous case. Since the wave length of C exceeds the probable thickness of the first layer the pulse can not be expected to have a distinct path there.

The travel-time curve of C has also a third leg, so we can use the velocities determined from it to calculate the thicknesses of the third layer (figure 26). In this case:

$$T_\Delta = \frac{h_1 - s}{V_{c1} \cos i_{13}} + \frac{h_2}{V_{c2} \cos i_{23}} + \frac{\Delta - (h_1 - s)\tan i_{13} - 2h_2 \tan i_{23} - h_1 \tan i_{13}}{V_{c3}} \tag{5-12}$$

$$+ \frac{h_2}{V_{c2} \cos i_{23}} + \frac{h_1}{V_{c1} \cos i_{13}}$$

Snell's law becomes:

$$\frac{\sin i_{nm}}{V_{cn}} = \frac{1}{V_{cm}} \tag{5-13}$$

Solving (5-12) we find:

$$h_2 = \frac{T_\Delta - \frac{2h_1 - s}{V_{c1} \cos i_{13}} - \frac{\Delta - (2h_1 - s)\tan i_{13}}{V_{c3}}}{\frac{2}{V_{c2} \cos i_{23}} - \frac{2 \tan i_{23}}{V_{c3}}} \tag{5-14}$$

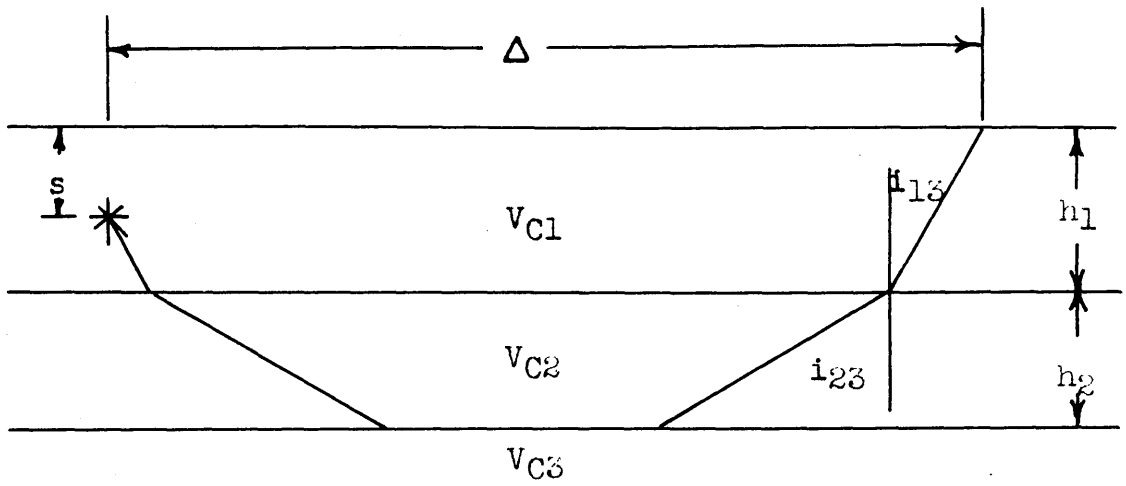

Ray path for shear wave whose deepest penetration is the top of the third layer.

Figure 26.

C arrives at 3284 meters from 5.100 sec. to 11.076 sec. from an explosion at 8.53 meters depth. Using $h_1 = 72.5$ meters and the values of V_{C_n} and V'_{C_n} given above we find $h_2 = 835$ meters using the minimum phase velocities, and $h_2 = 365$ meters using the maximum phase velocities. Though these values differ widely, this is not surprising considering that V_{C_3} is determined from a part of the travel-time curve where there is only one observed arrival time to determine its slope.

These calculated thicknesses should not be taken too seriously, as it is very doubtful if C is a refracted shear wave.

It is of interest to compare the angles of emergence observed for C with those computed using formula (5-13). The first breaks of C at short distances move upward and toward the shot. At 97 meters the angle of incidence, as determined from the ratio of the vertical to the horizontal amplitude of motion at the surface, is 21°; at 189 meters, it is 6°; at larger distances it is smaller or unmeasurable. Using (5-13):

$$\text{if } V_{C_1} = 225 \text{ m/s. and } V_{C_2} = 675 \text{ m/s.}$$
$$\sin i_{12} = .333 \qquad i_{12} = 19^\circ$$
$$\text{if } V_{C_1} = 225 \text{ m/s. and } V_{C_3} = 1225 \text{ m/s.}$$
$$\sin i_{13} = .184 \qquad i_{13} = 11^\circ$$

However, at 97 meters the ray presumably penetrates only the first layer, and at 189 meters it may or may not have penetrated thru the second layer. It therefore appears that C arrives at the surface at steeper angles than are predicted by these formulas. This is to be expected, as the velocity of C in the weathered layer is unknown, and is presumably smaller than V_{C1}.

It is also of interest to see what the values of Poisson's ratio, σ, are if C is a refracted shear wave. The well known expression for Poisson's ratio in terms of the compressional and shear wave velocities is:

$$\sigma = \frac{2 - \left(\frac{V_P^2}{V_C^2}\right)}{2 - 2\left(\frac{V_P^2}{V_C^2}\right)} \qquad (5\text{-}15)$$

In section IV we estimated that for the weathered layer V_P lay between 120 and 735 m/s., that in the first layer beneath the weathered layer V_P = 1565 m/s., and in the second layer beneath the weathered layer V_P = 1950 m/s. Since we do not know V_C in the weathered layer, we can not calculate σ there. However, using V_{C1} = 225-163 m/s. and V_P = 1565 m/s., we find σ = .488-.494. Where V_{C2} = 675-275 m/s., and V_P = 1950 m/s., we find σ = .44-.49. In section VII it will be shown that if the last pulse of measurable amplitude recorded is a Rayleigh wave, and if the velocity of compressional waves is 1565 m/s., σ = .49. This value is in good agreement with that

found assuming that C is a refracted shear wave.

However, the evidence certainly is not good enough to prove that it is of this nature. In conclusion, it is clear that our ideas of wave transmission must be somewhat modified before we can describe properly such a ground motion as C. Its similarity to the motion described by existing theories suggests that all that is needed is modification of these theories to include the effects of the special properties of the surface materials.

VI. THE "H" PULSE.

Description of the pulse.

Starting shortly before the end of C is a pulse which appears on both the longitudinal and vertical components. It is recognizable by phase-related motion on these two components as compared to the restriction to the longitudinal in the case of C. The maximum of this pulse is labeled "H" on the records. Figure 27 is a plot of the magnitude of the particle velocity during the later part of the passage of this pulse at a distance of 1493 meters from the explosion. The first part of the motion is distorted by the co-incident arrival of the end of C. The velocity of the maximum, as determined from the travel-time curve, chart V, is 345 meters per second; but this is probably a group velocity, and not the wave velocity. H is followed by a relatively quiet period during which the motion of the ground is irregular, but what motion there is appears to be generally of the same nature as H. This may all be a part of the dispersed H pulse, or it may be that there are several pulses of this type. At the larger distances it is possible to pick out several successive groups of oscillations of this sort.

During the time of arrival of H the particles move

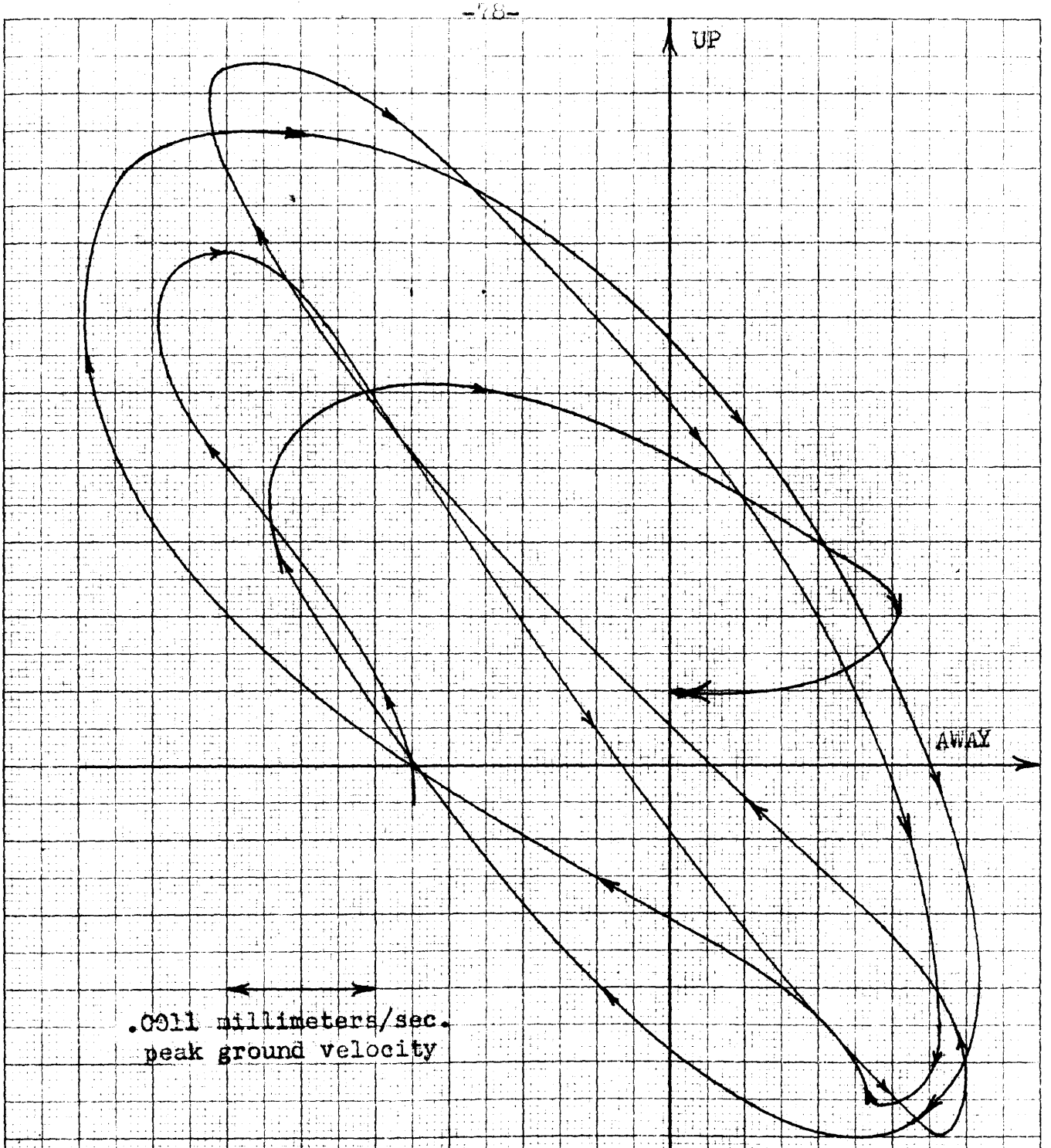

Particle motion during the passage of H at 1493 meters.

Figure 27.

in elliptical paths. The motion is direct, not retrograde as in the case of a Rayleigh wave. The horizontal component of motion has about twice the amplitude of the vertical. The ellipses are tilted with their tops toward the shot at an angle of about 45°. The average period of the waves is about .22 seconds.

There is some motion on the transverse component during the time of arrival of H. At places this energy seems to be related to that on the other two components, but there is no consistent correlation.

Because the motion of H and C overlap, a special travel-time curve has been made for H alone, chart V. The beginning of the pulse can not be determined, as it appears to be dispersed. The amplitude gradually increases to a maximum, then dies out again. The beginning appears to be at some time shortly before the time of maximum amplitude of C. On chart V are plotted the times of arrival of the outstanding maximum downward velocities. The average velocity of this pencil of motions is 270 meters per second.

Leet (1946) gave the name "Hydrodynamic" waves to similar motion which he found on the records of the Los Alamos atomic bomb test in about the same position with respect to other arrivals as the wave called H here. The implication presumably is that this motion is related to that of gravity waves in water.

H treated as a gravity wave.

The basic equations for gravity waves in two dimensions are well known (see for instance Lamb, 1932, p.363 ff). Choose a horizontal coordinate axis, x, in a free surface and a vertical coordinate axis, z, directed downward. The equation of continuity, which must be satisfied, is:

$$\nabla^2 \phi = 0 \tag{6-1}$$

Where ϕ is the velocity potential.

If we have a layer of incompressible fluid of depth, h, overlying a solid half-space, the boundary condition at the surface, z = h, is that the vertical component of velocity be zero, or:

$$\frac{\partial \phi}{\partial z} = 0 \tag{6-2}$$

If we seek a solution wherein the surface moves with simple harmonic motion, we must satisfy the equation of motion:

$$\eta = \frac{1}{g}\left[\frac{\partial \phi}{\partial t}\right] \tag{6-3}$$

where η is the elevation of the surface, and g is the acceleration of gravity.

A solution which satisfies (6-1) is:

$$\phi = P_z e^{i(pt - fx)} \tag{6-4}$$

where P_z depends only on z

$$p = \frac{2\pi}{\text{period}}$$

$$f = \frac{2\pi}{\text{wave length}} = \frac{2\pi}{L}$$

Substituting (6-4) in (6-1):

$$\frac{\partial^2 P_z}{\partial z^2} - f^2 P_z = 0 \tag{6-5}$$

which has the solution:

$$P_z = A e^{fz} + B e^{-fz} \tag{6-6}$$

Substituting this in (6-2), we see:

$$A e^{fh} = B e^{-fh} \tag{6-7}$$

Using this (6-4) becomes:

$$\phi = A_c \cosh f(z-h) e^{i(\rho t - fx)} \tag{6-8}$$

where $A_c = 2Be^{-fh}$. Since the velocity of the free surface is $\frac{\partial \eta}{\partial t}$, we find from (6-3) as a condition for the existence of such waves:

$$\frac{1}{g} \frac{\partial^2 \phi}{\partial t^2} = \frac{\partial \phi}{\partial z} \tag{6-9}$$

at the free surface, to the first approximation for small motion.

Substituting (6-8) in (6-9), at $z = 0$:

$$\frac{\rho^2}{g} = -f \tanh(-fh) = f \tanh(fh) \tag{6-10}$$

The velocity, V_g, of such waves is given by:

$$V_g = \frac{\text{wave length}}{\text{period}} = \frac{p}{f} \tag{6-11}$$

or

$$V_g = \frac{1}{f}\left(f_g \tanh (fh)\right)^{1/2} = \left[\frac{gL}{2\pi} \tanh\left(2\pi \frac{h}{L}\right)\right]^{1/2} \qquad (6\text{-}12)$$

If $h \gg L$:

$$V_g \approx \left(\frac{g}{f}\right)^{1/2} = \left(\frac{gL}{2\pi}\right)^{1/2} \qquad (6\text{-}13)$$

Squaring (6-13) and dividing by (6-11) we find:

$$V_g = \frac{g}{\rho} = \frac{g \times \text{period}}{2\pi} \qquad (6\text{-}14)$$

From the records we find that the period is of the order of .22 seconds, or $V_g = \frac{9.80 \times .22}{2\pi} = .34$ m/s. If L is not small compared to h, V_g will be even smaller. From chart V we see that the velocity of H is of the order of 270 m/s.

The above was derived on the assumptions that the layer was fluid and incompressible, neither of which conditions is satisfied by the ground in the Los Alamitos area. It is doubtful if the ground is even elastic, which means that the more fundamental condition, of which incompressibility is a special case, that the density of the medium be a function only of pressure, may not be satisfied. The other two assumptions, plane waves and very small amplitudes, though resulting in approximations to the true conditions, are probably sufficiently well satisfied. It is possible, that if the special conditions of the ground at Los Alamitos were taken into account, the velocity of "gravity" waves would be that observed. However, the theory

would have to be radically extended, and at present there seems to be no relation between gravity wave theory and the Los Alamitos observations except for the similarity of the particle paths.

H treated as a Stoneley wave.

Another possible explanation for H is that it is some form of Rayleigh wave wherein the direction of particle motion around the ellipse has been reversed from what is normal for a Rayleigh wave. A wave where this condition exists was described by Stoneley (1924) and is now known as a "Stoneley wave". It is a surface wave confined to the neighborhood of a contact between two distinct, but not too different, media.

Assume coordinate axes such that the x axis lies in the direction of propagation of the waves and the z axis is perpendicular to the contact. The equations to be satisfied are:

The equations of motion in the two media:

$$\rho \frac{\partial^2 u}{\partial t^2} = (\lambda + \mu) \frac{\partial \theta}{\partial x} + \mu \nabla^2 u \qquad (6\text{-}15)$$

$$\rho \frac{\partial^2 v}{\partial t^2} = (\lambda + \mu) \frac{\partial \theta}{\partial y} + \mu \nabla^2 v \qquad (6\text{-}16)$$

$$\rho \frac{\partial^2 w}{\partial t^2} = (\lambda + \mu) \frac{\partial \theta}{\partial z} + \mu \nabla^2 w \qquad (6\text{-}17)$$

where u, v, and w are the displacements, λ and μ are Lame's constants, and θ is the dilatation:

$$\theta = \frac{\partial u}{\partial x} + \frac{\partial v}{\partial y} + \frac{\partial w}{\partial z} \tag{6-18}$$

The boundary conditions are;

No motion far from the interface:

$$u = v = w = 0 \qquad \text{at} \quad z = \pm\infty \tag{6-19}$$

No openings at the interface:

$$\left.\begin{aligned} u_1 &= u_2 \\ v_1 &= v_2 \\ w_1 &= w_2 \end{aligned}\right\} \quad \text{at} \quad z = 0 \tag{6-20, 6-21, 6-22}$$

(Subscripts "1" and "2" will henceforth be used to distinguish the two media, the z axis being directed into medium 1.)

The tractions must be continuous across the interface:

$$\mu_1\left(\frac{\partial u_1}{\partial z} + \frac{\partial w_1}{\partial x}\right) = \mu_2\left(\frac{\partial u_2}{\partial z} + \frac{\partial w_2}{\partial x}\right) \tag{6-23}$$

$$\mu_1\left(\frac{\partial v_1}{\partial z} + \frac{\partial w_1}{\partial y}\right) = \mu_2\left(\frac{\partial v_2}{\partial z} + \frac{\partial w_2}{\partial y}\right) \tag{6-24}$$

$$\lambda_1\theta_1 + 2\mu_1\frac{\partial w_1}{\partial z} = \lambda_2\theta_2 + 2\mu_2\frac{\partial w_2}{\partial z} \tag{6-25}$$

A motion which satisfies all these conditions is:

$$u_1 = \left(-i\frac{V_{P1}^2}{f V_H^2} D_1 e^{-r_1 z} + s_1 Q_1 e^{-s_1 z}\right) e^{if(x - V_H t)} \tag{6-26}$$

$$v_1 = 0 \tag{6-27}$$

$$w_1 = \left(\frac{V_{P1}^2}{f^2 V_H^2} r_1 D_1 e^{-r_1 z} + if Q_1 e^{-s_1 z}\right) e^{if(x - V_H t)} \tag{6-28}$$

$$u_2 = \left(-i\frac{V_{P2}^2}{f V_H^2} D_2 e^{r_2 z} + s_2 Q_2 e^{s_2 z}\right) e^{if(x - V_H t)} \tag{6-29}$$

$$v_2 = 0 \tag{6-30}$$

$$w_2 = \left(-\frac{V_{P2}^2}{f^2 V_H^2} r_2 D_2 e^{r_2 z} + if Q_2 e^{s_2 z}\right) e^{if(x - V_H t)} \tag{6-31}$$

where:

$$r_n^2 = f^2\left(1 - \frac{V_H^2}{V_{Pn}^2}\right) \tag{6-32}$$

$$s_n^2 = f^2\left(1 - \frac{V_H^2}{V_{Sn}^2}\right) \tag{6-33}$$

$$f = \frac{2\pi}{\text{wave length}}$$

V_H = velocity of Stoneley waves

D_n and Q_n are constants determined by the boundary conditions. The other symbols have the same meaning as they have had up till now.

The condition which must be satisfied if such waves are to exist is:

$$V_H^4\left\{(\rho_1-\rho_2)^2-(\rho_1 A_2+\rho_2 A_1)(\rho_1 B_2+\rho_2 B_1)\right\}$$
$$+2KV_H^2\left\{\rho_1 A_2 B_2-\rho_2 A_1 B_1-\rho_1+\rho_2\right\}$$
$$+K^2(A_1B_1-1)(A_2B_2-1)=0 \qquad (6\text{-}34)$$

where:

$$A_n=\left(1-\frac{V_H^2}{V_{Pn}^2}\right)^{1/2} \qquad (6\text{-}35)$$

$$B_n=\left(1-\frac{V_H^2}{V_{Sn}^2}\right)^{1/2} \qquad (6\text{-}36)$$

$$K=2(\rho_1 V_{S1}^2-\rho_2 V_{S2}^2) \qquad (6\text{-}37)$$

V_{P_n} is the velocity of compressional waves in the nth medium and V_{S_n} is the velocity of shear waves in the nth medium.

It will be seen at once from equations (6-26) to (6-31) that the particles move in ellipses. The direction of the particle motion around the ellipse will depend on the velocities of body waves in the two media. It is not possible to show in what direction the motion will be in any particular case without substituting values in the above equations. However, it can be easily demonstrated that the motion may be either retrograde or direct. Suppose that we are standing in medium 1 looking at the interface as a train of Stoneley waves passes, as shown in figure 28, and that the motion

Viewed from this side the motion is retrograde.

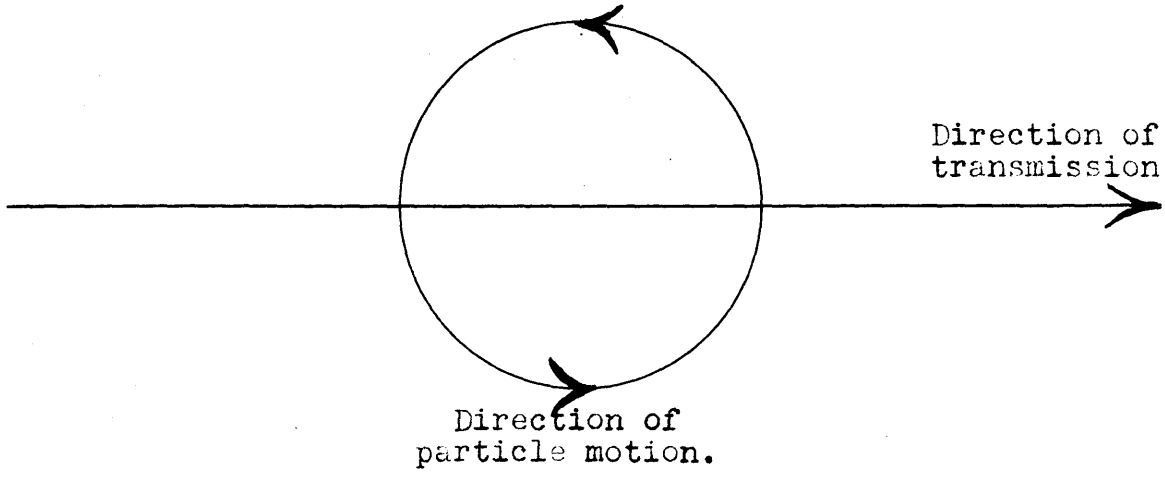

Viewed from this side the motion is direct.

Particle motion during the passage of a Stoneley wave at an interface.

Figure 28.

appears to us to be retrograde. If we view the motion from medium 2 instead, as we may do simply by turning the page upside down, the motion will appear to be direct. Thus for a Stoneley wave the direction of particle motion depends on from which side of the interface we look at it.

Because of the complexity of equation (6-34) it is not obvious when such waves can exist in an interface. Stoneley (1924, p.421) has shown that in general "when the wave velocities are not too widely different for the two media a wave of the Rayleigh type can exist at the interface". The presence of other interfaces in one or both media may make it more or less likely that such waves exist, particularly if one of these interfaces is essentially a free surface such as the surface of the earth. However, if conditions were right, it is possible that a Stoneley wave in a shallow interface might result in motion at the surface such as observed during the passage of H.

Unfortunately, too little is known about the thickness and elastic constants of the first layers at Los Alamitos to make a good quantitative check on whether or not Stoneley waves could exist there. Some notion of the velocities of compressional waves was developed in section IV. However, the shear wave velocities are unknown. Although the C waves may be

some sort of shear waves, they are certainly different from the shear waves whose velocities are needed to solve equation (6-34). Furthermore, the densities of the layers are completely unknown.

It is necessary to make additional simplifying assumptions before the problem can be treated further. To do this let us assume that the densities in the two layers are the same, a not too unlikely assumption if both are sedimentary layers. In this case (6-34) reduces to:

$$-\rho^2 V_H^4 (A_1 + A_2)(B_1 + B_2) + 2\rho K V_H^2 (A_2 B_2 - A_1 B_1)$$
$$+ K^2 (A_1 B_1 - 1)(A_2 B_2 - 1) = 0 \qquad (6\text{-}38)$$

where $\rho = \rho_1 = \rho_2$

Next we observe that except in the weathered layer, the velocity of compressional waves greatly exceeds that of H. When this is the case, A_1 and A_2 differ very little from 1. If we assume that $A_1 = A_2 = 1$, (6-38) simplifies to:

$$2\rho_2 V_H^4 (B_1 + B_2) + 2\rho K V_H^2 (B_2 - B_1) + K^2 (B_1 - 1)(B_2 - 1) = 0 \qquad (6\text{-}39)$$

(6-36) can be rewritten:

$$V_{Sn}^2 = \frac{V_H^2}{1 - B_n^2} \qquad (6\text{-}40)$$

(6-37) can now be written:

$$K = 2\rho\left(V_{S1}^2 - V_{S2}^2\right) = 2\rho V_H^2 \frac{B_1^2 - B_2^2}{(B_2^2-1)(B_1^2-1)} \tag{6-41}$$

Substituting (6-41) in (6-39) we find:

$$-2\rho^2 V_H^4 (B_1+B_2) + 4\rho^2 V_H^4 \frac{(B_1^2-B_2^2)(B_2-B_1)}{(B_2^2-1)(B_1^2-1)} + 4\rho^2 V_H^4 \frac{(B_1^2-B_2^2)^2(B_1-1)(B_2-1)}{(B_2^2-1)^2(B_1^2-1)^2} = 0 \tag{6-42}$$

On cancelling out common terms, if $B_2 \neq 1$ and $B_1 \neq 1$:

$$-(B_2^2-1)(B_1^2-1)(B_2+1)(B_1+1) - 2(B_1-B_2)^2(B_2+1)(B_1+1) + 2(B_2+B_1)(B_1-B_2)^2 = 0 \tag{6-43}$$

Which reduces to:

$$C_3 B_2^3 + C_2 B_2^2 + C_1 B_2 + C_0 = 0 \tag{6-44}$$

Where:

$$\begin{aligned} C_3 &= B_1^3 + B_1^2 + B_1 - 1 \\ C_2 &= B_1^3 - 3B_1^2 - B_1 + 1 \\ C_1 &= B_1^3 - B_1^2 - 3B_1 + 1 \\ C_0 &= -B_1^3 + B_1^2 + B_1 + 1 \end{aligned} \tag{6-45}$$

If we assume that $V_{S1} \rangle V_H$, then $0 \langle B_1 \langle 1$, and we can solve (6-44) for B_2 getting three roots, as shown in figure 29. Below $B_1 = .54$ two of the roots are imaginary, and nowhere are there any real roots between 0 and 1. Therefore B_2 must always be imaginary, and we may conclude that if $V_{S1} \rangle V_H$, $\rho_1 = \rho_2$ and V_{P1} and $V_{P2} \rangle\rangle V_H$, Stoneley waves can not exist.

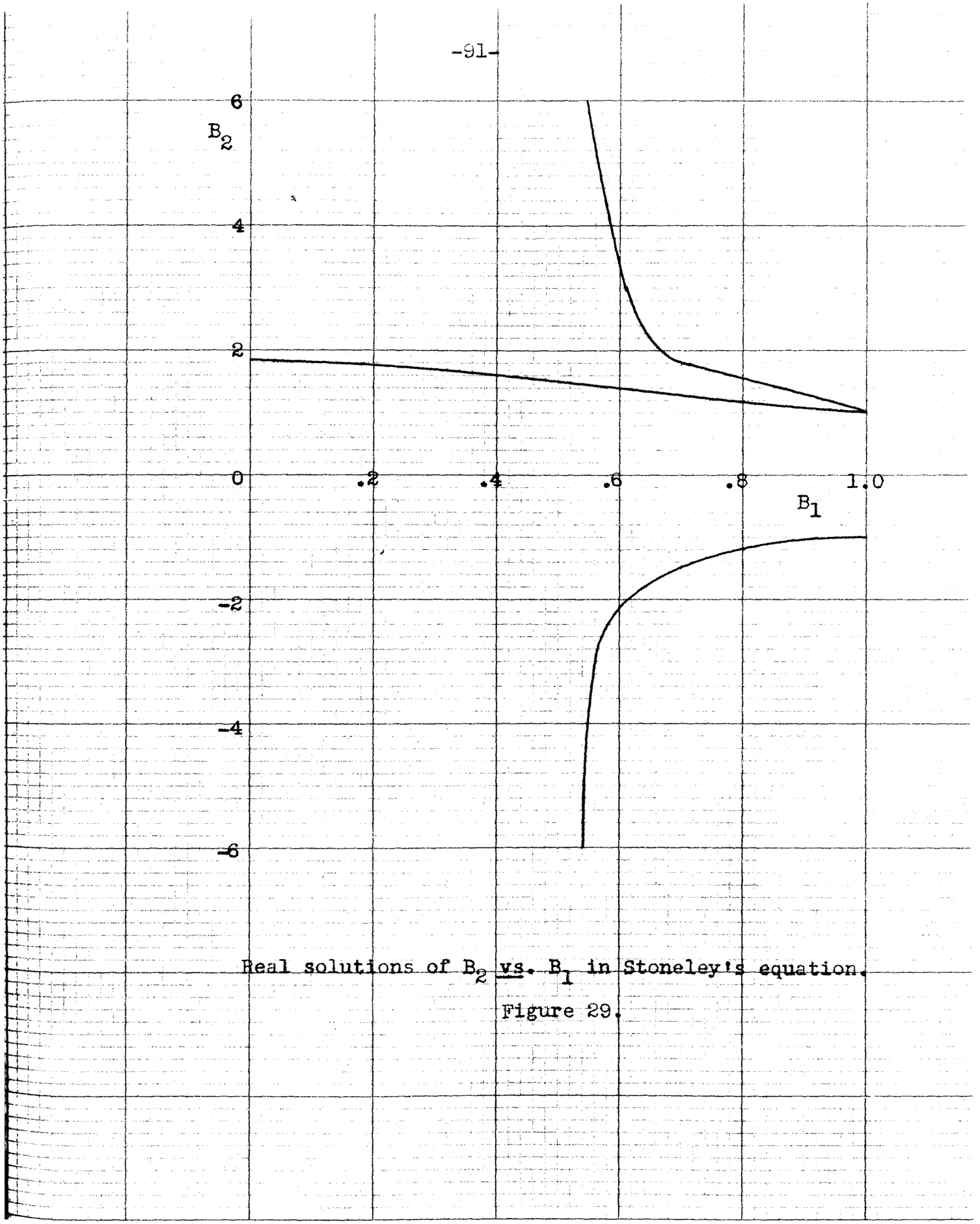

Real solutions of B_2 vs. B_1 in Stoneley's equation.

Figure 29.

Since these conditions were approximately what we would expect at any interface within the sedimentary section except the first one, it is unlikely that Stoneley waves with the velocity of the observed H waves can exist above the basement contact at Los Alamitos unless they are related to the interface at the base of the weathered layer.

Therefore we must determine if there is a solution of (6-34), using the velocities of compressional and shear waves in the weathered layer, and in the layer immediately beneath it.

V_H we know from the travel-time curves is approximately 270 m/s., V_{P2} is 1565 m/s., the other velocities are unknown. It will be suggested in section VII that the average value of Poisson's ratio, σ, is unusually large in the near surface material, being almost certainly over .4 and probably between .45 and .49. Large values of σ were similarly found on the assumption that C is a shear wave. If we assume $\sigma = .485$ in the first layer beneath the weathered layer, $V_{S2} = V_H$ and $B_2 = 0$. If we also assume as before that $\rho_1 = \rho_2$, using the value of A_2 determined from (6-35), (6-34) becomes:

$$-B_1(A_1 + .970) - 4A_1B_1\left(\frac{V_{S1}^2}{V_H^2} - 1\right) - 4(A_1B_1 - 1)\left(\frac{V_{S1}^2}{V_H^2} - 1\right)^2 = 0 \qquad (6\text{-}46)$$

Which can be solved for A_1 giving:

$$A_1 = \frac{4\left(\frac{V_{S1}^2}{V_H^2} - 1\right)^2 - .970\left(1 - \frac{V_H^2}{V_{S1}^2}\right)^{1/2}}{\left(1 - 2\frac{V_{S1}^2}{V_H^2}\right)^2 \left(1 - \frac{V_H^2}{V_{S1}^2}\right)^{1/2}} \qquad (6\text{-}47)$$

Multiplying both the numerator and denominator by $\frac{V_H^4}{V_{S1}^4}$ (6-47) becomes:

$$A_1 = \frac{4\left(1 - \frac{V_H^2}{V_{S1}^2}\right)^{1/2} - .970\ \frac{V_H^4}{V_{S1}^4}}{\left(2 - \frac{V_H^2}{V_{S1}^2}\right)^2} \qquad (6\text{-}48)$$

If V_H exceeds V_{S1}, A_1 is complex. Therefore, we need consider only the range $V_{S1} \geq V_H$.

From (6-35) we find:

$$V_{P1} = \frac{V_H}{(1 - A_1^2)^{1/2}} \qquad (6\text{-}49)$$

From (6-48) and (6-49) we calculate V_{P1} for all values of $V_{S1} \geq V_H$. The resulting relation between V_{P1} and V_{S1} is shown by figure 30. There is only one value of V_{P1} above 1102 m/s. since we are not concerned with values of V_{S1} less than 270 m/s. Equation (6-49) shows that V_H can never exceed V_{P1} for the assumed conditions.

Not all of the solutions are physically possible. To determine which are possible we calculate Poisson's ratio, σ, using the well known relation:

$$\sigma = \frac{2 - \left(\frac{V_P}{V_S}\right)^2}{2 - 2\left(\frac{V_P}{V_S}\right)^2} \qquad (6\text{-}50)$$

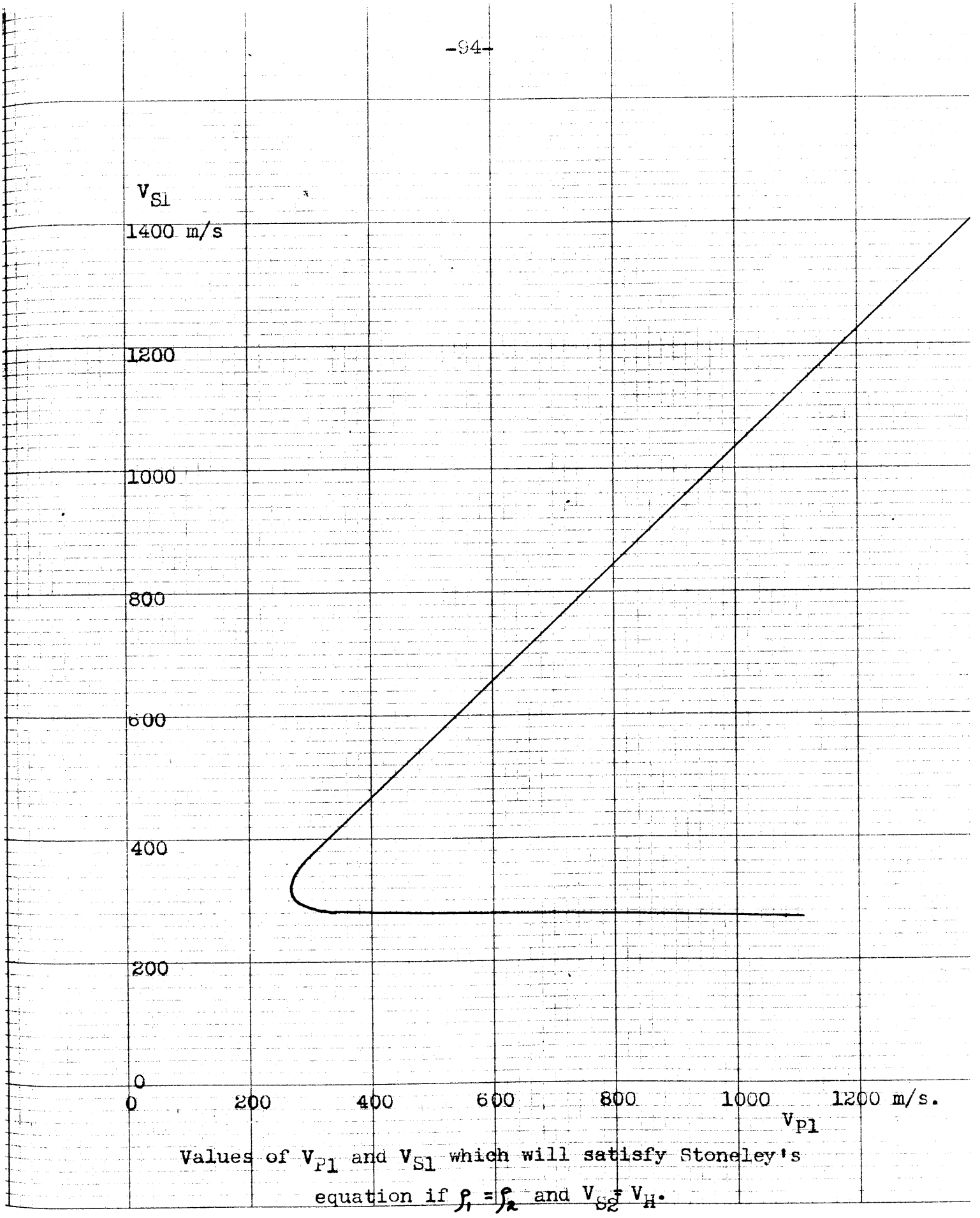

Values of V_{P1} and V_{S1} which will satisfy Stoneley's equation if $\rho_1 = \rho_2$ and $V_{S2} = V_H$.

Figure 30.

The resulting values are shown in figure 31. Only one of the roots of V_{P1} shown in figure 30 corresponds to a physically possible value of σ, as values of $\sigma > \frac{1}{2}$ are impossible; and all values of V_{P1} less than about 395 m/s. correspond to unlikely physical conditions, since negative values of Poisson's ratio have never been observed. We showed in section IV that V_{P1} probably lay between 120 m/s. and 735 m/s. If the larger figure is more nearly the true one, Stoneley waves may be possible in the interface beneath the weathered layer.

This analysis does not prove that Stoneley waves do exist, or even can exist in this interface, since as has already been pointed out the weathered layer is not the semi-infinite elastic medium required by Stoneley's theory; but if the differences are not too great, the approximation may be so good that something closely resembling Stoneley waves may exist. The range where this is likely has now been narrowed to $395 \text{ m/s.} \leq V_{P1} \leq 735 \text{ m/s.}$

If Stoneley waves can exist, we must consider whether or not their particle motion will be direct or retrograde. To do this consider equations (6-26) and (6-28). Since we do not know if D_1 and Q_1 have the same sign, we must clear the equations of one or the other. By substituting (6-26) thru (6-31) in

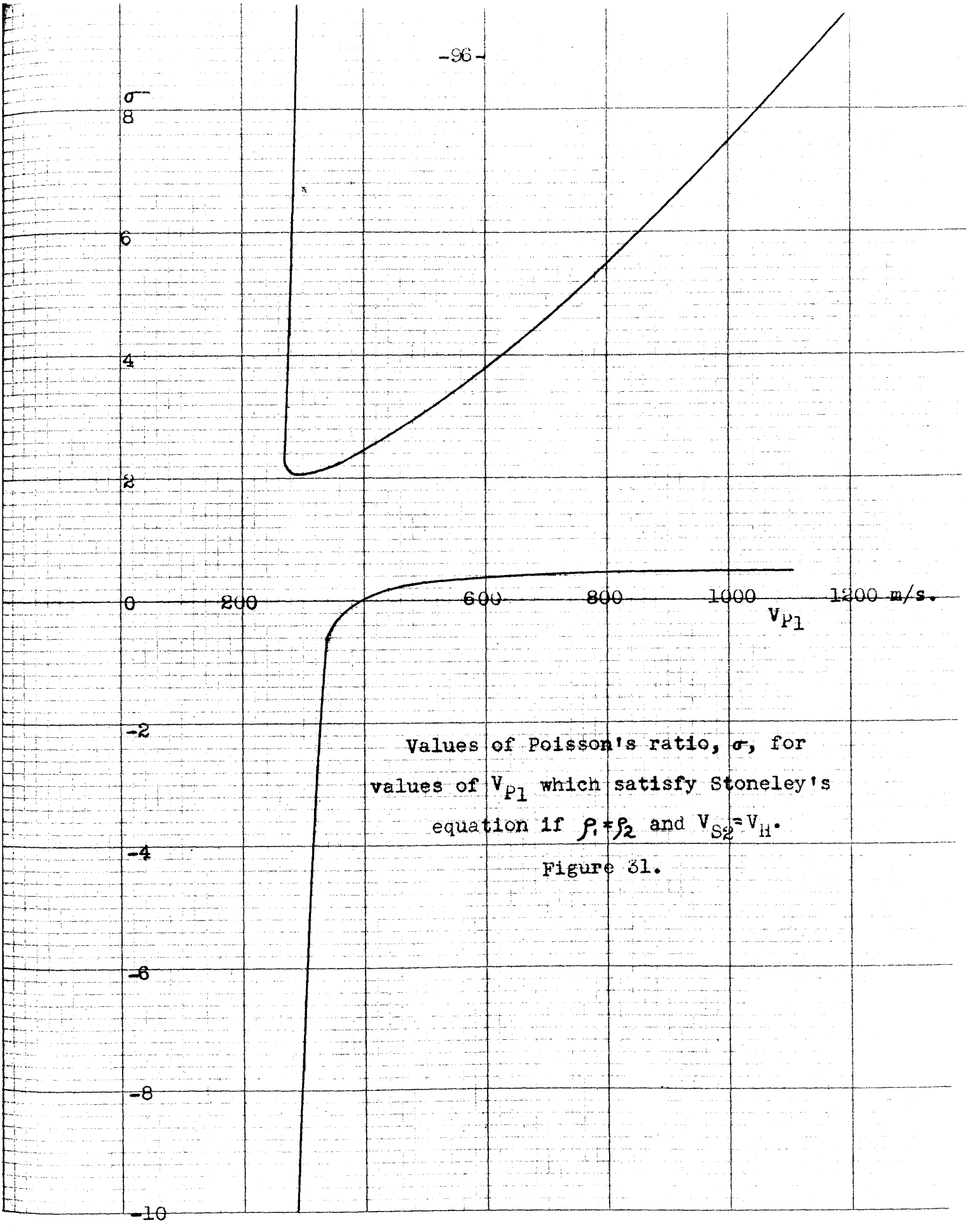

Values of Poisson's ratio, σ, for values of V_{P1} which satisfy Stoneley's equation if $\rho_1 = \rho_2$ and $V_{S2} = V_H$.

Figure 31.

(6-20) and (6-25) we get, at z = 0:

$$-i\frac{V_{P1}^2 D_1}{V_H^2 f} + s_1 Q_1 = -i\frac{V_{P2}^2 D_2}{V_H^2 f} + s_2 Q_2 \tag{6-51}$$

$$\lambda_1\left(\frac{V_{P1}^2}{V_H^2} D_1 + ifs_1 Q_1\right) + (\lambda_1 + 2\mu_1)\left[-\frac{r_1^2 V_{P1}^2}{f^2 V_H^2} D_1 - ifs_1 Q_1\right]$$

$$= \lambda_2\left(\frac{V_{P2}^2}{V_H^2} D_2 + ifs_2 Q_2\right) + (\lambda_2 + 2\mu_2)\left[-\frac{r_2^2 V_{P2}^2}{f^2 V_H^2} D_2 + ifs_2 Q_2\right] \tag{6-52}$$

On rearranging (6-52) we get:

$$\left[\lambda_1\frac{V_{P1}^2}{V_H^2} - (\lambda_1 + 2\mu_1)\frac{V_{P1}^2}{V_H^2}\left(1 - \frac{V_H^2}{V_{P1}^2}\right)\right] D_1 - 2i\mu_1 fs_1 Q_1 \tag{6-53}$$

$$= \left[\lambda_2\frac{V_{P2}^2}{V_H^2} - (\lambda_2 + 2\mu_2)\frac{V_{P2}^2}{V_H^2}\left(1 - \frac{V_H^2}{V_{P2}^2}\right)\right] D_2 + \lambda_2 ifs_2 Q_2 + (\lambda_2 + 2\mu_2) ifs_2 Q_2$$

or:

$$\left[\lambda_1\frac{V_{P1}^2}{V_H^2} - (\lambda_1 + 2\mu_1)\left(\frac{V_{P1}^2}{V_H^2} - 1\right)\right] D_1 - 2i\mu_1 fs_1 Q_1 \tag{6-54}$$

$$= \left[\lambda_2\frac{V_{P2}^2}{V_H^2} - (\lambda_2 + 2\mu_2)\left(\frac{V_{P2}^2}{V_H^2} - 1\right)\right] D_2 + 2(\lambda_2 + \mu_2) ifs_2 Q_2$$

Now if we assume $V_{S2} = V_H$ and $f_1 = f_2 = f$, s_2 becomes zero, and (6-51) and (6-54) become:

$$\frac{V_{P1}^2}{V_H^2} D_1 + ifs_1 Q_1 = \frac{V_{P2}^2}{V_H^2} D_2 \tag{6-55}$$

$$\left[-2\mu_1 \frac{V_{P1}^2}{V_H^2} + (\lambda_1 + 2\mu_1)\right] D_1 - 2i\mu_1 f s_1 Q_1$$

$$= \left[-2\mu_2 \frac{V_{P2}^2}{V_H^2} + (\lambda_2 + 2\mu_2)\right] D_2 \qquad (6\text{-}56)$$

or substituting $V_{Pn}^2 = \frac{\lambda_n + 2\mu_n}{\rho}$ and $V_{Sn}^2 = \frac{\mu_n}{\rho}$ into (6-56):

$$\left[-2V_{S1}^2 \frac{V_{P1}^2}{V_H^2} + V_{P1}^2\right] D_1 - 2i V_{S1}^2 f s_1 Q_1 = \left[-2V_{P2}^2 + V_{P2}^2\right] D_2 \qquad (6\text{-}57)$$

Clearing D_2 from (6-55) and (6-57):

$$V_{P1}^2 \left(1 - 2\frac{V_{S1}^2}{V_H^2}\right) D_1 - 2i V_{S1}^2 f s_1 Q_1 = -V_{P1}^2 D_1 - i f s_1 V_H^2 Q_1 \qquad (6\text{-}58)$$

Which simplifies to:

$$2V_{P1}^2 \left(1 - \frac{V_{S1}^2}{V_H^2}\right) D_1 - i f s_1 Q_1 (2V_{S1}^2 - V_H^2) = 0 \qquad (6\text{-}59)$$

Clearing D_1 from (6-26) and (6-28) by using (6-59):

$$u_1 = \left[\frac{s_1 Q_1 (2V_{S1}^2 - V_H^2)}{2(V_H^2 - V_{S1}^2)} e^{-r_1 z} + s_1 Q_1 e^{-s_1 z}\right] e^{if(x - V_H t)} \qquad (6\text{-}60)$$

$$w_1 = \left[\frac{i r_1 s_1 Q_1 (2V_{S1}^2 - V_H^2)}{2f(V_H^2 - V_{S1}^2)} e^{-r_1 z} + i f Q_1 e^{-s_1 z}\right] e^{if(x - V_H t)} \qquad (6\text{-}61)$$

If $z = 0$, neglecting the time dependent exponential:

$$u_1 = \frac{s_1 Q_1 (2V_{S1}^2 - V_H^2) + 2 s_1 Q_1 (V_H^2 - V_{S1}^2)}{2(V_H^2 - V_{S1}^2)} = \frac{s_1 Q_1 V_H^2}{2(V_H^2 - V_{S1}^2)} \qquad (6\text{-}62)$$

$$w_1 = i\left[\frac{r_1 s_1 Q_1 (2V_{S1}^2 - V_H^2) + 2f^2 Q_1 (V_H^2 - V_{S1}^2)}{2f(V_H^2 - V_{S1}^2)}\right] \tag{6-63}$$

$$\frac{w_1}{u_1} = i\,\frac{r_1 s_1 (2V_{S1}^2 - V_H^2) + 2f^2 (V_H^2 - V_{S1}^2)}{f s_1 V_H^2} \tag{6-64}$$

For real, positive values of r_1 and s_1 this reduces to:

$$\frac{w_1}{u_1} = -i\left[\left(1 - \frac{V_H^2}{V_{P1}^2}\right)^{1/2}\left(1 - 2\frac{V_{S1}^2}{V_H^2}\right) + 2\,\frac{V_{S1}}{V_H}\left(\frac{V_{S1}^2}{V_H^2} - 1\right)^{1/2}\right] \tag{6-65}$$

If V_{P1} lies between 400 m/s. and 735 m/s., the physically acceptable part of figure 30 gives $i.32 \leq w_1/u_1 \leq i.67$. This means that the particle motion is retrograde elliptical, the reverse of what was observed for H waves.

Actually to compute w_1/u_1 properly we should examine its magnitude at the surface of the ground, not at the interface. To do this we would have to consider the case of a surface layer of finite thickness, which was not done here, as the equations are too cumbrous. However, since the surface layer is probably considerably less than a wave length in thickness, the motion at the surface, if Stoneley waves will exist at all in this case, might be expected to be similar to that at the interface. Since the Stoneley wave equations predict

motion other than that observed, we are still lacking an adequate explanation for H.

H the sum of two pulses.

Another approach which the author has not yet had time to investigate thoroughly is to examine the possibility that H is the sum of a compressional and a shear pulse arriving from below at different angles but with the same frequencies. This approach seems to show promise, and will be made the subject of a later paper.

VII. RAYLEIGH WAVES.

Description of the pulse.

The last pulse of energy of measurable size recorded is also the most distinctive. Its maxima are labeled "R" on charts I-III. It appears on the longitudinal and vertical components only. Chart VI is a plot of the particle velocity during the passage of this pulse at a distance of 1493 meters. The velocity of its maximum is 193 meters per second. This is obviously a group velocity, as can be seen from the travel-time curve, chart IV. The average phase velocity, determined from the slope of the line thru this maximum and the origin is 167½ meters per second. The retrograde elliptical pattern of the particle motion suggests that this wave is of the Rayleigh type. It is notable, however, that the ellipses are "tilted" at about 45°, with their tops away from the shots. A possible explanation for this is that, since the velocity of propagation increases with depth, energy travelling along the deeper paths tends to get ahead of the shallower energy, and the arrivals give the impression of coming from below because of the earlier arrival of the pulse along these deeper paths. If this is the case, one would expect that, since the ellipses are tilted back, the larger component of chart VI would correspond to what would normally be the horizontal

component of motion if the pattern were not tilted.

Figure 32 is a plot of the ratio of the amplitudes of the vertical to horizontal motion against distance (disregarding any tilt of the ellipses). It is plain that this ratio never exceeds one. This has been observed for the Rayleigh waves from earthquakes also (Byerly 1933, p.182). The points are badly scattered, but there appears to be a decrease in this ratio at increasing distance. The two points at less than 200 meters have been disregarded as at these distances the different pulses all overlap, and it is uncertain how much of the motion attributed to R was really due to one of the other phases. If these two points should not be disregarded then it is questionable whether the ratio of amplitudes does decrease with distance.

Figure 33 is a plot of the periods of the maximum motions of R against time after the explosions at different distances. This period clearly increases with increasing distance. However, at any distance, the period decreases during the time of arrival of R.

Using the velocity of the maximum of the pulse of 167½ meters per second as taken from the travel-time chart, the wave lengths of the largest motions can be computed from these periods, and are shown in figure 34. Periods of more than one third of a second correspond to frequencies below the pass band of the

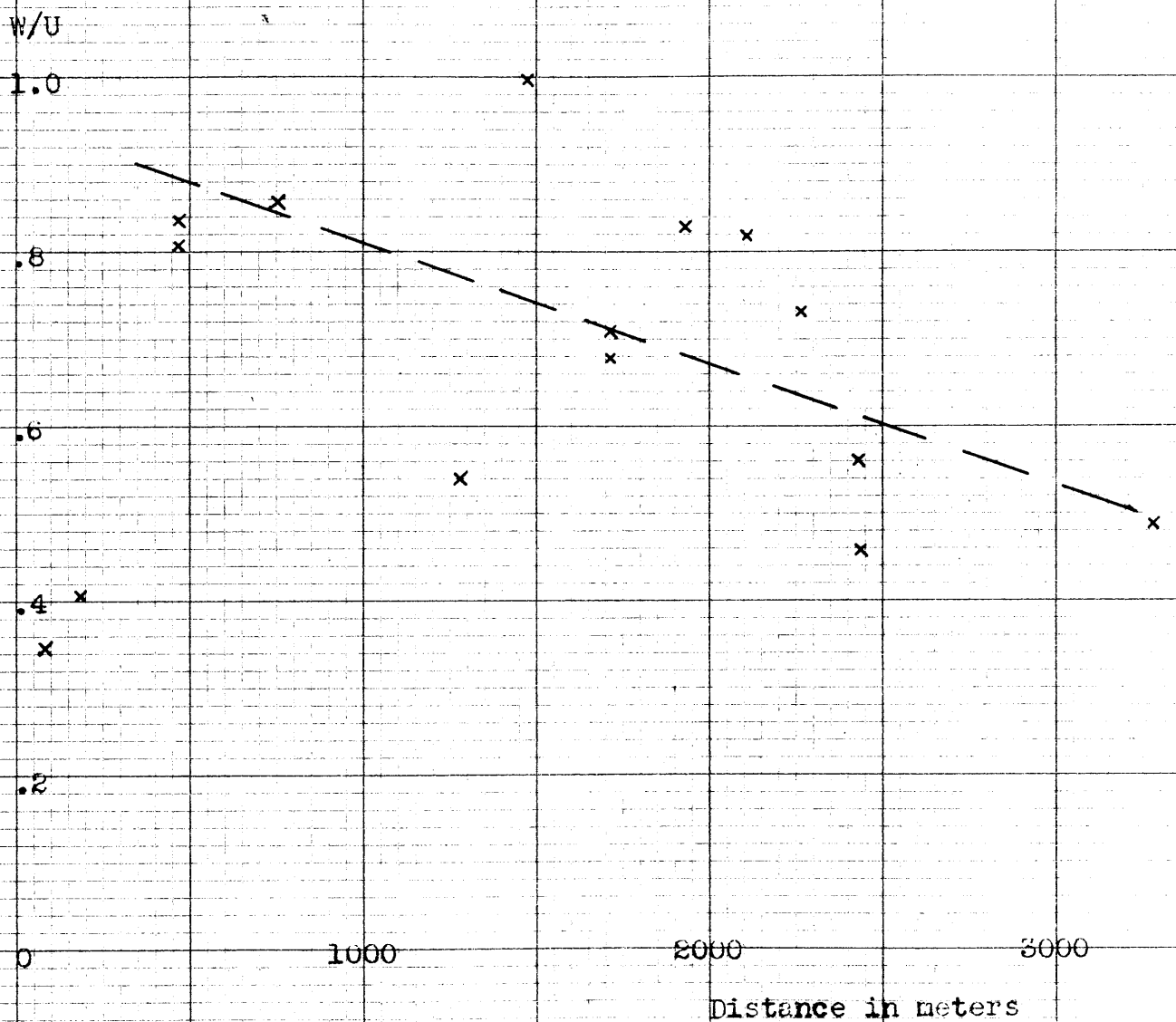

Variation of the ratio of the vertical to the horizontal amplitude of motion of R with distance from the explosion.

Figure 32.

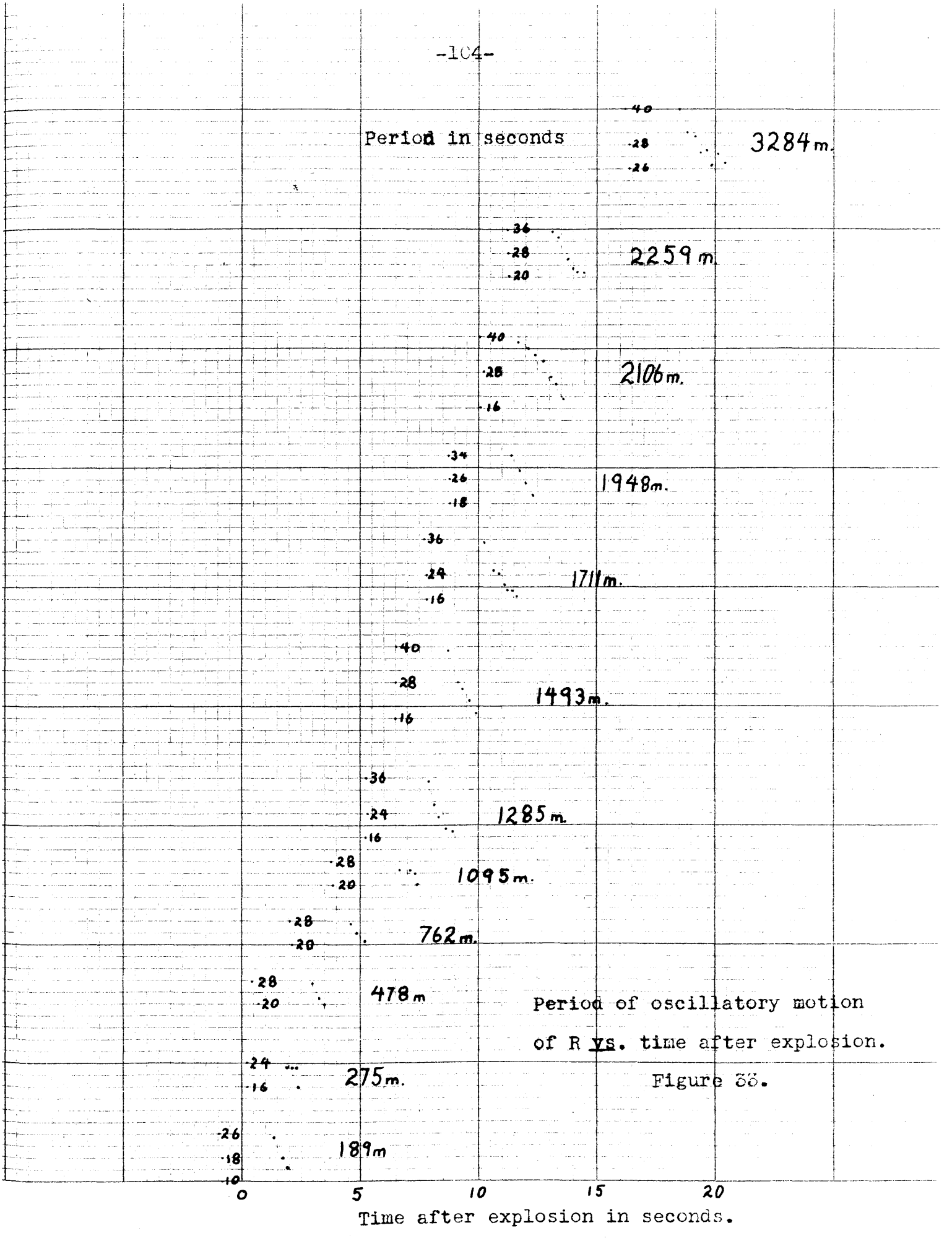

Period of oscillatory motion of R vs. time after explosion.

Figure 38.

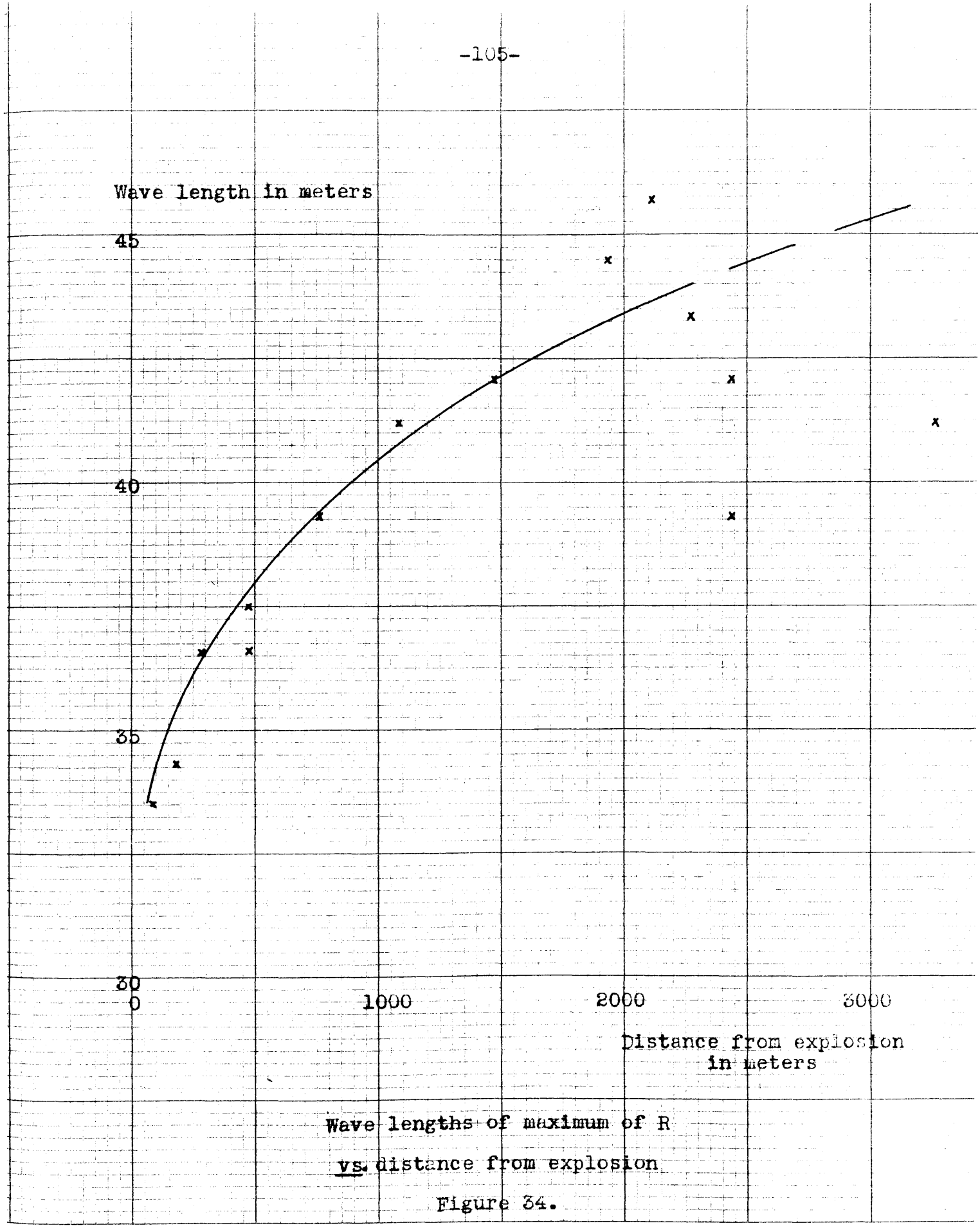

Wave lengths of maximum of R

vs. distance from explosion

Figure 34.

seismic recorders, and therefore at these frequencies there is a tendency of the apparatus to attenuate the fundamental frequency of the ground motion and record only the higher harmonics. This causes scattering of the points at large wave lengths.

Amplitude of R vs. distance.

To determine the rate at which the amplitude of R decreases with distance, we use the formula:

$$J_n = \frac{J_o}{\Delta_n} e^{-\alpha' \psi_n} \qquad (7\text{-}1)$$

taken from Gutenberg (1932, p.225), where

J_n is the maximum energy of the surface waves at the recording station at a distance Δ_n from the shot.

J_o is a constant for any one source, or for identical sources of seismic energy.

$\Delta_n = \Delta_o \sin \psi_n$

Δ_o is the radius of the earth.

ψ_n is the angular distance to the nth recording station along the great circle path.

α' is the attenuation factor, a function of the ground. Note that α' is twice the α used in section V to describe the attenuation of C, since (5-1) was set up in terms of amplitude variations, whereas (7-1) is in terms of energy.

Since the energy of the waves is proportional to the square of the velocity, we can also say, similarly:

$$A_n^2 = \frac{A_o^2}{\Delta_n} e^{-\alpha' \psi_n} \qquad (7\text{-}2)$$

where A_n is the magnitude of the ground velocity as computed from the record, and A_o is a constant similar to J_o. Gutenberg (loc. cit.) uses $J_\Delta = (\frac{a}{\text{period}})^2$ where a is the amplitude of the displacement of the ground, but our calibrations are already made in terms of the velocity, so we can neglect variations in frequency. A_o can be cleared from the equation by using the data from any two observations at different distances from the shot, thus:

$$\frac{A_{\Delta 1}^2}{A_{\Delta 2}^2} = \frac{\Delta_2}{\Delta_1} e^{-\alpha'(\psi_1 - \psi_2)} \tag{7-3}$$

Or, returning to the notation of section V by substituting 2α for α':

$$\frac{A_{\Delta 1}^2}{A_{\Delta 2}^2} = \frac{\Delta_2}{\Delta_1} e^{-2\alpha(\psi_1 - \psi_2)} \tag{7-4}$$

Which can also be written:

$$\left(\frac{\Delta_1}{\Delta_2}\right)^{1/2} \frac{A_{\Delta 1}}{A_{\Delta 2}} = e^{-\alpha(\psi_1 - \psi_2)} \tag{7-5}$$

This can be solved for α giving:

$$\alpha = \frac{1}{\psi_2 - \psi_1} \log_e \frac{A_{\Delta 1}}{A_{\Delta 2}} \left(\frac{\Delta_1}{\Delta_2}\right)^{1/2} \tag{7-6}$$

Since $\psi_n = \frac{\Delta_n}{\Delta_o}$

$$\alpha = \frac{\Delta_o}{\Delta_2 - \Delta_1} \log_e \frac{A_{\Delta 1}}{A_{\Delta 2}} \left(\frac{\Delta_1}{\Delta_2}\right)^{1/2} \tag{7-7}$$

where the units of α are inverse radians; or

$$\alpha = \frac{1}{\Delta_2 - \Delta_1} \log_e \frac{A_{\Delta 1}}{A_{\Delta 2}} \left(\frac{\Delta_1}{\Delta_2}\right)^{1/2} \qquad (7\text{-}8)$$

where the units of α are inverse distance.

Substituting the data from figure 35 into (7-6) we find that α is .0036 per meter or about .14 per wave length (α' is .0072 per meter). If one compares this with the values of α' found from earthquake studies (Gutenberg, 1932, p.255-258) of .00013 to .00053 per kilometer, it is clear that the near surface layers have a very high coefficient of absorption.

The plot of the amplitudes against distance, figure 35, shows a lot of scattering of the points. This is not surprising as the ground conditions at the shot hole vary from one explosion to the next, particularly when the records are made on different days. After many shots in one hole the ground becomes much broken up. Also, the amount of surface waves depend greatly on the depth below the surface at which the explosion was detonated. Five pounds of dynamite were exploded at 3284 meters, while only $2\frac{1}{2}$ were used at the shorter distances. There may also have been variations in the plants of the seismometers in the loose soil at the different recording locations. In short, successive explosion measurements depend on so many unknown and unmeasurable factors that the amplitudes of resulting motion can not be expected to fall on a line.

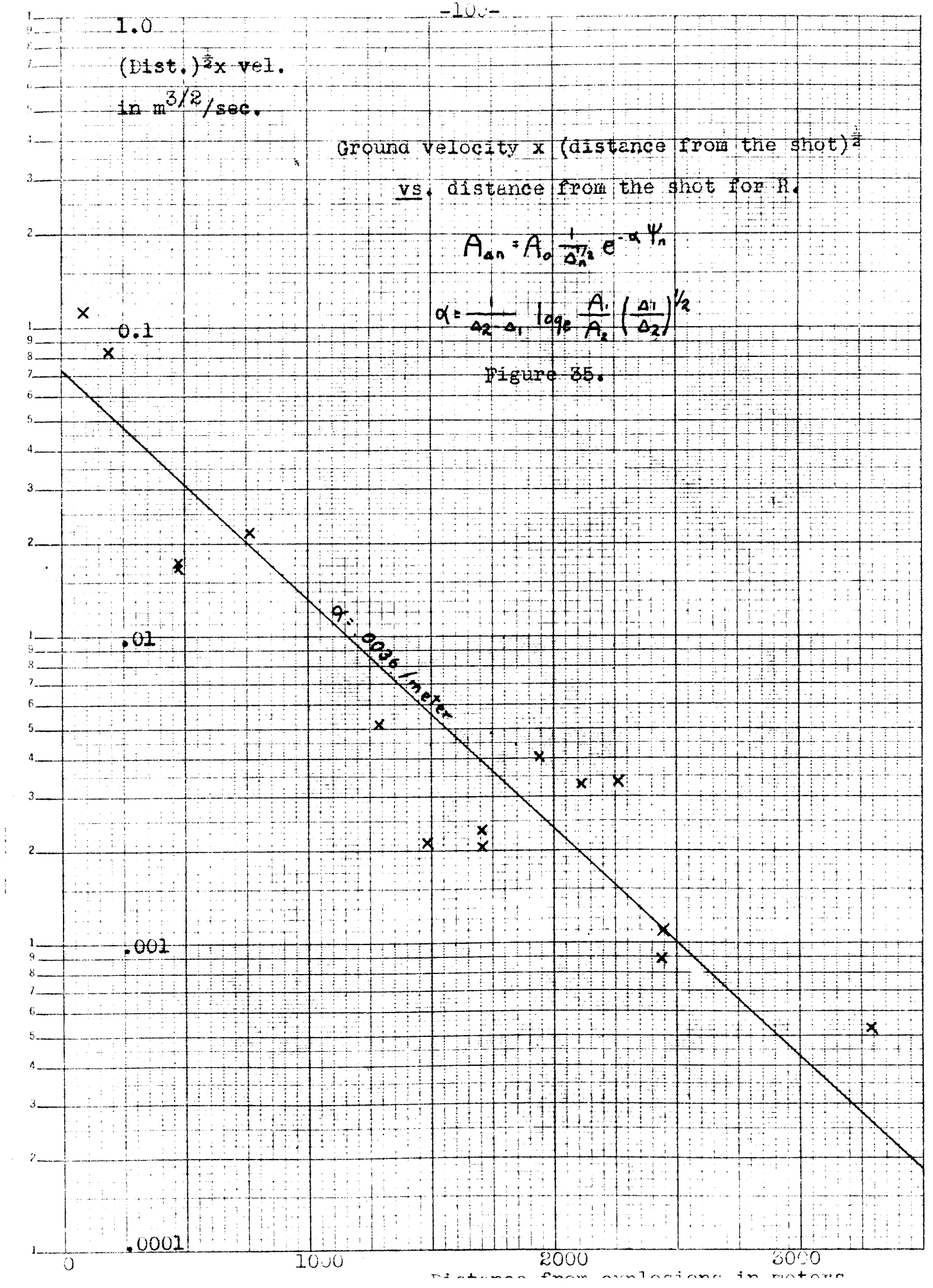

Ground velocity x (distance from the shot)$^{\frac{3}{2}}$ vs. distance from the shot for R.

$$A_{\Delta n} = A_0 \frac{1}{\Delta_n^{3/2}} e^{-\alpha \psi_n}$$

$$\alpha = \frac{1}{\Delta_2 - \Delta_1} \log_e \frac{A_1}{A_2} \left(\frac{\Delta_1}{\Delta_2}\right)^{1/2}$$

Figure 35.

The Rayleigh wave was plainly felt at almost all the recording locations; and it is a part of what is known as ground roll in the seismic exploration industry. Probably C also contributes to the ground roll, but it does not give the characteristic rolling sensation which R gives. H may contribute something, but as it is generally smaller in amplitude, its arrival is not so easily recognized by the physical sensation it produces.

Rayleigh's theory.

The R waves on the records are, in general, similar to the type which was first predicted by Lord Rayleigh (1885), and which are named after him. Rayleigh found that along the surface of a homogeneous, isotropic, elastic, half space, in which the velocities of the body waves are V_P (compressional) and V_S (shear), surface waves, that is waves whose amplitudes decrease rapidly with increasing depth, can be propagated. It has already been pointed out that the near surface material is probably neither homogeneous nor elastic, so that Rayleigh's theory does not strictly apply to the observations. However, as it is a first approximation to the conditions, although a poor one, we will examine it in some detail since we lack a development of the wave mechanics for a better approximation. It must be kept in mind that because the conditions required by Rayleigh's theory are not

met, we can not expect the ground motion to be exactly what it would be if the actual ground closely resembled the ideal medium. Any similarity of the motion could be a pure coincidence.

We choose a coordinate system with the z axis perpendicular to the free surface and directed into the solid half space, and the x axis along the free surface in the direction of propagation of the waves. The equations to be satisfied are similar to those required for Stoneley waves (section VI). The first ones are the equations of motion:

$$\rho \frac{\partial^2 u}{\partial t^2} = (\lambda + \mu) \frac{\partial \theta}{\partial x} + \mu \nabla^2 u \qquad (7\text{-}9)$$

$$\rho \frac{\partial^2 v}{\partial t^2} = (\lambda + \mu) \frac{\partial \theta}{\partial y} + \mu \nabla^2 v \qquad (7\text{-}10)$$

$$\rho \frac{\partial^2 w}{\partial t^2} = (\lambda + \mu) \frac{\partial \theta}{\partial z} + \mu \nabla^2 w \qquad (7\text{-}11)$$

where as before ρ is the density, u, v, and w are the particle displacements along the x, y, and z axes respectively, λ and μ are Lame's constants, and θ is the cubical dilatation:

$$\theta = \frac{\partial u}{\partial x} + \frac{\partial v}{\partial y} + \frac{\partial w}{\partial z} \qquad (7\text{-}12)$$

At great depths, $z = \infty$, there must be no motion:

$$u = v = w = 0 \qquad (7\text{-}13)$$

At the free surface, z = 0, there must be no traction:

$$\frac{\partial w}{\partial x} + \frac{\partial u}{\partial z} = 0 \tag{7-14}$$

$$\frac{\partial w}{\partial y} + \frac{\partial v}{\partial z} = 0 \tag{7-15}$$

$$\lambda \theta + 2\mu \frac{\partial w}{\partial z} = 0 \tag{7-16}$$

As in the case of Stoneley's waves, we find that there is no motion in the transverse direction; the displacements in the other two directions are:

$$u = i\left(-\frac{f}{h_R^2} e^{-rz} + \frac{2frs}{h_R^2(f^2+s^2)} e^{-sz}\right) e^{i(fx+pt)} \tag{7-17}$$

$$w = \left(\frac{r}{h_R^2} e^{-rz} - \frac{2f^2 r}{h_R^2(f^2+s^2)} e^{-sz}\right) e^{i(fx+pt)} \tag{7-18}$$

where $f = \dfrac{2\pi}{\text{wave length}} = \dfrac{2\pi}{L}$ (7-19)

$$p = \frac{2\pi}{\text{period}} \tag{7-20}$$

$$r^2 = f^2 - h^2_R \tag{7-21}$$

$$s^2 = f^2 - k^2_R \tag{7-22}$$

$$k^2_R = \frac{p^2}{V_S^2} \tag{7-23}$$

$$h^2_R = \frac{p^2}{V_P^2} \tag{7-24}$$

The necessary condition for the existence of such waves is:

$$\frac{k_R^8}{f^8} - 8\frac{k_R^6}{f^6} + 24\frac{k_R^4}{f^4} - 16\frac{k_R^2}{f^2} - 16\frac{k_R^2 h_R^2}{f^4} + 16\frac{h_R^2}{f^2} = 0 \tag{7-25}$$

From (7-19) and (7-20) it is plain that:

$$V_R = \frac{\rho}{f} \tag{7-26}$$

Therefore (7-23) and (7-24) become:

$$k_R^2 = f^2 \frac{V_R^2}{V_S^2} \tag{7-27}$$

$$h_R^2 = f^2 \frac{V_R^2}{V_P^2} \tag{7-28}$$

Substituting these values of h_R and k_R in (7-25):

$$\frac{V_R^8}{V_S^8} - 8\frac{V_R^6}{V_S^6} + 24\frac{V_R^4}{V_S^4} - 16\frac{V_R^2}{V_S^2} - 16\frac{V_R^4}{V_P^2 V_S^2} + 16\frac{V_R^2}{V_P^2} = 0 \tag{7-29}$$

This is an equation for V_R in terms of V_P and V_S. V_P and V_S are further related by equation (5-13), which can be rewritten:

$$\frac{V_S^2}{V_P^2} = \frac{1-2\sigma}{2-2\sigma} \tag{7-30}$$

σ is Poisson's ratio.

(7-29) can be reduced to the form which is generally called "Rayleigh's equation" by dividing thru by $\frac{V_R^2}{V_S^2}$ yielding:

$$\frac{V_R^6}{V_S^6} - 8\frac{V_R^4}{V_S^4} + \left(24 - 16\frac{V_S^2}{V_P^2}\right)\frac{V_R^2}{V_S^2} - 16\left(1 - \frac{V_S^2}{V_P^2}\right) = 0 \tag{7-31}$$

Thus the condition for the existence of Rayleigh waves in a homogeneous earth, in which Poisson's ratio has the value σ, is that there exists a V_R such that (7-29) can be satisfied. For every value of V_R/V_S

except $V_R/V_S = 1$ or -1 there exists a unique value of V_R^2/V_P^2 given by (7-29).

Let us now suppose that these equations can be applied to the ground motions we have observed, always remembering, however, that the fundamental assumptions of Rayleigh were not satisfied. Although the R pulse is dispersed, V_R can be approximately determined from the travel-time curve, chart IV, and is found to be $167\frac{1}{2}$ m/s. as noted earlier. Using this value of V_R and equation (7-29), we get the values of V_P which correspond to all real values of V_S as shown in figure 36.

Plainly there are some values of V_P for which Rayleigh waves with the observed velocity can not exist. This can also be seen from figure 37, which shows what value σ must have to give the observed value of V_R for different values of V_P. There is no real value of σ corresponding to $167\frac{1}{2}$ m/s. $< V_P <$ 259 m/s.; and no value of σ where $0 < \sigma < .5$ for $V_P <$ 105 m/s. Therefore R can be a true Rayleigh wave only if V_P falls outside of these ranges.

In section IV above it was shown that V_P varied with depth. In particular, it was shown that we could approximate the conditions in the Los Alamitos area by assuming three layers, a shallowest layer between 1.2 and 8.4 meters thick whose compressional wave

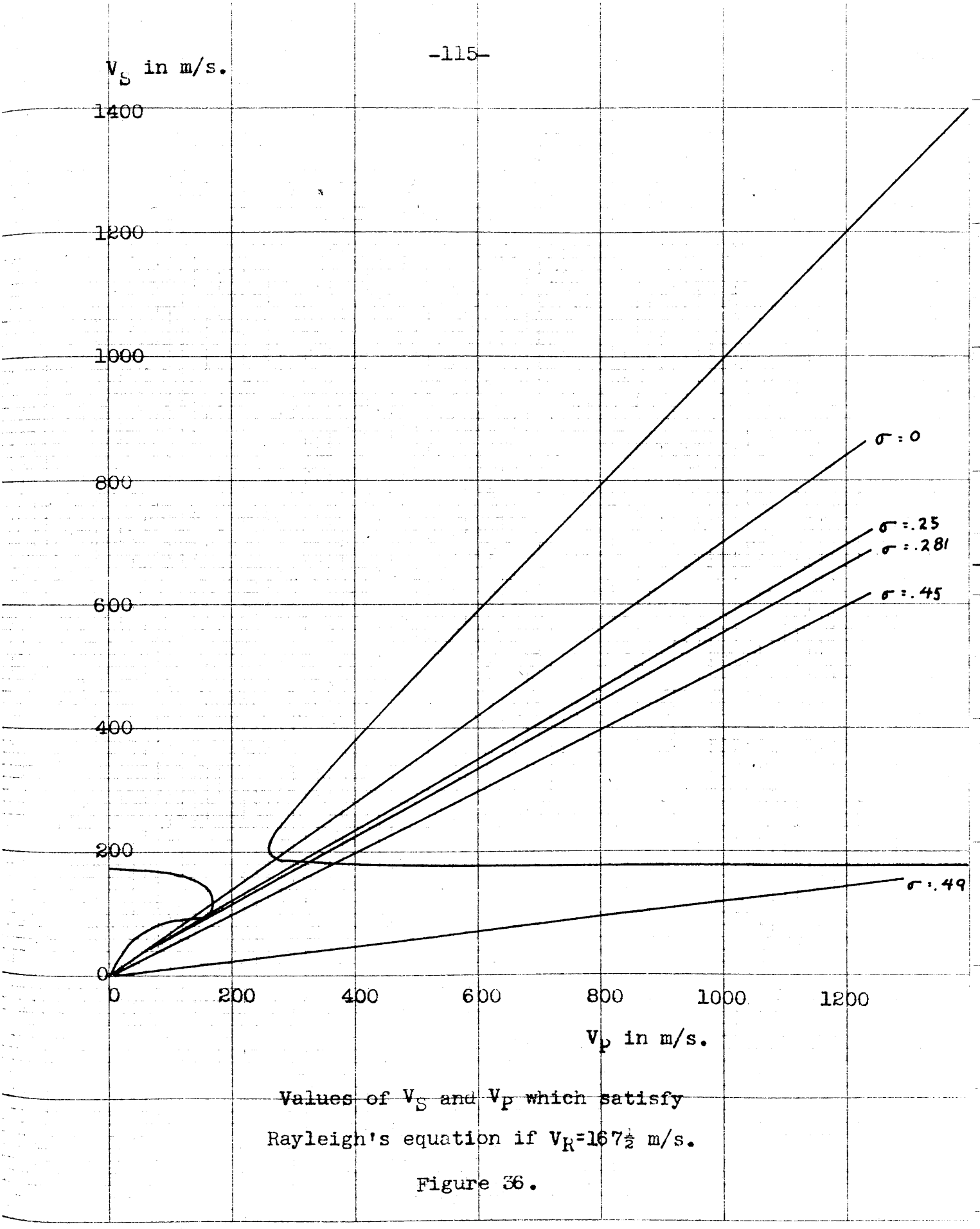

Values of V_S and V_P which satisfy Rayleigh's equation if V_R=167½ m/s.

Figure 36.

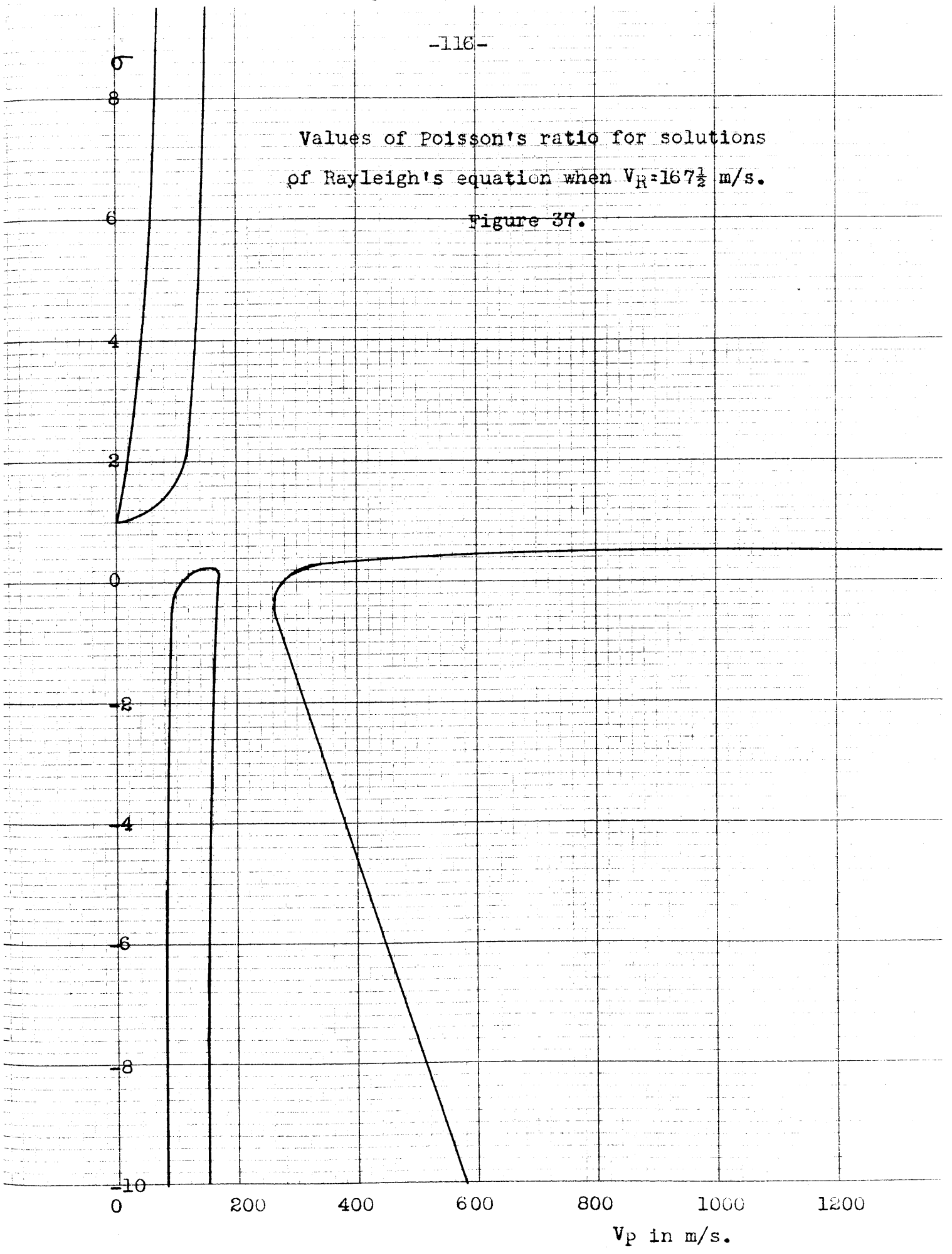

Values of Poisson's ratio for solutions of Rayleigh's equation when $V_R = 167\frac{1}{2}$ m/s.

Figure 37.

velocity lies between 120 m/s. and 735 m/s., a second layer between 29 and 106 meters thick whose compressional wave velocity is 1565 m/s., and a third layer of unknown thickness whose compressional wave velocity is 1950 m/s. Since the wave length of our R waves is of the order of 40 meters, it must penetrate at least into the second layer, and its velocity will be affected by this layer; but since the third layer lies at a depth of the order of a wave length or more from the surface, it will probably be little affected by this material as was shown by Fu (1946, p.21). Neither compressional wave velocity corresponds to the Rayleigh wave velocity for substitution in equation (7-29), as the observed compressional waves being of much shorter wave length were primarily transmitted along distinct paths in each layer though they passed thru both layers; while the Rayleigh waves were transmitted in the two in a more complicated fashion. However, the appropriate V_P, if there is one, presumably lies between 120 m/s. and 1565 m/s., the extremes of the compressional wave velocities in the upper two layers. Thus the observed value of V_R is possible for any value of σ from 0 to .49. Since the wave length of R is over four times the probable maximum depth of the weathered layer, the velocity of V_R is probably more dependent on the elastic constants of the second than the first layer, and therefore, σ must be about .49, neglecting the

negative root. For this value of σ, V_S = 175 m/s. This is so close to the value of V_R that we would expect the direct shear wave, if it existed, to arrive coincident with the Rayleigh waves. No such waves were recognized on the records, though there is sometimes some motion on the transverse component which may represent body shear waves or more likely Love waves. Even if body shear waves did exist, unless they were of larger amplitude than R, they could not be distinguished from it unless they were horizontally polarized.

In section V we suggested that C might be a modified shear wave. On the assumption that at short distances the first arrivals of C represented shear waves travelling in the first layer beneath the weathered layer, we found that C's velocity of 163-200 m/s. corresponded to a Poisson's ratio of from .491-.494. These figures are in good agreement with the values of V_S and Poisson's ratio of 175 m/s. and .49 found from Rayleigh's equation. This agreement supports the idea that the value of V_S of 163-200 m/s. found from the travel-time curves is for a combined layer which corresponds to the first two layers found using the P wave data.

Now let us examine the ratio of the vertical to the horizontal component of motion for Rayleigh waves. From (7-17) and (7-18), at z = 0:

$$\frac{w}{u} = \frac{r\left(1 - \frac{2f^2}{f^2+s^2}\right)}{-if\left(1 - \frac{2rs}{f^2+s^2}\right)} \qquad (7\text{-}32)$$

this can be reduced to:

$$\frac{w}{u} = \frac{-i\left(1 - \frac{1}{2}\left(\frac{V_R}{V_S}\right)^2\right)}{\left(1 - \frac{V_R^2}{V_S^2}\right)^{1/2}} \qquad (7\text{-}33)$$

At any one frequency this equation applies whether the motion is measured in units of displacement, velocity, or acceleration.

We have already solved equation (7-29) for all values of V_S in order to obtain figure 36. Using this data and (7-33) we can obtain w/u as shown in figure 38 for all possible values of V_P.

Note that if V_R exceeds V_S r and s as determined from equations (7-19) thru (7-24) become imaginary; and, therefore, the displacements u and w given by equations (7-17) and (7-18) no longer decrease exponentially with depth. In this case, also, equation (7-32) becomes:

$$\frac{w}{u} = \frac{\pm\left(1 - \frac{V_R^2}{2V_S^2}\right)}{\left(\frac{V_R^2}{V_S^2} - 1\right)^{1/2}} \qquad (7\text{-}34)$$

The motion is no longer either elliptical or confined to the neighborhood of the surface. The solutions of Rayleigh's equation are body waves. The motion is, except in one special case, neither parallel nor perpendicular to the surface along which the waves

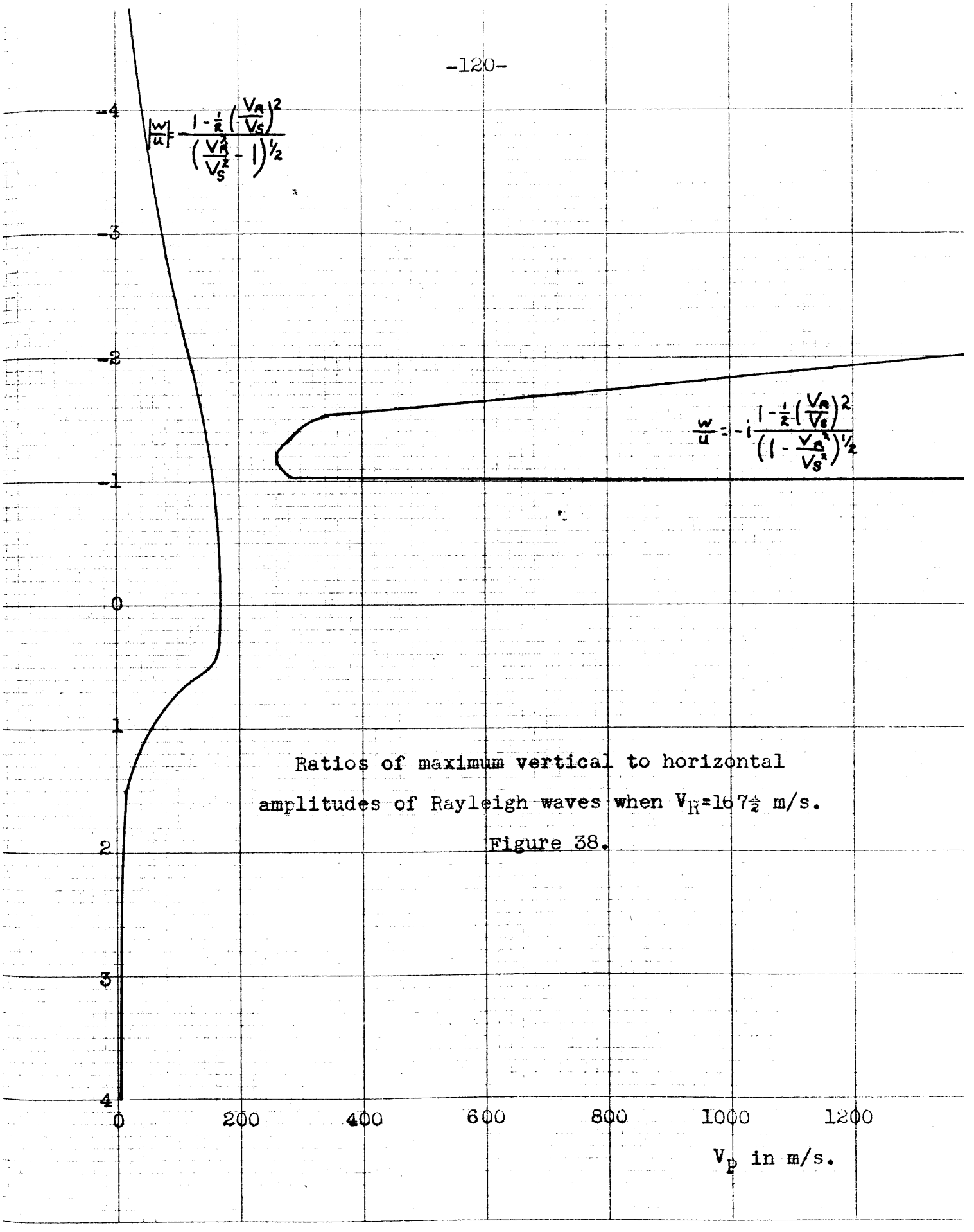

Ratios of maximum vertical to horizontal amplitudes of Rayleigh waves when V_R=167½ m/s.

Figure 38.

are travelling, but is at some intermediate angle. It appears from equation (7-34) that w/u can have any values except $\pm\infty$, which correspond to the cases $V_S = 0$ and $V_S = V_R$ for which Rayleigh's equation is indeterminate or reduces to a contradiction. However, only a small range of these values corresponds to positive values of Poisson's ratio less than $\frac{1}{2}$. This is the range $0 \leq |w/u| \leq .787$. It can be shown that except in the case $V_P = V_R$ the motion is the sum of a compressional and a shear wave of the same frequency arriving from different directions.

The $\pm$ sign in equation (7-34) arises from the uncertainty whether s (and similarly r) becomes of the form $i|s|$ or $-i|s|$. If s is of the former form, then the negative sign applies in (7-34). There is no preferred choice of sign on physical grounds. The compression and shear waves involved in this case must arrive at angles such that their surface velocities are both V_R. Since V_P, V_S and V_R are related by Rayleigh's equation (7-31), there is a fixed relation between these angles. However, the only limitation on the relative amplitudes of the two component waves is that they must satisfy (7-34). If the shear wave can be either in time phase or 180° out of time phase with respect to the compressional wave, then by proper choice of the amplitudes of the two either angle of

motion shown by (7-34) can be realized.

The case w/u = 0 is of interest. Here $(\frac{V_R}{V_S})^2 = 2$, and (7-31) reduces to $(\frac{V_S}{V_P})^2 = \frac{1}{2}$, which means $\sigma = 0$. This is the special case when all three roots of Rayleigh's equation are identical and $V_P = V_R$.

Physically this means that if a body can be compressed without the sides tending to bulge, the Rayleigh wave degenerates into a compressional body wave travelling along the surface and extending to infinite depths. Loose earth is easily compressed, and may very well be a good approximation to this condition. If this is the case then our C waves might be this degenerate type of Rayleigh waves, as noted in section V.

Figure 38 shows that for true Rayleigh waves, where V_S exceeds V_R and the particle motion is elliptical, w/u must exceed 1. Figure 33 (p.104) is a plot of the ratios of the maximum values of the vertical and horizontal velocities as determined from the records. It can be seen that it varies with distance from the shot, but is never more than one. Therefore, the simple theory of surface waves described by Rayleigh is inadequate to explain the observed ground motion, although it agrees with observation in certain important respects. The two principal ways in which R resembles Rayleigh waves are its retrograde elliptical particle motion, and the dying out of the motion with depth.

The particle motion is shown in chart VI. The dying out of the motion with depth has not yet been demonstrated.

The evidence is indirect. As was discussed previously, the R waves are the principal cause of the ground roll from explosions. It is a well known fact that ground roll is pronounced only for explosions at or near the surface, as was pointed out by Sharpe (1942). By analogy with tectonic earthquakes, where the relative amplitudes of the surface to the body waves are less the greater the depth of focus of the earthquake, this decrease in ground roll amplitude with increase in shot depth indicates that the ground roll, or R waves, is also a form of surface wave, and they too must die out with depth.

Stoneley's theory.

Several extensions of Rayleigh's theory have been made to include special surface conditions. Stoneley (1926) has studied the case where a homogeneous isotropic, elastic, half space (the earth) is overlain by a layer of fluid such as water of thickness, h. The coordinates used are a horizontal axis in the interface between the fluid and the solid earth in the direction of propagation of the surface waves, and a vertical axis directed into the layer of fluid. The notation is the same as that used for Rayleigh waves.

The first equation to be satisfied is the equation of continuity in the water (See for instance Stewart and Lindsey, 1930, p.21):

$$\frac{\partial \rho_1}{\partial t} + \frac{\partial(\rho_1 U)}{\partial x} + \frac{\partial(\rho_1 W)}{\partial z} = 0 \qquad (7\text{-}35)$$

where ρ_1 is the density of the water and U and W are the horizontal and vertical velocities. As in the case of Rayleigh waves, it can be shown that because of our choice of coordinates the transverse motion will be zero, so our problem is a two dimensional one.

If we introduce the velocity potential in the water:

$$U = \frac{\partial \phi}{\partial x} \qquad W = \frac{\partial \phi}{\partial z} \qquad (7\text{-}36)$$

(7-35) can be rewritten:

$$\frac{\partial \rho_1}{\partial t} + \rho_1 \nabla^2 \phi + U \frac{\partial \rho_1}{\partial x} + W \frac{\partial \rho_1}{\partial z} = 0 \qquad (7\text{-}37)$$

If we neglect gravity, $U\frac{\partial \rho_1}{\partial x}$, and $W\frac{\partial \rho_1}{\partial z}$ are both of the second order of small quantities, and (7-36) becomes:

$$\frac{\partial \rho_1}{\partial t} + \rho_1 \nabla \phi = 0 \qquad (7\text{-}38)$$

It is well known that in water (see for instance Stewart and Lindsey, 1930, p.27-28):

$$\frac{d\rho_w}{d\rho_1} = \frac{k}{\rho_1} = V_o^2 \qquad (7\text{-}39)$$

Where V_o is the velocity of compressional waves in water, k is the bulk modulus of water, and p_w is the pressure in the water.

Using (7-38) and (7-39) we get:

$$\frac{\partial \rho_w}{\partial t} = \frac{\partial \rho_1}{\partial t}\cdot\frac{d\rho_w}{d\rho_1} = -\frac{k}{\rho_1}\rho_1 \nabla^2 \Phi = -k\nabla^2\Phi \qquad (7\text{-}40)$$

which is the equation of motion in the water. As in the case of Rayleigh's analysis, the equations of motion in the solid are:

$$\rho_2 \frac{\partial^2 u}{\partial t^2} = (\lambda+\mu)\frac{\partial \theta}{\partial x} + \mu\nabla^2 u \qquad (7\text{-}41)$$

$$\rho_2 \frac{\partial^2 w}{\partial t^2} = (\lambda+\mu)\frac{\partial \theta}{\partial z} + \mu\nabla^2 w \qquad (7\text{-}42)$$

where ρ_2 is the density in the earth, λ and μ are Lame's constants, and u and w are the particle displacements. θ is again the cubical dilatation:

$$\theta = \frac{\partial u}{\partial x} + \frac{\partial w}{\partial z} \qquad (7\text{-}43)$$

Next we have the boundary conditions. The vertical velocity must be continuous across the interface between solid and fluid:

$$\frac{\partial \Phi}{\partial z} = \frac{\partial w}{\partial t} \qquad \text{at } z = 0 \qquad (7\text{-}44)$$

The horizontal traction at the interface is 0:

$$\frac{\partial w}{\partial x} + \frac{\partial u}{\partial z} = 0 \qquad \text{at } z = 0 \qquad (7\text{-}45)$$

The vertical traction is continuous across the interface:

$$\frac{\partial \rho_w}{\partial t} = \frac{\partial}{\partial t}\left\{(\lambda+2\mu)\frac{\partial w}{\partial z} + \lambda\frac{\partial u}{\partial z}\right\} \qquad \text{at } z = 0 \qquad (7\text{-}46)$$

At the free surface there is no stress:

$$p_w = 0 \qquad \text{at } z = h \qquad (7\text{-}47)$$

The wave motion which satisfies these conditions is:

$$\phi = A \frac{\sin f_1(z-h)}{f \cos f_1 h} e^{if(x - V_R t)} \tag{7-48}$$

where:

$$f_1^2 = f^2\left(\frac{V_R^2}{V_o^2} - 1\right) \tag{7-49}$$

and A is an amplitude constant.

$$U = \frac{\partial \phi}{\partial x} = if\phi \tag{7-50}$$

$$W = \frac{\partial \phi}{\partial z} = f_1\left[\cot f_1(z-h)\right]\phi \tag{7-51}$$

The necessary condition for the existence of such waves is:

$$\frac{f V_S^2 k \tan f_1 h}{f_1 \mu_2 V_o^2} = \frac{V_S^4}{V_R^4}\left[4\left(1 - \frac{V_R^2}{V_S^2}\right)^{1/2} - \frac{f}{r}\left(2 - \frac{V_R^2}{V_S^2}\right)^2\right] \tag{7-52}$$

We know that:

$$r^2 = f^2 - h_R^2 \tag{7-21}$$

$$h_R^2 = f^2 \frac{V_R^2}{V_P^2} \tag{7-24}$$

$$\frac{k}{\rho_1} = V_o^2 \tag{7-39}$$

and

$$V_S^2 = \frac{\mu}{\rho_2} \tag{7-53}$$

Using these relationships, (7-52) becomes:

$$\frac{\rho_1 \tan f_1 h}{\rho_2 f_1} = \frac{V_S^4}{V_R^4}\left[4\left(1 - \frac{V_R^2}{V_S^2}\right)^{1/2} - \frac{\left(2 - \frac{V_R^2}{V_S^2}\right)^2}{\left(1 - \frac{V_R^2}{V_P^2}\right)^{1/2}}\right] \tag{7-54}$$

(Since f_1 occurs in these equations in the form $\frac{\tan f_1 h}{f_1}$ we need not be concerned with its sign as long as $f_1 h$ lies in the first quadrant. This argument still applies if f_1 is imaginary, since $\frac{\tanh f_1 h}{f_1}$ is always positive. Discussion of how other values of f_1 than the one observed would effect the equations is beyond the scope of this work.)

Using (7-49), (7-54) becomes:

$$\frac{V_R^4 \rho_1}{V_S^4 \rho_2} \tan f_1 h \frac{\left(1 - \frac{V_R^2}{V_P^2}\right)^{1/2}}{\left(\frac{V_R^2}{V_0^2} - 1\right)^{1/2}} = \left[4\left(1 - \frac{V_R^2}{V_S^2}\right)^{1/2}\left(1 - \frac{V_R^2}{V_P^2}\right)^{1/2} - \left(2 - \frac{V_R^2}{V_S^2}\right)^2\right] \tag{7-55}$$

Let us define

$$\frac{V_R^2}{V_P^2} = X \qquad \frac{V_R^2}{V_S^2} = Y \qquad \frac{V_R^2}{V_0^2} = Z \tag{7-56}$$

(7-55) becomes:

$$Y^2 \frac{\rho_1}{\rho_2}\left(\tan f_1 h\right)\left(\frac{1 - X}{Z - 1}\right)^{1/2} = 4(1-Y)^{1/2}(1-X)^{1/2} - (2-Y)^2 \tag{7-57}$$

If we further define

$$\frac{4}{C} = \left[\left(\frac{\rho_1}{\rho_2}\right)\frac{(1-X)^{1/2}}{(Z-1)^{1/2}} \tan f_1 h \quad + 1\right] \tag{7-58}$$

(7-57) becomes:

$$\left(\frac{4}{C} - 1\right)Y^2 = 4(1-Y)^{\frac{1}{2}}\ (1-X)^{\frac{1}{2}} - (2-Y)^2 \tag{7-59}$$

or

$$\frac{4Y^2}{C} - 4Y + 4 = 4(1-Y)^{\frac{1}{2}}\,(1-X)^{\frac{1}{2}} \qquad (7\text{-}60)$$

On dividing by 4 and squaring:

$$\frac{Y^4}{C^2} - \frac{2Y^3}{C} + (\frac{2}{C}+1)Y^2 - 2Y + 1 = 1 - X - Y + XY \qquad (7\text{-}61)$$

or

$$Y^4 - 2CY^3 + (2C + C^2)Y^2 - C^2(1+X)Y + C^2X = 0 \qquad (7\text{-}62)$$

if $C = 4$, this becomes:

$$Y^4 - 8Y^3 + 24Y^2 - 16(1+X)Y + 16X = 0 \qquad (7\text{-}63)$$

Or in the ordinary notation:

$$\frac{V_R^8}{V_S^8} - 8\frac{V_R^6}{V_S^6} + 24\frac{V_R^4}{V_S^4} - 16\frac{V_R^2}{V_S^2} - \frac{16V_R^4}{V_S^2 V_P^2} - 16\frac{V_R^2}{V_P^2} = 0 \qquad (7\text{-}64)$$

which is simply equation (7-29). Therefore, when $C = 4$ the condition (7-52) reduces to Rayleigh's condition. This is the case if:

$$\left(\frac{4}{C}-1\right) = \frac{\rho_1(1-X)^{1/2}}{\rho_2(2-1)^{1/2}}\tan f_1 h = \frac{\rho_1\left(1-\frac{V_R^2}{V_P^2}\right)^{1/2}}{\rho_2\left(\frac{V_R^2}{V_0^2}-1\right)^{1/2}}\tan\left[2\pi\frac{h}{L}\left(\frac{V_R^2}{V_0^2}-1\right)^{1/2}\right] \qquad (7\text{-}65)$$

Where L is the wave length. If V_0 is greater than V_R:

$$\left(\frac{4}{C}-1\right) = \frac{\rho_1\left(1-\frac{V_R^2}{V_P^2}\right)^{1/2}}{\rho_2\left(1-\frac{V_R^2}{V_0^2}\right)^{1/2}}\tanh\ 2\pi\frac{h}{L}\left(1-\frac{V_R^2}{V_0^2}\right)^{1/2} \qquad (7\text{-}66)$$

$(\frac{4}{C}-1) \approx 0$ if $\rho_1 \ll \rho_2$, $V_R \approx V_P$, or $h \ll L$.

$V_R = V_P$ corresponds to the special case where all four roots of (7-64) are $Y = 2 = \frac{V_R^2}{V_S^2}$. In this case, as pointed out earlier, $\sigma = 0$, which is a very special and unusual condition. The meanings of the other two conditions where $(\frac{4}{c}-1)\approx 0$ are obvious.

This means that if a solid such as the earth is overlain by a light or thin layer of fluid, beneath this layer Rayleigh waves can be transmitted with velocities identical with normal Rayleigh waves, but if the conditions are other than this, the waves will have different velocities. It is possible that under the proper conditions, Rayleigh waves can not exist at all under a fluid layer.

If we consider the air to be a fluid layer, since $\rho_1 \ll \rho_2$, $C\approx 4$, and equation (7-66) will apply if our R waves are this sort of Rayleigh waves.

Dividing (7-51) by (7-50):

$$\frac{W}{U} = \frac{-if_1 \cot f_1(z-h)}{f} \qquad (7\text{-}67)$$

Using (7-49) this becomes at $z = 0$:

$$\frac{W}{U} = i\left(1-\frac{V_R^2}{V_0^2}\right)^{1/2} \coth\left[\frac{2\pi h}{L}\left(1-\frac{V_R^2}{V_0^2}\right)^{1/2}\right] \qquad (7\text{-}68)$$

Since for air V_0 equals 344 m./sec. (Stewart and Lindsey, 1930, p.328), and V_R equals 167½ m./sec. from the travel-time curve:

$$\frac{W}{U} = +i\ .874 \coth\ 5.49\frac{h}{L} \qquad (7\text{-}69)$$

Unless $h < L$, $\coth 5.49\frac{h}{L}\approx 1$, and the motion in the

air is retrograde elliptical with the amplitude of the vertical component .874 times the amplitude of the horizontal. (Remember that Stoneley's vertical axis is directed oppositely from Rayleigh's, so that in this case the + sign corresponds to retrograde motion, whereas previously the reverse was true.) Comparing this with figure 32 we see that the calculated amplitude ratio is of the same order of magnitude as those observed. If $h < L$, $\coth 5.49 \frac{h}{L} > 1$, and W/U becomes larger as the ratio h/L decreases.

These figures, however, are for the amplitudes in the air, not those in the ground. To find the motion in the ground we must calculate u and w. These are given by Stoneley as:

$$u = \left(- \frac{V_P^2}{f V_R^2} i E e^{rz} - s Q e^{sz} \right) e^{if(x - V_R t)} \tag{7-70}$$

$$w = \left(- \frac{V_P^2}{f^2 V_R^2} r E e^{rz} + i f Q e^{sz} \right) e^{if(x - V_R t)} \tag{7-71}$$

Substituting these in (7-45) at $z = 0$:

$$if \left(- \frac{V_P^2}{f^2 V_R^2} r E + i f Q \right) + \left(- \frac{V_P^2}{f V_R^2} i r E - s^2 Q \right) = 0 \tag{7-72}$$

This reduces to:

$$Q = -i \frac{2 \frac{r V_P^2}{f V_R^2}}{f^2 + s^2} E \tag{7-73}$$

Substituting this in (7-70) and (7-71), at $z = 0$:

$$u = -i \frac{E V_P^2}{f V_R^2} \left(\frac{f^2 + s^2 - 2rs}{f^2 + s^2} \right) e^{if(x - V_R t)} \tag{7-74}$$

$$w = -\frac{E V_\rho^2}{f^2 V_R^2}\left(\frac{r(s^2-f^2)}{f^2+s^2}\right)e^{if(x-V_R t)} \tag{7-75}$$

Therefore:

$$\frac{w}{u} = \frac{r(s^2-f^2)}{if(f^2+s^2-2rs)} = -i\,\frac{r\left(\frac{s^2}{f^2}-1\right)}{f\left(1+\frac{s^2}{f^2}-\frac{2rs}{f^2}\right)} \tag{7-76}$$

From (7-21) thru (7-24) and (7-26):

$$\frac{r^2}{f^2} = 1 - \frac{V_R^2}{V_\rho^2} \tag{7-77}$$

$$\frac{s^2}{f^2} = 1 - \frac{V_R^2}{V_S^2} \tag{7-78}$$

Substituting these in (7-78):

$$\frac{w}{u} = -i\,\frac{\left(1-\frac{V_R^2}{V_\rho^2}\right)^{1/2}\left(-\frac{V_R^2}{V_S^2}\right)}{2-\frac{V_R^2}{V_S^2}-2\left(1-\frac{V_R^2}{V_\rho^2}\right)^{1/2}\left(1-\frac{V_R^2}{V_S^2}\right)^{1/2}} \tag{7-79}$$

(We use the positive roots of r^2 and s^2 since we are considering only waves which die out with increasing depth.)

(7-59) can be written:

$$\left(\frac{4}{C}-1\right)\frac{V_R^4}{V_S^4} = 4\left(1-\frac{V_R^2}{V_S^2}\right)^{1/2}\left(1-\frac{V_R^2}{V_\rho^2}\right)^{1/2}-\left(2-\frac{V_R^2}{V_S^2}\right)^2 \tag{7-80}$$

Which can be rearranged to give:

$$\left(1-\frac{V_R^2}{V_\rho^2}\right)^{1/2} = \frac{\left(\frac{4}{C}-1\right)\frac{V_R^4}{V_S^4}+\left(2-\frac{V_R^2}{V_S^2}\right)^2}{4\left(1-\frac{V_R^2}{V_S^2}\right)^{1/2}} \tag{7-81}$$

Substituting this in (7-79) and simplifying:

$$\frac{w}{u} = i\,\frac{\frac{1}{2}\left[\left(\frac{4}{C}-1\right)\frac{V_R^4}{V_S^4}+\left(2-\frac{V_R^2}{V_S^2}\right)^2\right]}{\left(1-\frac{V_R^2}{V_S^2}\right)^{1/2}\left[\left(2-\frac{V_R^2}{V_S^2}\right)-\left(\frac{4}{C}-1\right)\frac{V_R^2}{V_S^2}\right]} \qquad (7\text{-}82)$$

If $(\frac{4}{C}-1) = 0$ this reduces to (7-33), the w/u for true Rayleigh waves, except that the sign is reversed since Stoneley's z axis is oppositely directed from Rayleigh's. For real positive values of $r = f(1-\frac{V_R^2}{V_P^2})^{\frac{1}{2}}$, $(\frac{4}{C}-1)$ is positive, as shown by (7-66). Therefore w/u is greater than the w/u obtained from Rayleigh's theory. Thus the values of this ratio found assuming that the air is a fluid layer of Stoneley's type is not any closer to the observed ones than those shown in figure 38.

If it is the air acting in the manner described by Stoneley which causes the low values of w/u observed, then the surface of the ground must be behaving as if it were a part of that medium instead of a part of the ground. This suggests an explanation of why we observe only relatively low frequency surface waves. The transition from the air to the ground may be so gradual that it looks like a sharp boundary only to vibratory movements whose wave lengths exceed a certain value. Vibrations of shorter wave length might not be transmitted by such an interface at all.

The air is not of constant density as was assumed in the above derivation; but it is much thicker than a wave length, and the density changes very slowly with height, so that the arguments may apply reasonably well to an ideal earth. It must not be forgotten, however, that the real earth differs greatly from the ideal one assumed in this derivation.

Stoneley derived his equations to describe the effect of a layer of water on the surface waves in the interface beneath the water. We might ask, next, if we could treat the weathered layer in the Los Alamitos area as a fluid layer, and then study the effect on the Rayleigh type waves. In this case, since our observations would then have to be made at $z = h$, equation (7-50) reduces to $U = 0$, which is not the case; so this approach is of no assistance in understanding the actual motion.

Bateman's theory.

A somewhat similar approach has been made by Bateman (1938). He assumed that the half-space was overlain by a layer of gas of thickness h, which acted as a cushion, so that the upper surface of the layer was not displaced. The justification of this assumption is beyond the scope of this work. Bateman believed that certain aspects of loudspeaker theory supported it. The coordinate axes are a horizontal

axis lying in the surface of the half space in the direction of propagation of the waves, and a vertical axis directed into the solid half-space. Bateman took into account the velocity of any wind which might be moving the air, but we will neglect the effect of such movements. Gravity is neglected also. Since the air is a fluid, the basic equation to be satisfied is:

$$\frac{\partial^2 \phi}{\partial t^2} = V_A^2 \nabla^2 \phi \qquad (7\text{-}83)$$

V_A is the sound velocity in the air. Otherwise our notation is the same as previously.

The solution must also satisfy the wave equations in the ground:

$$\rho \frac{\partial^2 u}{\partial t^2} = (\lambda + \mu) \frac{\partial \theta}{\partial x} + \mu \nabla^2 u \qquad (7\text{-}84)$$

$$\rho \frac{\partial^2 w}{\partial t^2} = (\lambda + \mu) \frac{\partial \theta}{\partial z} + \mu \nabla^2 w \qquad (7\text{-}85)$$

Where ρ is the density of the ground, u and w are the particle displacements. The equation for v is omitted since it can be shown that there is no component in this direction.

The first boundary condition is that there be no vertical velocity at the top of the layer of air:

$$\frac{\partial \phi}{\partial z} = 0 \qquad \text{at } z = h \qquad (7\text{-}86)$$

Secondly, the vertical velocity must be continuous across the interface between the air and solid:

$$\frac{\partial w}{\partial t} = \frac{\partial \phi}{\partial z} \qquad \text{at } z = 0 \qquad (7\text{-}87)$$

Thirdly, neglecting any viscous drag of the air at the interface, there must be no shearing traction here:

$$\frac{\partial u}{\partial z} + \frac{\partial w}{\partial x} = 0 \qquad \text{at } z = 0 \qquad (7\text{-}88)$$

Fourthly, the normal excess pressure of the air must equal the normal traction at the interface:

$$\rho_A \frac{\partial \phi}{\partial t} = \rho V_\rho^2 \left(\frac{\partial u}{\partial x} + \frac{\partial w}{\partial z} \right) - 2\rho V_S^2 \frac{\partial u}{\partial x} \qquad (7\text{-}89)$$

ρ_A is the density of the air.

The wave motion which satisfies these equations and is confined to the neighborhood of the surface is:

$$U = -2ifK_B \cosh f_B(z+h)\, e^{-if(x-V_R t)} \qquad (7\text{-}90)$$

$$W = 2f_B K_B \sinh f_B(z+h)\, e^{-if(x-V_R t)} \qquad (7\text{-}91)$$

where

$$f_B^2 = f^2 \left(1 - \frac{V_R^2}{V_A^2}\right) \qquad (7\text{-}92)$$

U and W are the particle velocities in the air, and K_B is an amplitude constant. The other symbols are the same as used up till now.

The condition for the existence of such waves is:

$$\rho V_S^4 \left(1 - \frac{V_R^2}{V_A^2}\right)^{1/2} (\tanh f_B h) \left[4\left(1 - \frac{V_R^2}{V_\rho^2}\right)^{1/2} \left(1 - \frac{V_R^2}{V_S^2}\right)^{1/2} - \left(2 - \frac{V_R^2}{V_S^2}\right)^2 \right] \qquad (7\text{-}93)$$

$$= \rho_A V_R^4 \left(1 - \frac{V_R^2}{V_\rho^2}\right)^{1/2}$$

Which can be rearranged in the form:

$$\frac{\rho_A V_R^4 \left(1-\frac{V_A^2}{V_P^2}\right)^{1/2}}{\rho V_S^4 \left(1-\frac{V_A^2}{V_A^2}\right)^{1/2}} \coth f_B h = 4\left(1-\frac{V_A^2}{V_S^2}\right)^{1/2}\left(1-\frac{V_A^2}{V_P^2}\right)^{1/2} - \left(2-\frac{V_R^2}{V_S^2}\right)^2 \qquad (7\text{-}94)$$

Which differs from (7-55) only in the presence of

$$\rho_A \frac{\coth f_B h}{\left(1-\frac{V_R^2}{V_A^2}\right)^{1/2}} \quad \text{instead of} \quad \rho_1 \frac{\tan f_1 h}{\left(\frac{V_R^2}{V_0^2}-1\right)^{1/2}} = \rho_1 \frac{\tanh i f_1 h}{\left(1-\frac{V_R^2}{V_0^2}\right)^{1/2}}$$

For $f_1 h > 2.65$, $\tanh f_1 h = 1 = \coth f_1 h$ to within 1%. Therefore Bateman's and Stoneley's conditions are alike if

$$f_1 h = 2\pi \frac{h}{L}\left(1-\frac{V_R^2}{V_A^2}\right)^{1/2} > 2.65 \qquad (7\text{-}95)$$

Since for air $V_A = 344$ m/s., and $V_R = 167\frac{1}{2}$ m/s.:

$$f_1 h = 5.49\, h/L \qquad (7\text{-}96)$$

and equation (7-95) is satisfied unless the layer of air is very thin.

For Bateman's condition (7-58) becomes:

$$\frac{1}{C_B} = \frac{1}{4}\left[\frac{\rho_A\left(1-\frac{V_R^2}{V_P^2}\right)^{1/2}}{\rho\left(1-\frac{V_R^2}{V_A^2}\right)^{1/2}}\left\{\coth 2\pi\frac{h}{L}\left(1-\frac{V_R^2}{V_A^2}\right)^{1/2}\right\}+1\right] \qquad (7\text{-}97)$$

If we assume $\rho_A = .001205$ g/cc. (Stewart and Lindsey, 1930, p.328), $\rho = 1.7$ g/cc., $\coth f_1 h = 1$, and if V_P exceeds V_R, C is between 3.996 and 4. Thus the velocities of the surface waves will be the same as those found using Rayleigh's equation unless the layer

of air is very thin. This is true if the air is treated as a fluid with a free surface as Stoneley did, or if it is treated as a cushion as Bateman did.

Using equations (7-90) and (7-91):

$$\frac{W}{U} = i \frac{f_B}{f} \tanh f_B(z+h) \tag{7-98}$$

Using also equations (7-19) and (7-92):

$$\frac{W}{U} = i\left(1 - \frac{V_R^2}{V_A^2}\right)^{1/2} \tanh\left[2\pi \frac{z+h}{L}\left(1 - \frac{V_R^2}{V_A^2}\right)^{1/2}\right] \tag{7-99}$$

Compare this with (7-67) which can be written:

$$\frac{W}{U} = i\left(1 - \frac{V_R^2}{V_0^2}\right)^{1/2} \coth\left[2\pi \frac{h-z}{L}\left(1 - \frac{V_R^2}{V_0^2}\right)^{1/2}\right] \tag{7-100}$$

(7-99) and (7-100) are similar in form if we recall that z is oppositely directed in the two sets of coordinate axes.

Since for our case:

$$\tanh 2\pi \frac{z+h}{L}\left(1 - \frac{V_R^2}{V_A^2}\right)^{1/2} \approx 1 \approx \coth 2\pi \frac{h-z}{L}\left(1 - \frac{V_R^2}{V_0^2}\right)^{1/2} \tag{7-101}$$

at z = 0, in the air:

$$\frac{W}{U} = i\left(1 - \frac{V_R^2}{V_A^2}\right)^{1/2} = i.874 \tag{7-102}$$

as discussed previously.

In the ground in Bateman's case:

$$u = \left(if P_B e^{-rz} + is Q_B e^{-sz}\right) e^{if(x - V_R t)} \tag{7-103}$$

$$w = \left(r P_B e^{-rz} + f Q_B e^{-sz}\right) e^{if(x - V_R t)} \tag{7-104}$$

This is of the same form as (7-70) and (7-71), and similarly, it can be shown that it yields the relation:

$$\frac{w}{u} = i \frac{\left(1 - \frac{V_R^2}{V_P^2}\right)^{1/2} \frac{V_R^2}{V_S^2}}{2 - \frac{V_R^2}{V_S^2} - 2\left(1 - \frac{V_R^2}{V_P^2}\right)^{1/2}\left(1 - \frac{V_R^2}{V_S^2}\right)^{1/2}} \tag{7-105}$$

If we write (7-94) in the form:

$$\frac{V_R^2}{V_S^2}\left(\frac{4}{C_B} - 1\right) = 4\left(1 - \frac{V_R^2}{V_P^2}\right)^{1/2}\left(1 - \frac{V_R^2}{V_S^2}\right)^{1/2} - \left(2 - \frac{V_R^2}{V_S^2}\right)^2 \tag{7-106}$$

Where:

$$\left(\frac{4}{C_B} - 1\right) = \frac{\rho_A \left(1 - \frac{V_R^2}{V_P^2}\right)^{1/2}}{\rho \left(1 - \frac{V_R^2}{V_A^2}\right)^{1/2}} \coth 2\pi \frac{h}{L}\left(1 - \frac{V_R^2}{V_A^2}\right)^{1/2} \tag{7-107}$$

and use it to clear (7-105) of $(1 - \frac{V_R^2}{V_P^2})^{\frac{1}{2}}$, we get:

$$\frac{w}{u} = i \frac{\frac{1}{2}\left[\left(\frac{4}{C_B} - 1\right)\frac{V_R^4}{V_S^4} + \left(2 - \frac{V_R^2}{V_S^2}\right)^2\right]}{\left(1 - \frac{V_R^2}{V_S^2}\right)^{1/2}\left[\left(2 - \frac{V_R^2}{V_S^2}\right) - \left(\frac{4}{C_B} - 1\right)\frac{V_R^2}{V_S^2}\right]} \tag{7-108}$$

This is identical to (7-82) except that C_B replaces C. Thus the same arguments apply as in Stoneley's case.

Therefore, either Bateman's and Stoneley's assumptions lead to equations which predict motion with w/u larger than that observed, or the surface material itself reacts like the lower part of the fluid layer of which the air is the upper part.

Meissner's theory.

The problem was approached in a slightly different way by Meissner (1922). He assumed that a layer of density ρ_L and thickness h overlies the half space of Rayleigh. The layer is inert in that its only effect is to exert a force on the surface of the half space. The coordinate axes are the same as in Rayleigh's and Bateman's analyses, a horizontal axis in the interface in the direction of propagation, and a vertical axis into the solid half space. The basic equations to be satisfied are again the wave equations:

$$\rho \frac{\partial^2 u}{\partial t^2} = (\lambda + \mu) \frac{\partial \theta}{\partial x} + \mu \nabla^2 u \qquad (7\text{-}9)$$

$$\rho \frac{\partial^2 w}{\partial t^2} = (\lambda + \mu) \frac{\partial \theta}{\partial w} + \mu \nabla^2 w \qquad (7\text{-}11)$$

(As usual the equation involving v can be omitted, as v will be zero). The notation is that used for Bateman's and Stoneley's equations. The boundary conditions are that the added load of the layer equal the tractions at the interface:

$$\omega \frac{\partial^2 u}{\partial t^2} = \mu \left(\frac{\partial u}{\partial z} + \frac{\partial w}{\partial x} \right) \qquad (7\text{-}109)$$

$$\omega \frac{\partial^2 w}{\partial t^2} = \lambda \theta + 2\mu \frac{\partial w}{\partial z} \qquad (7\text{-}110)$$

where ω is the load at the surface, and is equal to ρ_L h per unit area.

The solution which satisfies these equations and is confined to the neighborhood of the interface

is:

$$u = \frac{K_M}{f h_R^2}\left[f^2 e^{-rz} + s\beta e^{-sz}\right] \sin\left(fx + pt - \alpha_M\right) \tag{7-111}$$

$$w = \frac{K_M}{h_R^2}\left[re^{-rz} + \beta e^{-sz}\right] \cos\left(fx + pt - \alpha_M\right) \tag{7-112}$$

where K_M is an amplitude constant, α_M is a phase angle, and

$$\beta = \frac{\frac{\omega}{\mu}\rho^2 r - 2f^2 + k_R^2}{2s - \frac{\omega}{\mu}\rho^2} \tag{7-113}$$

The condition for the existence of such waves is:

$$L'^2\left[4\left(1-\frac{V_R^2}{V_P^2}\right)^{1/2}\left(1-\frac{V_R^2}{V_S^2}\right)^{1/2} - \left(2-\frac{V_R^2}{V_S^2}\right)^2\right] - L'\frac{V_R^4}{V_S^4}\left[\left(1-\frac{V_R^2}{V_S^2}\right)^{1/2} + \left(1-\frac{V_R^2}{V_P^2}\right)^{1/2}\right] + \left[1-\left(1-\frac{V_R^2}{V_P^2}\right)^{1/2}\left(1-\frac{V_R^2}{V_S^2}\right)^{1/2}\right]\frac{V_R^4}{V_S^4} = 0 \tag{7-114}$$

where $L' = \frac{\rho}{f\omega} = \frac{L\rho}{2\pi h \rho_L}$ (7-115)

Using the abbreviations of equation (7-56):

$$\frac{V_R^2}{V_P^2} = X \qquad \frac{V_R^2}{V_S^2} = Y \tag{7-56}$$

(7-114) becomes:

$$L'^2\left[4(1-X)^{\frac{1}{2}}(1-Y)^{\frac{1}{2}} - (2-Y)^2\right] - L'Y^2\left[(1-Y)^{\frac{1}{2}} + (1-X)^{\frac{1}{2}}\right] + Y^2\left[1-(1-X)^{\frac{1}{2}}(1-Y)^{\frac{1}{2}}\right] = 0 \tag{7-116}$$

This can be solved for $(1-X)^{\frac{1}{2}}$ giving:

$$(1-X)^{\frac{1}{2}} = \frac{L'^2(2-Y)^2 + L'Y^2(1-Y)^{\frac{1}{2}} - Y^2}{4L'^2(1-Y)^{\frac{1}{2}} - L'Y^2 - Y^2(1-Y)^{\frac{1}{2}}} \tag{7-117}$$

Since V_R is known from the travel time curves, (7-117) is essentially an equation telling what values V_P must have for different L' and V_S to give the observed V_R. If we assume that the load is provided by the surface layer whose thickness we computed in section IV, then $1.2m. \leq h \leq 8.4m.$ If the density of the weathered layer approximately equals that of the material immediately below the weathered layer, $\rho = \rho_L$; and since the wave length is of the order of 40 meters, the range of L' is approximately $.75 \leq L' \leq 5.3$. Figure 39 shows V_P against V_S for L' = .75, 2 and 5.3. If L' = 2 or 5.3 there is only one real range for which solutions exist for (7-117); but if L' = .75 there are two ranges. These are not the same two ranges that we observed earlier for true Rayleigh waves, since in Meissner's case both occur where V_P and V_S both exceed V_R. When the body wave velocities are less than the surface wave velocities, (7-117) becomes complex.

Thus the special, degenerate solutions of Rayleigh's equation described earlier in which the motion is non-elliptical, and which can exist if V_R exceeds V_P when there is no surface load do not appear as solutions of the equations under the conditions assumed by Meissner.

Meissner (loc. cit.) has also shown that the ratio of the amplitudes of the vertical to horizontal components of motion is:

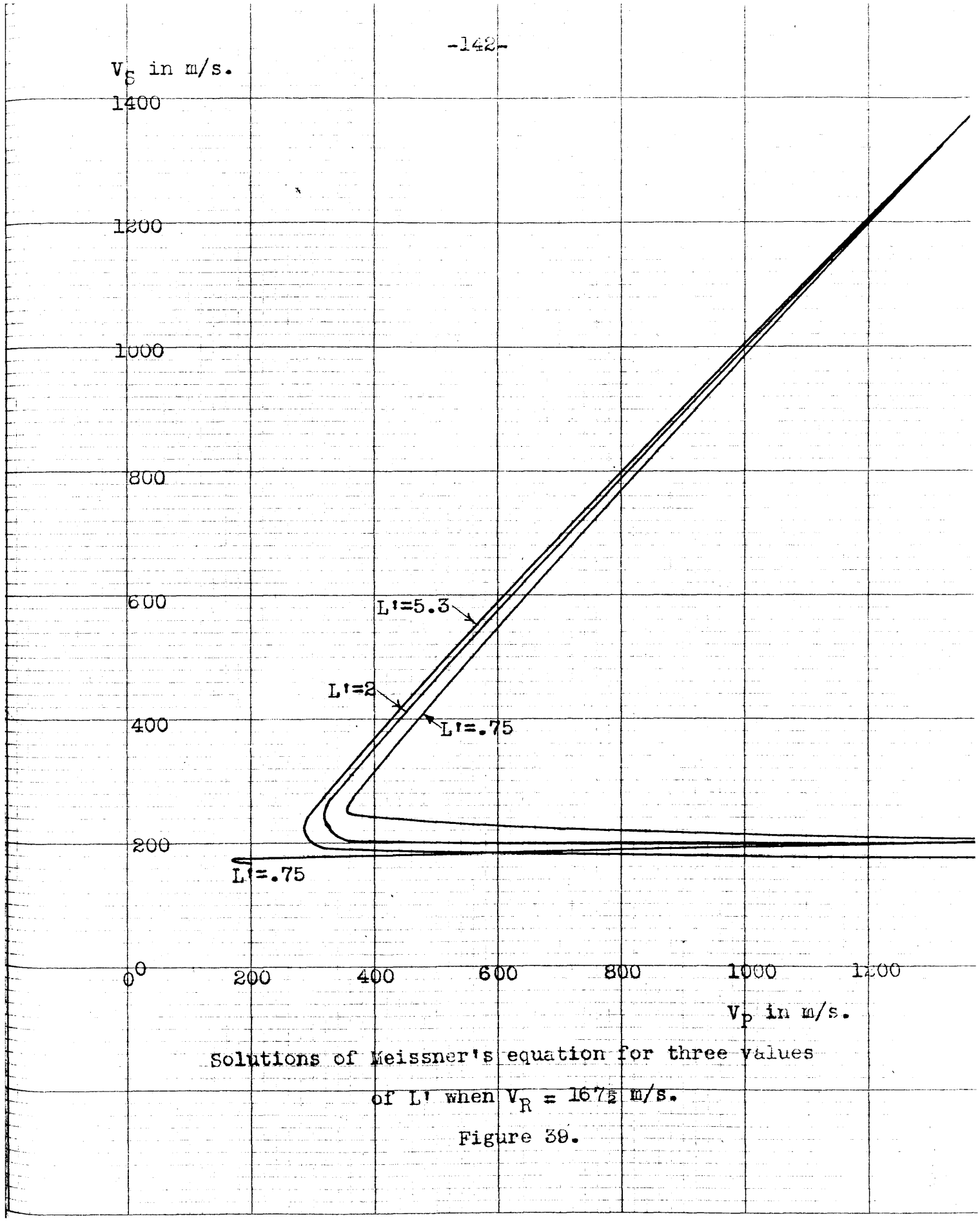

Solutions of Meissner's equation for three values of L' when V_R = 1675 m/s.

Figure 39.

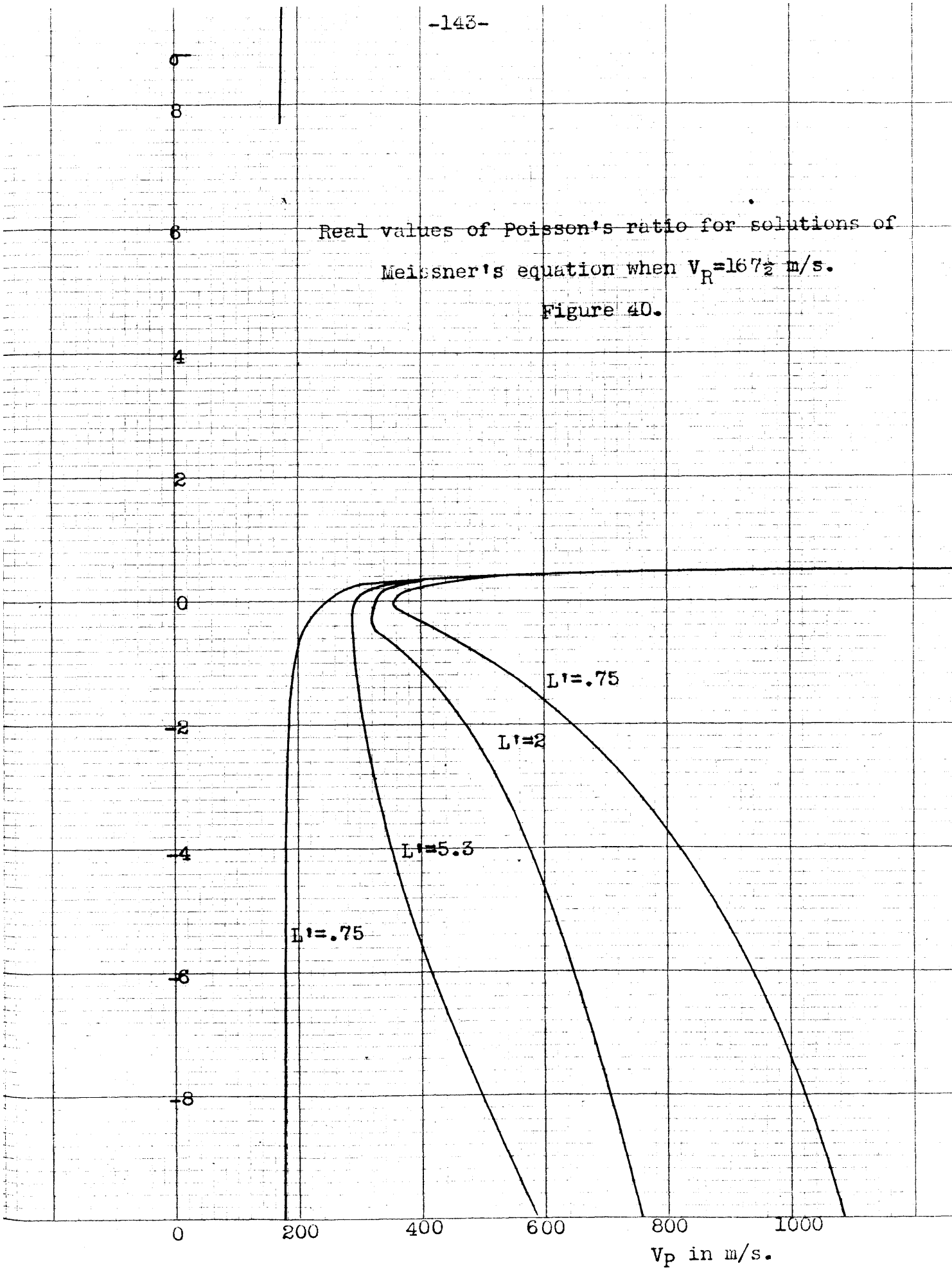

Real values of Poisson's ratio for solutions of Meissner's equation when V_R=167½ m/s.

Figure 40.

$$\frac{W}{U} = \left| \frac{\frac{V_R^2}{V_S^2} + 2\left(1-\frac{V_R^2}{V_S^2}\right)^{1/2}\left(1-\frac{V_R^2}{V_P^2}\right)^{1/2} - 2}{\frac{V_R^2}{V_S^2}\left[\left(1-\frac{V_R^2}{V_S^2}\right)^{1/2} - \frac{1-\left(1-\frac{V_R^2}{V_S^2}\right)^{1/2}\left(1-\frac{V_R^2}{V_P^2}\right)^{1/2}}{L'}\right]} \right| \qquad (7\text{-}118)$$

or in our abbreviated notation:

$$\frac{W}{U} = \left| \frac{L'_X Y + 2(1-Y)^{\frac{1}{2}}(1-X)^{\frac{1}{2}} - 2}{Y \quad L'(1-Y)^{\frac{1}{2}} - 1 + (1-Y)^{\frac{1}{2}}(1-X)^{\frac{1}{2}}} \right| \qquad (7\text{-}119)$$

Figure 41 is a graph of W/U for the cases considered above. It is plain that W/U can not have the values observed on our records for any solution of (7-117) that corresponds to a physically likely state of the ground.

Other treatments of Rayleigh waves.

The general case when the half space is overlain by a layer of solid material of different elastic properties is more difficult to treat. Fu (1946) has given the equations for this case, and has investigated them far enough to get theoretical dispersion curves by treating the effect of the layer as a perturbation of the Rayleigh waves in the lower medium. Love (1911, p.165-177) has examined in some detail the case where the superficial layer is incompressible. Stoneley (1934) and Pekeris (1935) have investigated the case where there is no layering, but the elastic constants are a function of depth. These treatments, though they show

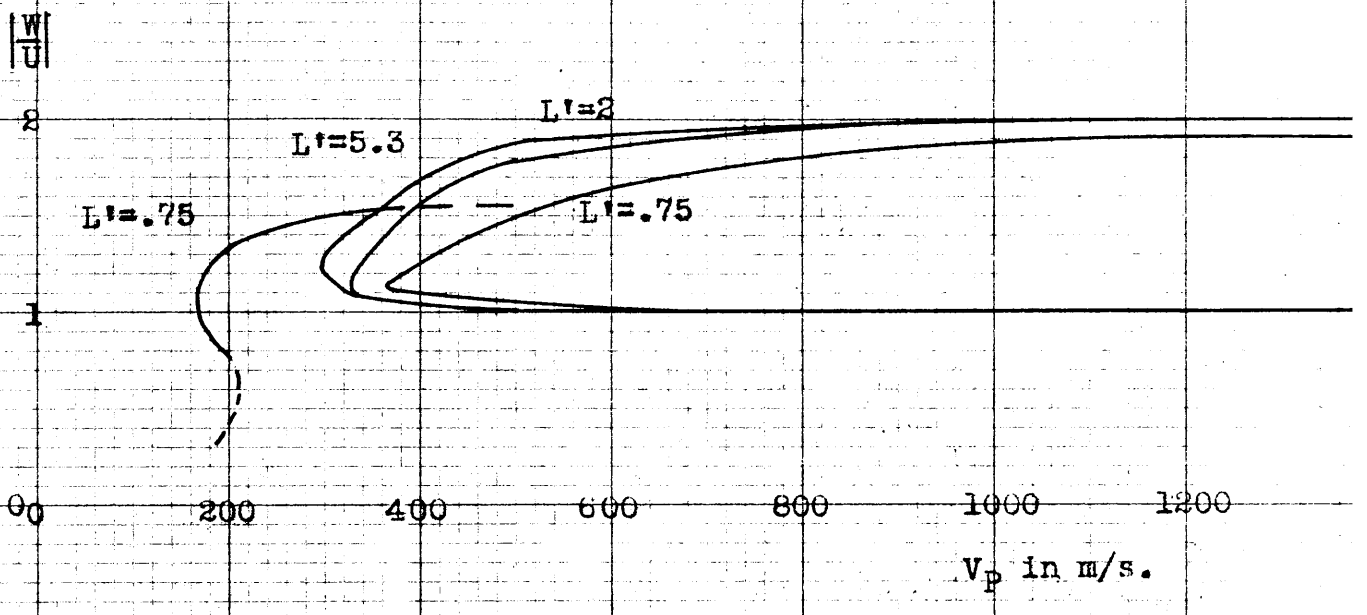

Ratio of the vertical to the horizontal amplitude of R for solutions of Meissner's equation when $V_R = 167\frac{1}{2}$ m/s.

Figure 41.

that Rayleigh waves can exist under a wide variety of conditions, have not as yet been developed in a form convenient for quantitative consideration using the experimental data of this investigation.

It will be noted that throughout the investigation so far the effect of gravity has been neglected. Of the various treatments mentioned of Rayleigh waves, only Stoneley's (1925) considered the effect of gravity in the presence of a superficial layer, though Rayleigh's original treatment has been modified by Love (1911, p.154-160) to include this effect. Love states (loc. cit., p.160) in referring to Rayleigh waves:

> "The modification necessitated by gravity is nothing more than a correction, which is trifling except in so far as it suggests as explanation of the observed fact that the motion is oscillatory."

Thus the effect of gravity will in general be merely to disperse the pulse. Stoneley (1926) also found that gravity had little effect, except for very long wave lengths.

Considerable work has also been done by Uller, who has developed the general equations for the existence of all kinds of surface waves in detail (see Gutenberg, 1932, p.115-124), but here again the results are so complicated that the author has been unable to correlate the observed data with Uller's equations.

In summary then, we can say that, in spite of the large differences between the earth and the ideal medium of theory, the retrograde, elliptical motion observed from shallow explosions in the Los Alamitos region is of the type which would be expected for a Rayleigh wave, except for the small values of the ratios of the vertical to the horizontal amplitudes of motion. These ratios can only be explained by the theories developed if the surface material behaves as though it were a part of the fluid air. The observed ratio of the vertical to the horizontal amplitude is such that some influence is needed to modify the true Rayleigh wave motion, since the horizontal component of movement everywhere exceeds the vertical.

VIII. MOTION ON THE TRANSVERSE COMPONENT.

It was noted earlier that transversely polarized energy is arriving coincident with C. Such waves continue to arrive at least until the maximum of R. It is possible that Love waves or transversely polarized body shear waves were recorded, in which case their origin must be sought in inhomogenieties in the earth which transform motions in radial planes perpendicular to the surface of the ground to motions in other directions. Structures such as faulting, tilting or folding of the rocks could have the effect of making the compressional or longitudinally polarized shear waves appear to be coming from a direction other than directly from the shot; but the origination of truly transversely polarized shear waves from an explosion in the ground is more difficult to visualize mechanically than the simple theory of plane or spherical waves.

On chart VII are plotted the times of arrival of the first recognizable pulses of energy in the transverse direction following X_3. This arrival is marked "T" on the records, charts I-III, where it has been identified. Following the arrival of T are plotted the arrivals of the outstanding maximum to-the-left-facing-the-shot velocities of motion.

This transverse motion begins roughly about the same time as C. It has a maximum velocity close to

the source of the energy of about 250 m/s., and at larger distances the velocity apparently increases to about 800 m/s., as compared to the corresponding velocities of C of 225 m/s. and 675 m/s. Close to the origin, alignment of the times of these maximum velocities indicates dispersion with a group velocity of about 275 m/s.

The data are so poor that the true velocities of this pulse and C could be the same. If this is true and the transverse motion is Love wave motion, or shear body wave motion, this would agree with the hypothesis that C is a body shear wave.

IX. SUMMARY AND CONCLUSIONS.

List of pulses observed.

In summary, the following pulses were recognized on many or all of the records taken in the Los Alamitos region:

P The first pulse to arrive, refracted thru one or both of the first two layers beneath the weathered layer.

P_3 A compressional pulse arriving later than P.

X_1, X_2, X_3 Three pulses presumed to be body waves travelling along deeper paths than P and P_3.

C A strongly dispersed pulse largely confined to the longitudinal component. Its nature is uncertain.

T Motion on the transverse component arriving largely coincident with C. Possibly Love waves.

H A direct, elliptical motion in a vertical plane. It partly overlaps the end of C, even at several kilometers from the explosion.

R A Rayleigh-type motion possibly influenced by loading of the surface by the air or weathered layer.

P, C and R are prominent on all of the records, though at distances less than 300 meters from the explosions, C and R overlap each other and are not clearly distinguishable. H is also recognizable on

almost all of the records, though its beginning is always indistinguishable because it starts to arrive before C is past. In the same manner H overlaps the beginning of R. C, H and R are all strongly dispersed, and their beginnings are therefore difficult to identify at best. It is the times of arrival of their maxima which are plotted in the travel-time curves.

Comparison with Leet's records.

As was noted previously, the only published, previous investigation with which these results are directly comparable are those of Leet. Reproductions of some of Leet's records appear in his report, "Earth motion from the atomic bomb test" (Leet, 1946); and two of these are reproduced here as figures 42 and 43. In comparing Leet's records with those of this investigation, it must be remembered that his apparatus is of the displacement type, while that used here responds more linearly to constant velocity. Also Leet's seismometers have resonant frequencies below three cycles per second, whereas those used here are resonant at about $3\frac{1}{2}$ c. p. s.

Consider first Leet's record obtained at 650 feet (198 meters) from an explosion in granite (figure 42) and the author's record taken at 189 meters in alluvium (Chart I). The records are very similar. Both start with relatively high frequency motion with

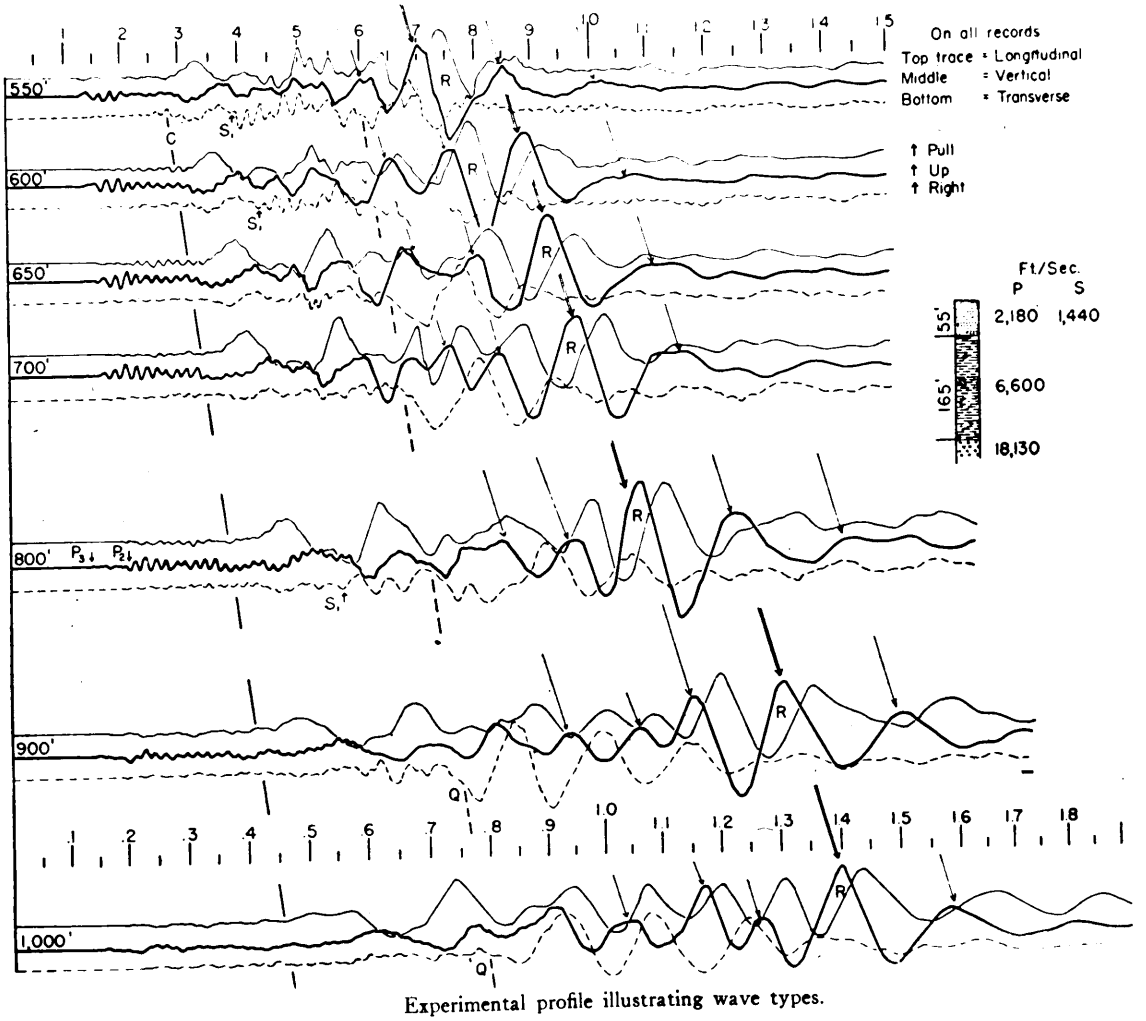

Experimental profile illustrating wave types.

Reproduction of records taken by L. Don Leet.

Earth motion from the atomic bomb test.

American Scientist v.34, 1946, p.202.

Figure 42

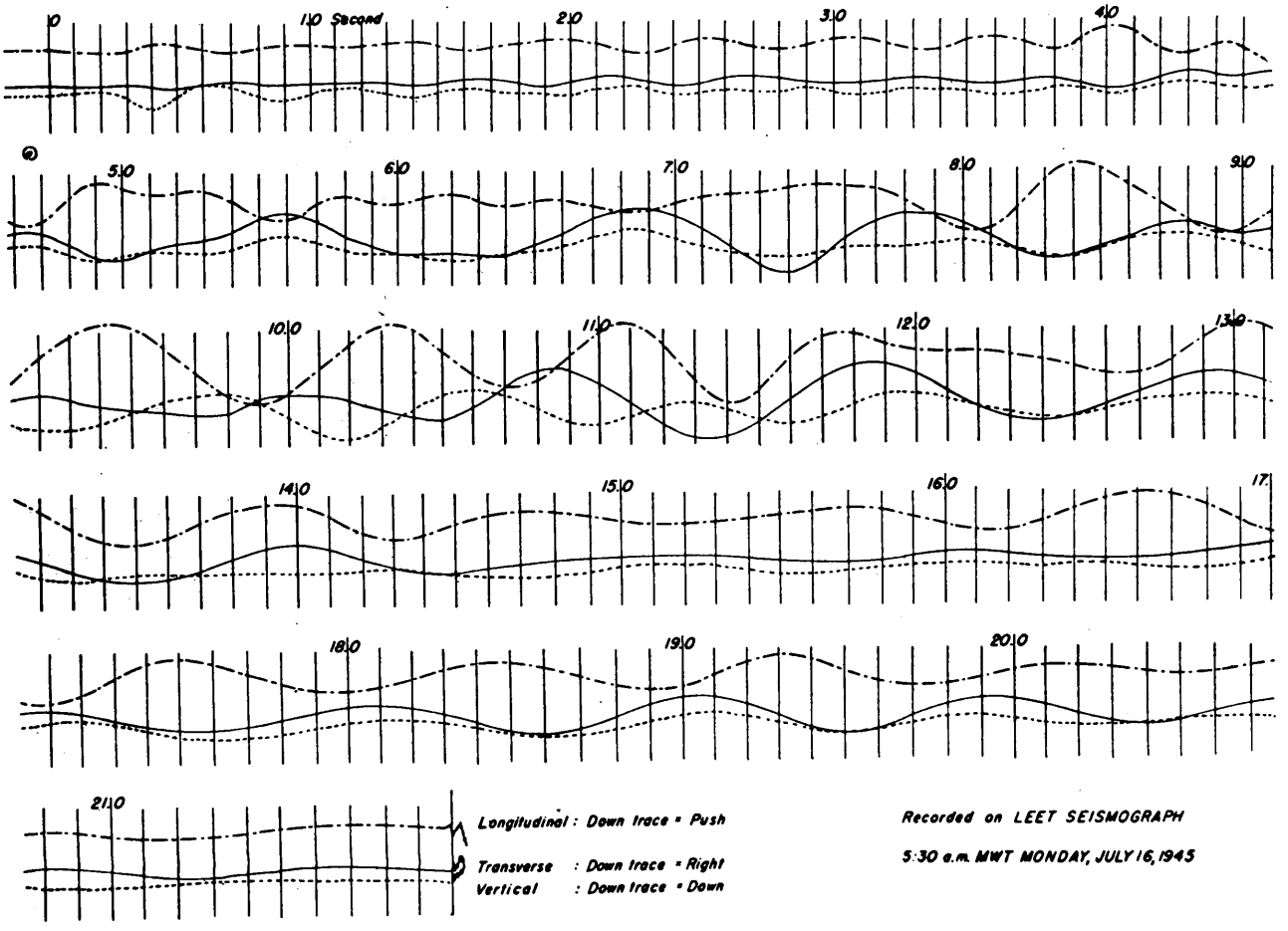

Record of earth motion at Atomic Bomb test in Jornada del Muerto Valley, New Mexico, July 16, 1945.

Reproduction of record taken by L. Don Leet.

Earth motion from the atomic bomb test.

American Scientist v.34, 1946, p.199.

Figure 43

the largest amplitudes on the vertical components. This is followed by some increase in the energy on the longitudinal components. Next comes the C pulse. Shortly after the beginning of this phase on Leet's records occurs a relatively high frequency pulse which he has concluded is the shear wave corresponding to his first arriving compressional waves. This pulse is not discernible in the records taken by the author. At a time equal to about twice the time from the origin time until the arrival of C, Leet's record shows motion beginning on the transverse component. A similar pulse occurs on the author's record, but somewhat earlier. This pulse is not always clearly distinguishable on records made at larger distances at Los Alamitos. This is followed by a pulse having the maximum amplitude on Leet's record, and identified as the Rayleigh wave. A similar pulse appears on the author's record, having motion of the same nature and predominant amplitude. After the arrival of this R pulse the amplitudes rapidly diminish on both records, and no more identifiable pulses are recorded. On Leet's record, the vertical motion arriving coincident with C appears to be related to it, whereas on the author's records, this is not the case, since H is already, even at this short distance, clearly recognizable.

Now let us compare Leet's record taken at the time

of the explosion of the atomic bomb at Los Alamos, New Mexico (Leet, 1946, p.199), which is reproduced as figure 43, with one taken by the author at the greatest distance at which he was able to record explosions with a useable amplitude. Leet's distance from the atomic bomb explosion has not been given for "security" reasons. The author's distance was 3284 meters. Both observations were taken in regions underlain by alluvial deposits. In each case the records begin with a compressional pulse, followed by energy probably representing other body wave pulses of both compressional and shear type. These are followed, as in the case of the records discussed above, by C in both cases. On Leet's record the motion is clear on all three components. On the author's records it is clear on only one component, the longitudinal. Four seconds after the arrival of the first pulse on Leet's records the amplitude of the transverse component begins to increase. Three seconds later that of the longitudinal component also increases, and at the same time the amplitude of the transverse motion is at a maximum. More striking, however, is the increase in the period of the predominant motion. This is accompanied by a phase shift of the longitudinal with respect to the transverse component of about 60°. The period of the motion on

the transverse trace is such as to suggest that an independent wave may be coming in on that trace. Leet identifies this as a Love wave. Because of the phase shift, he believes that a wave of a different type than the C wave is also being recorded on the other two components. He has called this an H or Hydrodynamic wave, because the particles follow paths similar to those in a gravity wave in a liquid. This is an assumption which should be investigated with care, as the period is approaching that corresponding to the natural frequency of his recording apparatus, and in this region there are rapid phase shifts of the recording mechanism. Hence the distinctly different appearance of the two motions could be entirely an effect of the change of frequency of the motion if the two recording channels do not have identical phase response at these frequencies. Some difference in phase is to be expected since the natural frequency and damping of the three seismometers is not identical, as shown in Leet's published response characteristics (Leet, 1939, p.489).

On the corresponding record taken by the author we find that the longitudinal trace becomes active at about 5 seconds (Chart III). A small amount of motion on the transverse component beginning at about 6½ seconds may correspond to Leet's Love wave. Also, beginning at ten seconds there is a train of

waves on the vertical and longitudinal which has a motion similar to that of Leet's Hydrodynamic wave. The appearance of strong motion on the previously quiet vertical trace makes it certain that this is a distinctly new arrival.

Leet identifies a second pulse of Love type motion while H is still arriving, and following the end of strong H motion considers the motion of the longitudinal trace to represent the arrival of the direct compressional wave along the surface.

Toward the end of Leet's record the amplitudes of all three traces build up again, the motion on the vertical and longitudinal components being correlatable. Leet interprets this as being due to simultaneous arrival of a Love wave pulse on the transverse, and a Rayleigh wave pulse on the longitudinal and vertical. The author's records show a similar pulse of the Rayleigh type, but lack significant motion on the transverse component.

Comparing all the records it can be said that the present investigation recorded waves in general similar to those recorded by Leet, with the exception of the notable absence of motion on the transverse component. The pulse called C by the author occupies the same place on the records as Leet's "coupled" waves, but differs from them in its lack of vertical and transverse

motion, especially the latter. However, it should be noted that Leet's coupled wave has its greatest amplitude on the longitudinal component.

Similarly, pulses called H and R by the author correlate with Leet's Hydrodynamic and Rayleigh waves. The greater amount of transverse motion on the atomic bomb record may be due to application of the explosive force, whereas the explosions used in this survey were detonated beneath the surface.

Other observations of surface waves are not comparable, record against record, with these investigations. Sharpe (1942) in his investigation of compressional waves did not record the horizontal components of motion, so that his records do not show most of the phenomena of the ground motion following an explosion. The waves recorded at distant permanent seismic observatories have travelled largely thru deeper parts of the earth, and the original seismic pulses have been changed so much in character in these long distances of transmission that they do not closely resemble the pulses recorded here. Records taken at distances of three to fifty kilometers would greatly help to fill the gap between the observations of small explosions such as are treated here, and the large blasts regularly recorded by the permanent seismic stations, and would help to correlate the

types of motion observed here with the better known waves of teleseisms.

Need of a new theory.

The recorded pulses of energy were all of types previously reported. For all except two, namely C and H, the ground motion is satisfactorily described by well known equations. If we could modify the theory of shear waves to include adequate dispersion, and that of Stoneley waves to include the proximity of the surface we might be able to explain C and H equally well. To describe these two pulses, called "coupled" and "hydrodynamic" by Leet, whether they are new types of ground motion, or are well known types modified by special near-surface conditions, requires a new theory. Such a theory must be based on a knowledge of the fundamental properties of the first few meters of the earth's crust, a complicated medium which is plainly neither homogeneous nor elastic, and hence for which the classical wave equations do not apply. The fact that such a medium can transmit both compressional and Rayleigh type waves is an encouraging sign, as it means that its behavior can not be radically different from that of elastic substances, especially since Rayleigh waves are essentially simply a combination of compressional and shear waves confined to the neighborhood of a surface. Relatively little is known about the properties of non-elastic

substances (Gutenberg, 1939, p.361-384); but it is to be hoped that the mathematical physicists will soon come to our aid and develop equations describing wave transmission thru such media similar to those we now have for elastic media.

LIST OF SYMBOLS AND ABBREVIATIONS USED IN THE TEXT.

a Magnitude of displacement.

A, A_o Amplitude constants.

A_c Amplitude coefficient depending on f and h.

A_n Magnitude of velocity at distance Δ_n.

A_1, A_2 $(1-\frac{V_H^2}{V_{Pn}^2})^{\frac{1}{2}}$, n = 1 or 2.

B Amplitude constant.

B_n $(1-\frac{V_H^2}{V_{Sn}^2})^{\frac{1}{2}}$

C A dispersed pulse on the longitudinal component, also the expression: $4\left[\frac{\rho_1}{\rho_2}\left(\frac{1-X}{Z-1}\right)^{1/2}\tan f_1 h + 1\right]^{-1}$

C_B A similar expression involving $\frac{\tanh f_\beta h}{f_\beta}$

C_o, C_1, C_2, C_3 Cubics in B_1.

CM, C_{M1}, C_{M2}, C_{M3} Three peak movements during the passage of C.

D_n Amplitude coefficients.

E Amplitude coefficient.

f 2π/wavelength

f_1 $f(\frac{V_R^2}{V_o^2}-1)^{\frac{1}{2}}$

f_B $f(1-\frac{V_R^2}{V_A^2})^{\frac{1}{2}}$

g Acceleration of gravity.

h Thickness of surface layer.

h_n Thickness of the nth layer.

h_r $p^2/V_P{}^2$

H A direct elliptical pulse.

i $\sqrt{-1}$

i_c Critical angle of incidence.

i_n Angle of incidence in the nth layer.

i_{nm} Angle of incidence in the nth layer of the ray which penetrates to the mth layer.

J_n Maximum energy of surface waves at a distance Δ_n.

k Bulk modulus.

k_R p^2/V_S^2

K $2(\rho_1 V_{S1}^2 - \rho_2 V_{S2}^2)$

K_M Amplitude coefficient.

L Wave length.

L' $\frac{\rho}{f \omega}$

p 2π/period

P The first wave to arrive at the recording station.

P_B Amplitude coefficient.

P_w Pressure in the water.

P_z A function depending only on z.

P_3 A refracted compressional pulse.

Q, Q_B, Q_n Amplitude coefficients.

r $f(1-\frac{V_R^2}{V_\rho^2})^{\frac{1}{2}}$

r_n $f(1-\frac{V_R^2}{V_{\rho n}^2})^{\frac{1}{2}}$

R A pulse similar to a Rayleigh wave.

s Shot depth, also $f(1-\frac{V_R^2}{V_S^2})^{\frac{1}{2}}$

s_n $f(1-\frac{V_R^2}{V_{Sn}^2})^{\frac{1}{2}}$

t Time.

t_o Time at which the explosion was detonated.

T Motion on the transverse component.

T_u Uphole time.

T_Δ Time of transmission over surface distance Δ.

u, v, w Displacements.

u_n, v_n, w_n Displacements in the nth medium.

U, V, W Velocity components of compressional waves in a fluid.

V_A Velocity of propagation of compressional waves in air.

V_C Surface velocity of C.

$V_{Cn}, V_{Cn'}$ Maximum and minimum phase velocities of C in the nth layer.

V_g Velocity of propagation of gravity waves.

V_H Surface velocity of H.

V_P Velocity of propagation of compressional waves in the ground.

V_{Pn} Velocity of propagation of compressional waves in the nth medium.

V_R Velocity of propagation of Rayleigh waves.

V_S Velocity of propagation of shear waves in the ground.

V_{Sn} Velocity of propagation of shear waves in the nth medium.

V_O Velocity of propagation of compressional waves in water.

x, y, z Coordinates.

X V_R^2/V_P^2

Y V_R^2/V_S^2

Z V_R^2/V_O^2

X_1, X_2, X_3 Three body waves.

α, α' Absorption coefficients.

α_M Phase angle.

β An amplitude coefficient.

Δ Distance.

Δ_n Distance to the nth recording location.

Δ_o Radius of the earth.

η Elevation of the surface of a fluid layer.

ρ Density.

ρ_n Density of the nth layer.

ρ_L Density of a surface load.

σ Poisson's ratio.

Θ Dilatation.

Θ_n Dilatation in the nth medium.

Ψ_n Angular distance along a great circle path.

λ / μ Lame's constants.

Φ Velocity potential.

BIBLIOGRAPHY.

The following abbreviations are used in the bibliography:

BSSA Bulletin of the Seismological Society of America.

MNRAS Monthly notices of the Royal Astronomical Society, Geophysical Supplement.

TAGU Transaction of the American Geophysical Union.

Bateman: 1938 Rayleigh waves. Proc. Natl. Ac. Sci. v.24, p.315-320.

Birch and Leet: 1942 Geol. Soc. Am. Special Pub. #36 Handbook of physical constants. p.63-100.

Byerly, P.: 1933 The records of earthquakes at intermediate and great distances. Bull. Natl. Res. Council #90. Physics of the earth VI. Seismology p.171-188.

1946 The seismic waves from the Port Chicago explosion. BSSA v.36 p.331-348.

- and Dyk: 1932 Richmond quarry blast of Sept. 12, 1931. BSSA v.22, p.50-55.

- and Wilson: 1934 The Richmond quarry blast of Aug. 16, 1934. BSSA v.25, p.259-268.

Dix, Fu, McLemore: 1945 Rayleigh waves and free surface reflections. Quart. Jour. Ap. Math. v.3, p.151-156.

Frenkel, J.: 1944 On the theory of seismic and seismoelectric phenomena in a moist soil. J. Phy. U. S. S. R., v.8, p.230-241.

Fu, C. Y.: 1946 Rayleigh waves in a superficial layer. Geophysics v.11, p.10-23.

1947 Propagation of elastic waves in the neighborhood of a free boundary. Geophysics v.12, p.57-71.

Gutenberg, B.: 1932 Handbuch der Geophysik. v.4 Erdbeben. Ch. 3 Theory of surface waves. Ch. 6 Observations of surface waves. Gebruder Borntraeger, Berlin.

1939 Internal Constitution of the earth. McGraw-Hill.

1944 Energy ratio of reflected and refracted seismic waves. BSSA v.34, p.85-102.

1946 Atomic bomb test, July 16, 1945. BSSA v.36, p.327-330.

- and Fu: 1948 Remarks on multiple reflections. Geophysics v.13, p.45-48. This paper is only one of a symposium on multiple reflections in the January 1948 issue of Geophysics.

- and Richter: 1946 Seismic waves from atomic bomb tests. TAGU v.27, p.776.

Hecher, O.: 1922 **Die Explosionkatastrophe von Oppau. Veroffentlichungen der Hauptstation fur Erdbebenforschung in Jena, v.2.**

Hoots, H. W.: 1932 General geology and oil development in the Los Angeles basin. XVI Internat. Geol. Congress, Guidebook 15, p.23-30.

Jeffreys, H.: 1925 On the surface waves of earthquakes. MNRAS v.1, p.282-291.

1947 On the Burton-on-Trent explosion of 1944 Nov.27. MNRAS v.5, p.99-104.

Lamb, H.: 1904 On the propagation of tremors over the surface of an elastic solid. Phil. Trans. Roy. Soc. London v.20, p.1-42.

1932 Hydrodynamics. Ch. 9, p.363-475. Cambridge Univ. Press.

Lee, A. W.: 1932 The effect of geologic structure upon microseismic disturbance. MNRAS v.3 p.83-105.

Leet: 1939 Ground Vibrations near dynamite blasts. BSSA v.29, p.487-496.

1946-A Earth Motion from the Atomic Bomb Test. American Scientist v.34, p.198-211.

1946-B Vibrations from blasting. Explosives Engineer. v.24, p.41-44, 55-59, 85-89.

- and Ewing: 1932 Velocity of elastic waves in granite. J. Ap. Phy. v.2, p.160-173.

Love, A. E. H.: 1911 Some problems of geodynamics. Ch. 11. Theory of propagation of seismic waves. p.144-178. Cambridge Univ. Press.

Macelwane: 1936 Theoretical Seismology. John Wiley and Sons.

Meissner, E.: 1922 Oberflachenwellen bei Mitschwingen einer tragen Rindenschicht. Vierteljahrs. Naturf. Ges. Zurich v.67, p.1. See also Gutenberg, 1932, Handbuch der Geophysik, p.94-97.

Pekeris, C. L.: 1935 The propagation of Rayleigh waves in Heterogeneous media. J. Ap.Phy. v.6, p.133-138.

Press and Ewing: 1948 A theory of microseisms with geologic applications. TAGU v.29 #2, p.163-174.

Rayleigh, Lord: 1885 On waves propagated along the plane surface of an elastic solid. Proc. London Math. Soc. v.17, p.4-11. Also Coll. Works v.2, p.441-447.

Sharp, J. A.: 1942 The production of elastic waves by explosion pressures. Geophysics v.7, p.144-154, 311-322.

Stewart and Lindsey: 1930 Acoustics. D. Van Nostrand Co., Inc.

Stoneley, R.: 1924 Elastic Waves at the surface of separation of two solids. Proc. Roy. Soc., Series A v.106, p.416-428.

1925 Dispersion of seismic waves. MNRAS v.1, p.280-282.

1926 The effect of the ocean on Rayleigh waves. MNRAS v.1, p.349-356.

1934 The transmission of Rayleigh waves in a heterogeneous medium. MNRAS v.3, p.222-232.

Willmore, P. L.: 1947 Seismic aspects of the Heligoland explosion. Nature v.160, p.350-351.

Wood, A.: 1941 Acoustics. Interscience Pub. Inc.

Wood and Richter: 1931 A study of blasting recorded in southern California. BSSA v.21, p.28-46.

1933 A second study of blasting recorded in southern California. BSSA v.23, p.95-110.

Wrinch and Jeffreys: 1922 On the seismic waves from the Oppau explosion. MNRAS v.1, p.15-22.